2012

Measurement, analysis and process planning for the layup of unidirectional fabrics

Fanqi Meng
Iowa State University

Measurement, analysis and process planning for the layup of unidirectional fabrics

by

Fanqi Meng

A dissertation submitted to the graduate faculty

in partial fulfillment of the requirements for the degree of

DOCTOR OF PHILOSOPHY

Major: Industrial Engineering

Program of Study Committee:
Frank E. Peters, Co-Major Professor
Matthew C. Frank, Co-Major Professor
Stephen B. Vardeman
Vinay Dayal
William Q. Meeker

Iowa State University

Ames, Iowa

2012

TABLE OF CONTENTS

ABSTRACT

Manual layup has been a common method in the manufacture of composite structures for complex geometries. However, when production volumes and/or the quality requirements increase, there is an urgent need for solutions to automate the layup process. In addition, the trend in designing composite structures with increasingly larger dimensions and more complex geometries requires advanced process planning tools to optimize process parameters and guarantee the feasibility of the layup process. This dissertation presents a three-phased study on the development of automated and optimized process planning tools for the layup of unidirectional fabrics onto complex three-dimensional mold surfaces. The first phase of the study introduces the development of a laser scanning based measurement system, with the capability of measuring in-plane shear and out-of-plane deformations of unidirectional fabrics at the resolution of tow level. Based on this fabric deformation measurement approach, the second phase of study analyzes the effects of process parameters on the generation of different deformation modes and the transformation between them. The findings from the analyses were further explored to provide generalized solutions for improving the process of fabric layup in the third phase of the study, where two process planning tools are presented: pre-shearing planning and in-process manipulation planning. It has been verified by both simulation and experiments that these process planning tools are effective in increasing the drapability of the fabrics and in securing a feasible layup plan. Implementation approaches in layup process automation and composite structure design for manufacturability are also presented. The results of this dissertation can provide a path

toward automated composite manufacturing that is both cost effective and reduces variability leading to flaws in large complex composites.

CHAPTER 1. GENERAL INTRODUCTION

In the manufacture of advanced composites of complex geometries, manual layup has been the one of the dominant [1,2] methods employed. However, when production volumes and/or the quality requirements increase, there is an urgent need for solutions to automate the layup process. In addition, the trend in designing composite structures with increasingly larger dimensions and more complex geometries requires advanced process planning tools to optimize process parameters and guarantee the feasibility of the layup process. This dissertation presents a three-phased study, on the development of automated and optimized process planning tools for the layup of unidirectional (UD) fabrics onto three-dimensional (3D) mold/tool surfaces. This first chapter discusses the challenges in process planning for the layup process and provides a set of research objectives for this dissertation.

1. Background and Motivation

Composite material has long been the choice for the aerospace, boat and wind turbine blade manufacturing industries due to its superior material properties, such as high strength-to-weight ratio, corrosion resistance, long fatigue life, and the ability to tailor layups for optimal strength and stiffness. Typical manufacturing processes involved in the fabrication of composite structures are vacuum forming, compression molding, vacuum resin transfer molding (VRTM), automated tape laying (ATL) and filament winding. Among these processes, VRTM plays a very important role in manufacture of large composite structures (Figure 1). Firstly, because an autoclave is not required for curing, the tooling cost is reduced. In addition, the relatively lower pressure used in the VRTM process allows light weight foam or balsa cores to be easily incorporated into the fabric plies during the layup process.

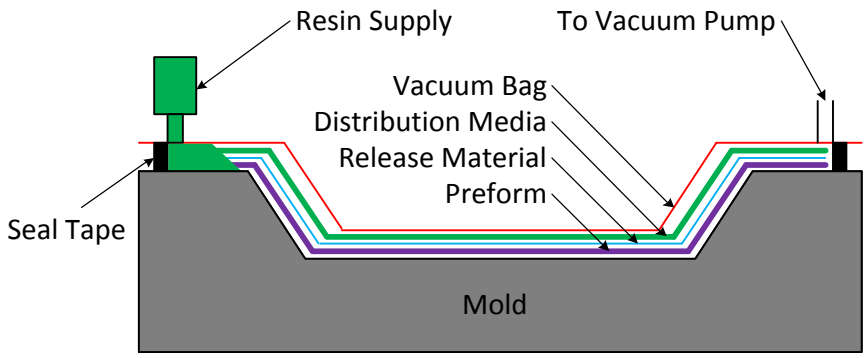

Figure 1. Vacuum resin transfer molding

Fabric Layup is the process performed prior to the VRTM process, where layers of fabric panels are placed into the mold in the location and orientation as specified in the process instruction and then smoothed to conform to the mold shape. During layup, in-plane shear (IPS) deformation occurs when the fabric panels are smoothed to conform to undevelopable mold surfaces or offsets of these surfaces. When deforming, the fabric material behaves as a pin-jointed cell network [3], and if the IPS angle is beyond the shear locking angle of the fabric at a cell, buckling or out-of-mold (OOM) deformation will occur [4-6]. An OOM deformation typically results in excessive fabric material covering the region on the mold where it occurs and induces wrinkling when vacuum is applied prior to and during the resin transfer stage. This wrinkling or fiber waviness will reduce the strength and fatigue endurance of the product. Thus, it is of great importance to plan and control the layup process, in order to manufacture defect-free composite structures.

A UD fabric is characterized by the feature that the majority of tows run in one direction only. Although a small fraction of fiber tows run in the perpendicular direction, their main purpose is holding the primary fiber tows in position with stitching lines (Figure 2). UD fabric is one of the primary reinforcement materials for the manufacture of three

dimensional structural composite. It offers better opportunities to optimize the strength to weight ratio of a part than offered by other types of fabrics, because the unidirectional fabric allows the designer full freedom to set the directions of all fabric layers independently [7]. In wind turbine blade design, for example, a spar cap is utilized as the main load carrying structural component. This component is primarily made of layers of UD fabrics to provide flap wise bending strength [8]. Unfortunately, the relatively simple structure of UD fabrics results in the limited capability in shear deformation [9]. The shear locking limits (SLL) for common types of UD fabrics are much less than the SLLs of biaxial woven fabrics, making the layup process more challenging. Additionally, with the trend of moving toward larger dimension components with more complex geometries, the layup process is more prone to excessive shear deformations which will more readily lead waviness or wrinkling defects.

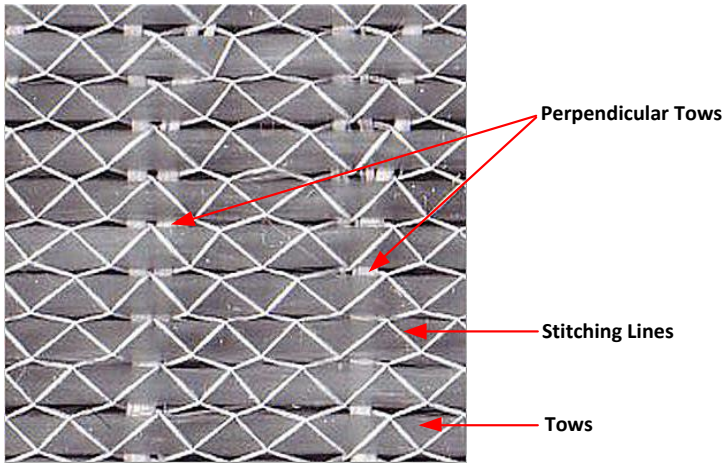

Figure 2. Structure of unidirectional fabric

Computer-based layup modeling has emerged since the late 1970s [10]. Typically, layup simulations involve iterative methods on the computation of the unit cell shapes in order to predict the overall draped shape of the fabrics onto specific 3D tool surfaces. These methods vary from purely kinematic approach [10], to more sophisticated finite element

analysis [11]. Some of these approaches have been integrated into commercial software packages such as FiberSIM [12] and QuickForm [13]. Generally, these simulation methods are not able to generate any layup process plans [1]. Although they can be utilized as a tool for the feasibility evaluation of existing process plans, only the binary answers of *feasible* or *unfeasible* can be provided. A feasible plan corresponds to the situation where all the IPS angle values are within the shear locking limits (SLLs) at every location of the fabric, while an unfeasible plan corresponds to the situation where the IPS angle magnitude exceeds the SLL in at least one location of the fabric. This is because a common assumption shared among these simulation methods is that the fabric panels always conform to the tool surface. This assumption ignores the phenomenon of OOM deformation that could be generated when the local shear angles are beyond the shear locking limit of the material. With this assumption, the prediction of the shear angle distribution is therefore not accurate beyond the point where shear locking limit is reached. Thus, using this type of layup simulations to evaluate a layup process plan could be error-prone. In addition, for a given layup plan that is predicted to be unfeasible, it is desirable that the layup simulation software is capable of automatically suggesting improvement methods, so that a feasible layup process can be determined. The development of such software tools with design for manufacturability feedback requires the knowledge of the mechanism of the interaction between IPS and OOM deformations, and the abstraction of that mechanism requires analysis of measured deformation data obtained from layup experiments.

Although some defects such as local wrinkling or fiber tow deviation from specification could be corrected manually, there is an inherent lack of repeatability in smoothing that will result in random and unpredictable locations of defects from time to

time. Handling these types of defects relies too heavily on the skill and experience of the operators. It is therefore desirable to have an automated machine system to perform or at least assist the layup process, in order to reduce overall product variation and the likelihood of defects. In industrial applications, there are generally two types of automated machines that can perform the lay-up process for open mold surfaces [9]. The first type is the ATL machine, which lays down narrow tapes to high performance composites, such as airplane wing skins. The second type of automated system is a fiber tow placement machine, which places individual tows to the mold surface. Because these systems place individual narrow tapes/tows that are hardly cross-linked, the excessive IPS deformation problem is avoided. However, none of the above automation techniques can be directly applied to the layup of a wide (e.g. 20 inches ~ 50 inches) piece of UD fabric ply onto a 3D mold with complex geometry. This is because a UD fabric typically has limited capability in shear deformation, which is not able to tolerate the excessive IPS deformation needed to conform to complex mold surfaces. In such situation, IPS deformation orientated process planning tools are critical to enable the automation of the layup process.

2. Research Objectives and Solution Approaches

The primary objective of this dissertation is to provide process planning tools for the layup of UD fabrics onto 3D molds, in the manufacture of large scale composite structures with complex geometries. In order to achieve the primary objective, multiple sub-objectives and the corresponding solution methodologies are proposed below.

The first sub-objective is to develop a measurement methodology, which is capable of capturing IPS distortion and out-of-plane (OOP) waviness. In this part of the study, a

modified laser scanning system and analysis technique were developed, with the capability of measuring the IPS and OOP deformations of UD fabrics at the resolution at the tow level.

The second sub-objective is to investigate the mechanism of generation and the relationships among different deformation modes within the fabric layup process. An experimental study was conducted to understand 1) the relationship among IPS angle distribution, geometry of the mold, position of the constraint, and material properties of the UD fabric, and 2) the interaction between IPS and OOM deformations.

Measurement of the different fabric deformation modes and understanding of the underlying mechanisms provide the foundation for achieving the primary objective, i.e. the development of the process planning tools. Two process planning methods were developed as part of this research. Pre-shearing planning addresses manipulation of fabric prior to the layup process, in order for the layup process to achieve optimal IPS angle distribution. In-process planning provides a robust solution to the unfeasible layup plans. By sacrificing a controlled amount of geometric conformity to the mold surface, this methodology redefines the tow positions of the given UD fabric, following which will guarantee the feasibility of the layup process.

3. Dissertation Organization

The reminder of this dissertation is organized as follows: Chapter 2 provides a general review of relative research found in the literature. Chapter 3 introduces the development of a modified laser scanning methodology for the measurement of fabric deformations. Chapter 4 discusses an experimental study on the layup of the UD fabrics. Chapter 5 and Chapter 6 present pre-shearing planning and in-process manipulation planning

methodologies for the UD fabric layup process, respectively. Lastly, Chapter 7 presents an overall conclusion to the dissertation and future research opportunities.

Reference

[1] Hancock SG, Potter KD. The use of kinematic drape modeling to inform the hand layup of complex composite components using woven reinforcements. Composites Part A 2006;37:413-422.

[2] Gutowski TGP. Advanced Composites Manufacturing: John Wiley &Sons, New York, 1997.

[3] Potter K. In-plane and out-of-plane deformation properties of unidirectional preimpregnated reinforcement. Composites Part A 2002;33:1469-1477.

[4] Prodromou AG, Chen J. On the Relationship between the shear angle and wrinkling in textile composite preforms. Composites Part A 1997;28(A):491-503.

[5] McBride TM, Chen J. Unit-cell geometry in plain-weave fabrics during shear deformation. Composites Science and Technology 1997;57:345-351.

[6] Mohammed U, Lekakou C, Bader MG. Experimental studies and analysis of the draping of woven fabrics. Composites: Part A. 2000;31:1409-20.

[7] Olsen HB, Craig JH. Automated composite tape layup using robotic devices. Proceedings of the IEEE international conference on robotics and automation, Los Alamitos, CA 1993.

[8] Yerramalli C, Miebach T, Chandraseker K, Quek S. Fiber waviness induced strength knockdowns in composite materials used in wind turbine blades. Proceedings of the European wind energy conference & exhibition, Warsaw, Poland 2010.

[9] Campbell FC. Manufacturing technology for aerospace structural materials: Elsevier; 2006.

[10] Potter K. The influence of accurate stretch data for reinforcements on the production of complex mouldings. Part 1: deformation of aligned sheets and fabrics. Composites 1979.

[11] Dong L, Lekakou C, Bader MG. Solid-mechanics finite element simulations of draping fabrics: sensitivity analysis. Composites Part A 2000;31:639-52.

[12] FiberSIM, Vistagy Inc., Waltham, Massachusetts.

[13] QuickForm, ESI Group, Paris, France.

CHAPTER 2. LITERATURE REVIEW

This chapter reviews previous research in the following fields: methodologies and techniques for dry fabric deformation measurements, studies and analyses on the relationship among mold geometry, IPS deformation, OOM deformation and wrinkling during the layup process, as well as approaches to formulate and implement process plans for automated fabric layup.

1. Measurement Methodologies for Dry Fabrics Deformations

In previous research, various methods had been developed to measure fabric distortions, especially the in-plane shear deformations occurring in the draping process. The first and perhaps the most basic type of measurement method is manually tracking the distorted grid, inscribed prior to the draping process [1,2]. This type of technique is laborious and lacks repeatability, because each of the individual grid elements has to be traced, and the diagonal lengths had to be manually measured using protractors, in order to calculate the local in-plane shear angle. Inherently, the resolution of this measurement technique is low. Lin et al. [2] reported the grid size of 10mm, while Mohammed et al. [1] used the grid size of 18mm. Although finer grids may be feasible, they are not practical.

As a second category of measurement approaches, image analysis was widely utilized in the work of several fabric deformation studies [3-8]. This technique is applicable to both 2D and 3D measurement situations. For 2D measurements, typically involved in the bias extension test or picture frame test, a single camera is required to be positioned perpendicular to a flat surface. The acquired digital image is analyzed using a digital image correlation (DIC) method in order to obtain both qualitative and quantitative information on the

heterogeneous deformation on the fabric surface. In the case of 3D fabric deformation measurements, [5,6] it requires the use of two cameras simultaneously or one camera to capture two images of the fabric distortion from two difference known positions. Comparing with the manual measurement method, the use of digital cameras and image analysis is contactless, which eliminates the possible distortion introduced during the measurement process. It also has much higher resolution and repeatability. However, its major drawbacks are: (i) light reflections can corrupt the measurements at certain places [5] (ii) at high magnifications it is difficult to keep the camera focused on a specific area [9].

The third type of measurement method was developed by Potluri et al. [9], where a flat-bed scanner was used to capture the unit cell deformations across the fabric in the bias extension test. In their work, points of tow interlacements were traced manually within the scanned image, in order to calculate the shear deformations. The advantages of this method are: (i) it eliminated the fabric inscription process, which is required (or partially required) in the previous two methods (ii) comparing with the digital camera method, this method has significantly larger measurement area. However, this method could only be applied in 2D measurements, due to the capability of a flat-bed scanner.

2. Analyses of Relationships among Mold Geometry, In-plane Shear, Out-of-plane Deformation and Wrinkling in the Layup Process

Previous research has studied the relationship among mold geometry, shear angle distribution, the generation of OOP deformation and wrinkling of fabrics. This literature basically falls into two categories. The first category is computer draping simulations, which predict the shear angle distribution based on a given mold shape and fabric material

properties. This type of analysis involves iterative methods on the computation of the unit cell shapes in order to predict the overall draped shape and the local shear deformations of the fabrics onto specific 3D tool surfaces.

Potter [10] used the pin-jointed net model to simulate the draping of a fabric over a semi-spherical mold. The simulation starts from the component surface geometry, with the assumption that the fabric is initially an orthogonal net. An initial point of contact is specified and an initial warp and weft tow path is generated from the start point over the surface. The fabric is then modeled as a net made up of equal sided cells corresponding to a free linkage of four bars of equal length defined by the warp and weft tows and constrained by the initial warp and weft tows. The computation is then performed in an iterative process, until all the cells of the fabric are in contact with the mold surface.

Improvements on the basic pin-joint model were made by several researchers in order to achieve better prediction capability and accuracy. Trochu et al. [11] illustrated how the classical draping technique, based on the pin-jointed net algorithm, can be combined with kriging, a new interpolation technique used to generate a differentiable parametric model of complex surfaces. Aono et al. [12] presented a Tchebychev net cloth model and described the method for simulating a fit of a sheet of woven cloth composites to an arbitrary curved surface. Two algorithms were developed in the work: a numerical algorithm that solves the mathematical formula of the Tchebychev net using a finite difference method, and an algorithm that solves the fitting problem by reducing the original problem to a surface-surface intersection problem. Potluri et al. [13] presented a comprehensive drape model with the capabilities to handle a range of surfaces from simple open surfaces to closed bent surfaces.

Besides the advancements in kinematic modeling approaches, Finite Element (FE) techniques were also introduced to enhance the simulation of the draping process. In the work by Dong et al. [14], the fabric was considered as a continuum and the analysis of the draping of fabrics was modeled as an extension of the deep drawing or diaphragm forming simulation of metal forming processes. Lin et al. [15] introduced numerical simulations of forming for textile composites over a hemisphere using a rate/temperature-dependent hybrid FE model. These solid mechanics analyses of the draping of fabrics by using FE methodology take into account the mechanical properties of the fabric, and the process parameters. Therefore, the simulation is closer to the actual physical process of draping.

Some of these approaches have been integrated into commercial software packages (eg. FiberSIM, QuickForm), which are widely utilized as analysis tools in the composite manufacturing industry. However, a common assumption shared among these simulation approaches is that the fabric is always conformed to the mold/tool surface. This assumption ignores the out-of-plane deformation of the fabric when the local shear deformation is beyond the shear locking limit of the material, in which case, the prediction of the shear angle distribution will not be accurate.

The second category of the research studies the relationship between the in-plane shear angle deformation and wrinkling of the fabric material. In the work by McBride and Chen [4], as well as Prodromou and Chen [16], the wrinkling mechanism was identified at the unit cell level by conducting a bias tension test and picture frame test, respectively. They claimed that the trellising results in a continuously changing yarn/unit cell structure. If the fabric continues to be deformed, local shear and in-plane compressive forces build up. This is compensated in the form of wrinkling or out-of-plane deformation. Such bias tension tests

and picture frame tests are not suitable to infer the fiber tow behavior in the layup process, where the fiber tows are only partially constrained (as opposed to complete constraint in bias tension and picture frame tests). The unconstrained end/ends will provide the flexibility to allow the generation of other deformations, which could mitigate the concentrated local in-plane shearing deformations.

In addition to 2D material property testing, research has attempted to understand the winkling mechanism from 3D deformation experiments, such as the forming process. In the work by Potter [17] and Lin et al. [15], the shape of the fabric material was initially flat. Then it was directly pressed by the punch tool into the die, without any draping or layup procedure involved. Mohammed et al. [1] conducted a forming experiment with a semispherical shaped lower male die, onto which the fabric material was placed. Then the upper female die was dropped upon the setup. This experiment was repeated for four different types of fabric materials; wrinkling was observed for three of them. For unwrinkled parts obtained from the forming process, the shear angle distribution can be directly measured by some optical methods. This distribution information is helpful for verifying the accuracy of the layup simulation models. In addition, by varying forming process parameters, such as temperature and forming speed, or material types, it is possible to find an optimal process condition or material combination to produce wrinkle free parts. However, such forming experiments do not provide direct links between local shear angle and the emergence of wrinkling, because, for a wrinkled region, it is not possible to measure the shear angle accurately.

3. Approaches to Planning and Automating the Layup Process

By far, hand layup persists as the method by which a majority of all advanced composite structure is made [18]. The popularity is due to its features of low cost, flexibility and capability of making a wide variety of complex geometric shapes. Nevertheless, as the production volumes increase and economic pressures intensify, hand layup would need to be replaced by emerging automation techniques.

Ruth and Mulgaonkar [19] proposed a robotic work cell for the automation of the layup process, capable of doing ply acquisition, transfer and placement, and stacking and smoothing operations. The entire process was planned by mimicking the hand layup sequence performed by an operator. A vision system was used for determining the ply position and orientation, and provided visual guidance during ply placement on the mold. A similar automated layup system was presented in the work by Sarhadi et al. [20], where an electrostatic gripping device (EGD) was utilized to overcome some of the disadvantages of the conventional fabric handling techniques. A vacuum-assisted large scale gripping system was introduced by Jarvis [21], which was capable of handling full sized fabric plies in the manufacture of high performance aircraft propeller blades.

In order to improve the automated layup process, many methods were developed on the analysis and modeling of the fabric gripping and transferring during the process. Chen and Sarhadi [22] investigated the force needed for gripping carbon fiber materials by EGD, where the dynamic behavior of charging process was analyzed, and the charging parameters were controlled to improve the EGD operation reliability. Ozcelik and Erzincanli [23] experimented with different levels of gripping force and speeds in the horizontal direction during the transporting of the woven fabrics using a non-contact end-effector. It was found

that the success rate of the fabric movement increased when a large gripping force was applied, and woven fabrics could be transferred at a higher speed in such situations. Lin et al. [24] provided modeling technique to predict the real-time deformed shape of textile reinforcements in 3D space during robotic handling operations. The deformed shape can be used to guide robotic end-effectors to ensure accurate fabric placement and avoid collisions.

In addition to the techniques and devices developed in research laboratory environments, there are commercial machines that are able to provide full automation solutions to a limited set of layup processes. These machines generally fall into the following categories: 1) tape laying machines, 2) fiber placement machines, and 3) fiber tow placement machines. These machines all apply a band of material, yet they have different application areas. Tape laying machines are suitable for parts whose shapes are nearly general cylinders, including nearly flat parts and nearly conventional cylinders. Filament winding machines are suitable for relatively long, round, convex shells of constant wall thickness such as pressure vessels and pipes. Fiber Tow Placement offers greater versatility and (for dry tows) reduced materials costs since the process is no longer limited by the transverse and shear compliance of a tape and (for tow-preg) the materials handling problem is simplified [25].

Improvements for these existing commercial machines were addressed by several researchers. Olsen et al. [26] claimed that almost all commercially available tape laying systems target the nearly flat parts, such as wing skins and control surfaces. (eg. B-2 wing skins from Boeing, and the vertical and horizontal stabilizer skins on aircraft from Airbus Industries.) In their work, automated tape laying systems were developed to be capable of laying tape on more strongly curved surfaces than commercially available systems. Many process parameters and constraints were considered for the layup process, including tape

distortion, spacing, orientations, application speed, force, tension temperature, pattern and region. It was emphasized that in addition to ensuring the coverage of the tool surface, wrinkling is the one of the most important problem during the layup of the tapes over complex 3D tool surfaces. Two general guidelines were provided to minimize the wrinkling problem in their work. The first solution is to find a best path for a single piece of tape, so that its distortion/shearing deformation is minimized; while the second one is to reduce the tape width, in order to increase the tolerance of local distortion. Longo and Bianchi [27] introduced mathematical modeling to provide the trajectories of the tape centerlines in a fashion that both wrinkling and stretching errors of the tape fibers and overlapping errors between contiguous tapes are minimized. These researchers addressed the significance of the wrinkling problem in the layup of tapes when the mold geometry is complex, and provided process planning solutions to minimize the in-plane shear deformation. However, minimization of the distortion is not a complete solution to the wrinkling problem. In the case of extremely complex mold geometries, even the minimized shear angles could exceed the shear locking limit, which will result in wrinkling.

Rudd et al. [28] argued that the capital equipment cost of conventional tow placement machine is much higher than their potential savings in material cost. They provided a solution where a kinematic draping algorithm was applied to define the net-shape, two-dimensional fiber pattern. Tow placement was performed in two rather than three dimensions, which simplified the handling problem and reduces setup costs. These tows were subsequently formed in to a three-dimensional shape using matched dies or diaphragm forming. The composite parts produced by this novel process were of comparable static performance to the conventional fabric reinforcements.

In the manufacture of advanced composite parts where the application of carbon fiber fabric is prohibited by its high cost, fiberglass fabric is an ideal alternative. In the production of large scale composite structures, such as a wind turbine blade, and its supporting structures (spar cap and shear web), single large pieces (for example, 2m wide x 30m long) of fiberglass fabrics are placed into 3D molds.

Zhang and Sarhadi [29] proposed an integrated CAD/CAM system for automated composite manufacture, where the application of non-crimp fabric dramatically simplified the layup process. The high drapability of this fabric material allowed the preforms to be laid up flat and then conformed to the required 3D geometry as they are placed into the mold. This significantly reduced the complexity of automating the layup operation and removes 3D tools from the process. The process planning is therefore simplified to a tool surface coverage-oriented one. However, this system is not able to handle fiberglass fabrics, for which, in-plane shear is the dominant deformation mode when draped in to a complex 3D tool/mold surface.

Hancock and Potter [30] presented a strategy through which the information provided by kinematic simulation can be enhanced to produce unambiguous manufacturing instructions that can be passed onto the layup operator. The strategy relates experimentally determined layup rules to the designed tow alignment pattern and uses tow curvature to extract the dynamic behavior of the forming process. The preform is split up into regions of similar in-plane curvature and an order-of-drape is established for these regions. In addition, the out-of-plane tow curvature is interpreted to identify areas of the preform that are susceptible to bridging of the fabric across concave areas of the mold shape. This work provided an important linkage between the drape simulation modeling and layup process

planning. The drawback of this strategy is that only qualitative instructions could be obtained from the simulation model. Although these instructions will guide operators with clear smoothing and manipulating sequences toward the draped pattern obtained from the simulation, they cannot change the inherent disadvantage of the hand layup – lack of repeatability and consistency.

Reference

[1] Mohammed U, Lekakou C, Bader MG. Experimental studies and analysis of the draping of woven fabrics. Composites Part A. 2000;31:1409-20.

[2] Lin H, Wang J, Long AC, Clifford MJ, Harrison P. Predictive modelling for optimization of textile composite forming. Composites Science and Technology 2007;67:3242-52.

[3] Prodrodromou AG, Chen J. On the relationship between shear angle and wrinkling of textile composite preforms. Composites Part A. 1997;28(A):491-503.

[4] McBride TM, Chen J. Unit-cell geometry in plain-weave fabrics during shear deformations. Composites Part A. 1997;57:345-51.

[5] Lomov SV, Boisse P, Deluycker E, Morestin F, Vanclooster K, Vandepitte D. Full-field strain measurements in textile deformability studies. Composites Part A. 2008;39:1232-44.

[6] Long AC, Rudd CD, Blagdon M, Smith P. Characterizing the processing and performance of aligned reinforcements during preform manufacture. Composites Part A. 1996;27(A):247-53.

[7] Zhu B, Yu TX, Tao XM. Large deformation and slippage mechanism of plain woven composite in bias extension. Composites Part A. 2007;38:1821-8.

[8] Lomov SV, Willems A, Verpoest I, zhu Y, Barburski M, Stoilova T. Picture frame test of woven composite reinforcements with a full-field strain registration. Textile Research Journal. 2006;76(3):243-52.

[9] Potluri P, Ciurezu DAP, Ramgulam RB. Measurement of meso-scale shear deformations for modelling textile composites. Composites Part A. 2006;37:303-14.

[10] Potter K. In-plane and out-of-plane deformation properties of unidirectional preimpregnated reinforcement. Composites Part A. 2002;33:1469-77.

[11] Trochu F, Hammami A, Benoit Y. Prediction of fibre orientation and net shape definition of complex composite parts. Composites Part A. 1996;27A:319-328.

[12] Aono M, Breen D, Wozny M. Modeling methods for the design of 3D broadcloth composite parts. Computer-Aided Design. 2001;33(13):989-1007.

[13] Potluri P, Sharma S, Ramgulam R. Comprehensive drape modelling for moulding 3D textile preforms. Composites Part A. 2001;32:1415-1424.

[14] Dong L, Lekakou C, Bader MG. Solid-mechanics finite element simulations of draping fabrics: sensitivity analysis. Composites Part A 2000;31:639-52.

[15] Lin H, Wang J, Long AC, Clifford MJ, Harrison P. Predictive modelling for optimization of textile composite forming. Composites Science and Technology 2007;67:3242-52.

[16] Prodromou AG, Chen J. On the Relationship between the shear angle and wrinkling in textile composite preforms. Composites Part A 1997;28(A):491-503.

[17] Potter K. In-plane and out-of-plane deformation properties of unidirectional preimpregnated reinforcement. Composites Part A 2002; 33: 1469-1477.

[18] Morais DTS, Avila AF. A methodology for quality control evaluation for laminated composites manufacturing. Journal of the Brazil Society of Mechanical Science and Engineering 2005;XXVII(3):248-254.

[19] Ruth D, Mulgaonkar P. Robotic layup of prepreg composite plies. Proceedings of the IEEE international conference on robotics and automation, Cincinnati, Ohio 1990.

[20] Sarhadi M, Nicholson PR, Simmons J. Advances in gripper technology for apparel manufacturing. IMechE 1986;C372(86):47-53.

[21] Jarvis SDH, Wilcox K, Chen XQ, McCarthy R, Sarhadi M. Design of handling device for composite ply lay-up automation. Proceedings of ICAR, Pisa, Italy 1991.

[22] Chen XQ, Sarhadi M. Investigation of electrostatic force for robotic layup of composite fabrics. Machatronics 1992;2(4):363-373.

[23] Ozcelik B, Erzincanli F. Examination of the movement of a eoven fabric in the horizontal direction using a non-contact end-effector. The International Journal of Advanced Manufacturing Technology 2005;25(5):527-532.

[24] Lin H, Clifford MJ, Long AC, Sherburn M. Finite element modeling of fabric shear. Modelling and Simulation in Materials Science and Engineering 2009;17:015008.

[25] Campbell FC. Manufacturing technology for aerospace structural materials: Elsevier; 2006.

[26] Olsen HB, Craig JH. Automated composite tape layup using robotic devices. Proceedings of the IEEE international conference on robotics and automation, Los Alamitos, CA 1993.

[27] Longo E, Pandolfi Bianchi M. Modeling and simulation of a lay-up process of composite material tapes. Mathematical and Computer Modeling 1994;19(2): 43-54.

[28] Rudd CD, Turner MR, Long AC, Middleton V. Tow placement studies for liquid composite moulding. Composites Part A 1999;30:1105-1121.

[29] Zhang Z and Sarhadi M. An integrated CAD/CAM system for automated composite manufacture. Proceedings of the 12th international conference on computer aided production engineering 1996.

[30] Hancock SG, Potter KD. The use of kinematic drape modeling to inform the hand layup of complex composite components using woven reinforcements. Composites Part A 2006;37: 413-422.

CHAPTER 3. MEASUREMENT OF IN-PLANE SHEAR AND OUT-OF-PLANE DEFORMATIONS ON THE DRAPING OF DRY UNIDIRECTIONAL FABRICS

A paper to be submitted to *Composites: Part A*

Fanqi Meng[1], Matthew C. Frank, Frank E. Peters[2]

Abstract

This paper presents a methodology for the measurement of dry fiberglass fabric being used in large scale composites. Specifically, it provides a new approach to measuring individual tows of unidirectional fabric, in an effort to evaluate in-plane distortion versus out-of-plane waviness. This type of distortion is inherent to the process of placing rectangular-shaped bolts of fiberglass fabric onto three dimensional molds, as in the process of vacuum resin transfer molding, used in the manufacturing of wind turbine blades.

Current fabric distortion measurement approaches are limited by the lack of measurement instruments and techniques that are capable of consistently and precisely capturing 3D deformation of the fabric surface. In this work, modified laser scanning methodologies were developed and utilized in order to obtain the out-of-plane deformations generated during the draping of fabric in a mold. Meanwhile, the deviations of individual tows of fabric were isolated, which allowed for the computation of shear angles between adjacent fiber tows with the resolution at tow width level. This technique represented the out-of-plane deformation of the fabric surface as deformations of individual fiber tows, which

[1] Primary researcher and author
[2] Author for correspondence

will facilitate characterizing the unit-cell behavior of fiberglass fabric under both in-plane and 3D out-of-plane deformations.

The overarching goal of this study is to provide an experimental method and an analysis procedure that will enable more advanced wrinkle prediction software tools, that are capable of simulating the out-of-plane deformations during the draping process. The method also has direct potential to provide real-time quality and process control for future automation technologies in wind turbine blade fabric layup.

1. Introduction

Composite material has long been the choice for the aerospace industry due to its superior material properties, such as high strength-to-weight ratio, corrosion resistance, long fatigue life, and the ability to tailor layups for optimal strength and stiffness. Due to these advantages, composite material has been widely applied in the rapidly growing wind energy manufacturing industry in recent years. Typical manufacturing processes involved in the fabrication of composite parts include vacuum forming, compression molding, vacuum resin transfer molding (VRTM), automated tape laying (ATL), filament winding, etc. Among these processes, VRTM plays the most important role in the manufacturing of wind energy components, due to the fact that the majority of wind turbine blades and the supporting structures, i.e. spar caps, shear webs, are fabricated using this process.

Fabric layup is a step that is performed prior to the VRTM process, where layers of fabric panels are placed into the mold. During layup, in-plane shear deformation, or trellising occurs when the fabric panels are smoothed to conform to the three dimensional mold surfaces or offsets of tool surfaces (laying on top of other fabric plies). When deforming, the

fabric material behaves as a pin-jointed net [1]. Therefore, if the local in-plane shear angle is beyond the shear locking angle of the fabric, buckling or out-of-plane deformation will occur [2-4]. The out-of-plane deformation typically results in excessive fabric material covering the region on the mold where it occurs and induces wrinkling when vacuum is applied during the resin transfer stage. This wrinkling defect is the primary cause for fiber waviness, which will reduce the strength and fatigue endurance of the composite parts. Thus it is of great importance to plan and control the layup process, in order to manufacture defect-free composite parts.

Prior to the implementation of the layup process, a feasible process plan is critical to ensure the quality of the parts to be manufactured. Such a plan should include the starting position and orientation of the fabric panels, the constraints to be applied, and the specifications on the sequence of smoothing operations. The feasibility of the plan is usually evaluated utilizing draping simulation software packages. Typically, draping simulations involve iterative methods on the computation of the unit cell shapes in order to predict the overall draped shape of the fabrics onto specific 3D tool surfaces. These methods vary from purely kinematic approaches [5], to more sophisticated finite element analysis [6]. Some of these approaches have been integrated into commercial software (For example, FiberSIM and QuickForm). However, a common assumption shared among these simulation methods is that the fabric panel is always conforming to the mold surface. This assumption ignores the phenomenon of out-of-mold deformation that could happen in the situation where the local shear angles are beyond the shear locking limit of the material. With this assumption, the prediction of the shear angle distribution may not be accurate. Therefore, using such type of draping simulations to evaluate a process plan could be error-prone. It is desirable to have the

draping simulation software to be capable of predicting out-of-mold deformations, in order to provide reliable assessment on the feasibility of a given layup process plan. The development of such software requires the integration of the mechanism on the interaction between in-plane and out-of-plane deformations, and the abstraction of such mechanism must be from the measurement data. Therefore, a measurement system providing consistent and reliable data of the in-plane and out-of plane deformations in the way that facilitates the abstraction of the mechanism is of great importance.

As a second approach, process control has been widely recognized as necessary in the manufacturing of composite materials [7]. Position and orientation of the delivery head are constantly monitored and controlled to ensure the accuracy of the Automated Tape Layup (ATL) process [8]. In addition, other control methodologies were developed for the VRTM process. Nalla et al. [9] developed a vision-based close loop control system, which utilized the real-time resin coverage information to determine the status of the resin flow, in order to guarantee a reliable resin infusion process. A model-assisted feedback control algorithm was implemented by Dunkers et al. [10] to control the curing stage during the VRTM process. Comparing with the wide applications in ATL and VRTM processes, feedback control is rarely applied in the layup process. While it is challenging to design the actuators that are able to feed and precisely place large pieces of fabric into 3D molds, lack of appropriate means of sensor to detect real-time fabric distortion brings more difficulty to the implementation of a feedback system. In such a system, the fabric's in-plane and out-of-plane deformations should be constantly monitored, and compared against the ideal process output. Based on this feedback information, the system makes adjustments to the current process parameters, in order to keep the deformations and deviations of the fabric panels

within the specified tolerance. Such type of system requires real-time, high precision measurement data on the fabric deformations.

The present study aims to develop a measurement methodology and an analysis procedure as a tool that is capable of providing consistent measurement data on the in-plane and out-of-plane deformations of the fabric panels draped into 3D mold surface, with the resolution at the fabric tow width level. This tool will help the understanding the mechanism of the interaction between in-plane and out-of-plane deformations during the layup process, enabling the development of draping simulation software packages that are capable of predicting out-of-plane deformations of the fabrics, which will provide more reliable and precise layup process plans. On the other hand, the tool developed in this paper could be directly utilized as a sensor to provide fabric distortions as feedback information to the control system, enabling the realization of the automated fabric layup system.

2. Related Work

In previous researches, various methods had been developed to measure fabric distortions, especially the in-plane shear deformations occurred in the draping process. The first and perhaps the most basic type of measurement methods is manually tracking the distorted grid, inscribed prior to the draping process [4, 11]. This type of technique is usually laborious and lack of repeatability, because each of the individual grid elements has to be traced, and the diagonal lengths had to be manually measured using protractor, in order to calculate the local in-plane shear angle. The resolution of this measurement technique is low. Lin et al. reported the grid size of 10mm, while Mohammed et al. used the grid size of 18mm.

As the second category of measurement approaches, digital camera and image analysis were widely utilized in the work of fabric deformation studies [2, 3, 12-15]. This technique is applicable to both 2D and 3D measurement situations. For 2D measurement case, typically involved in the bias extension test or picture frame test, a single camera is required to be positioned perpendicular to a flat surface. The acquired digital image was analyzed using digital image correlation (DIC) method, in order to obtain both qualitative and quantitative information on the heterogeneous deformation on the fabric surface. In the case of 3D fabric deformation measurement, usually seen in the draping and forming processes [12, 13], it is required to use two cameras simultaneously or use one camera and capture two images of the fabric distortion from two difference known positions. Comparing with the manual measurement method, the digital camera and image analysis method is contactless, which eliminates the possible distortion introduced during the measurement process. It also has much higher resolution and repeatability. However, its major drawbacks are: (i) light reflections can corrupt the measurements at certain places [12] (ii) at high magnifications, as the fabrics undergo large deformations, it is difficult to keep the camera focused on a specific area [16].

The third type of measurement method was develop by Potluri et al. [16], where flat-bed scanner was utilized to capture the unit cell deformations across the fabric in the bias extension test. In their work, points of tow interlacements were traced manually within the scanned image, in order to calculate the shear deformations. The advantages of this method are: (i) it eliminated the fabric inscription process, which is required (or partially required) in the previous two methods (ii) comparing with the digital camera method, this method has

significantly larger measurement area. However, this method could only be applied in 2D measurements, due to the capability of the flat-bed scanner.

3. Overview of the Solution Approach

The overarching goal of this research is to provide a measurement solution to the in-plane shear and out-of-plane deformations of a fabric piece draped onto 3D shaped mold. Particularly, this study focuses on the measurement of UD fabrics, because this category of fiberglass material has wide application in the wind energy manufacturing industries, primarily providing flap-wise bending and tensional loads. The entire measurement and analysis process consists of four parts: fabric preparation; laser scanning; individual fiber tows extraction; and calculation of the deformations.

In the fabric preparation step, a special pattern in black color was painted onto the fabric surface, with the purpose of modifying the regional reflectivity properties, in order to facilitate the fiber tow extraction and the calculation of shear angle distributions between each pair of the extracted fiber tows. The painted fabric region was then measured by using 3D laser scanning. The output of the laser scanning system is a single point cloud file, or a collection of multiple point clouds (in the case of large scanning area), which can be registered into a single point cloud.

After the scanning process, the individual fiber tows were extracted from the acquired point cloud. This extraction process included two steps. The first step was the segmentation of the point cloud, where the point cloud was separated into multiple sub point clouds, with each one containing the points representing a single fiber tow. These point clouds were filtered in the second step, in order to reduce noise introduced during the scanning process.

The extracted fiber tows were fitted to 3D curves, so that each of them had unique and continuous mathematical representation. Out-of-plane deformations of individual fiber tows were computed by tracing their change in 3D coordinates following the direction of the fitted curve. In-plane deformations were computed sequentially by tracking the local unit cell deformations between the neighboring pair of fiber tows.

The measurement and analysis processes are summarized in Figure 1, and the details of each part are presented in detail in subsequent sections.

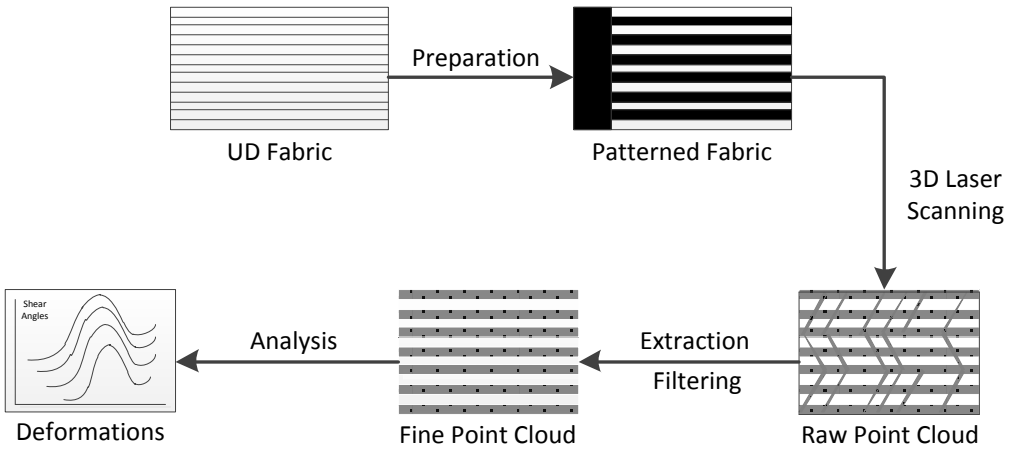

Figure 1. Overall Procedure.

4. Methodology

4.1 Fabric preparation and laser scanning

Prior to the layup process, the UD fabric piece (SAERTEX U14EU920, see Table 1 for specifications) was placed onto a two dimensional flat surface. A special pattern in black color was painted onto the fabric surface, aiming to create virtual boundaries for individual fiber tows, so that the measurement could reveal the behavior of these tows, rather than the

original fabric surface. The pattern was made according to the following procedure. A thick straight segment orthogonal to the fabric tow direction was drawn in the first place, serving as the starting line. Then from the starting line, along the fabric direction, every other fiber tow was painted in black. It is worthwhile to point out that the black paint material has to completely fill the target tows, in order to create clear and precise boundaries for the unpainted tows. Such painted pattern is shown in Figure 2.

Table 1. Properties of experiment UD fabric

Parameters	***Values***
Fabric width (mm)	*200*
Yarn width (mm)	*3.81*
Fabric area density (g/m^2)	*930*

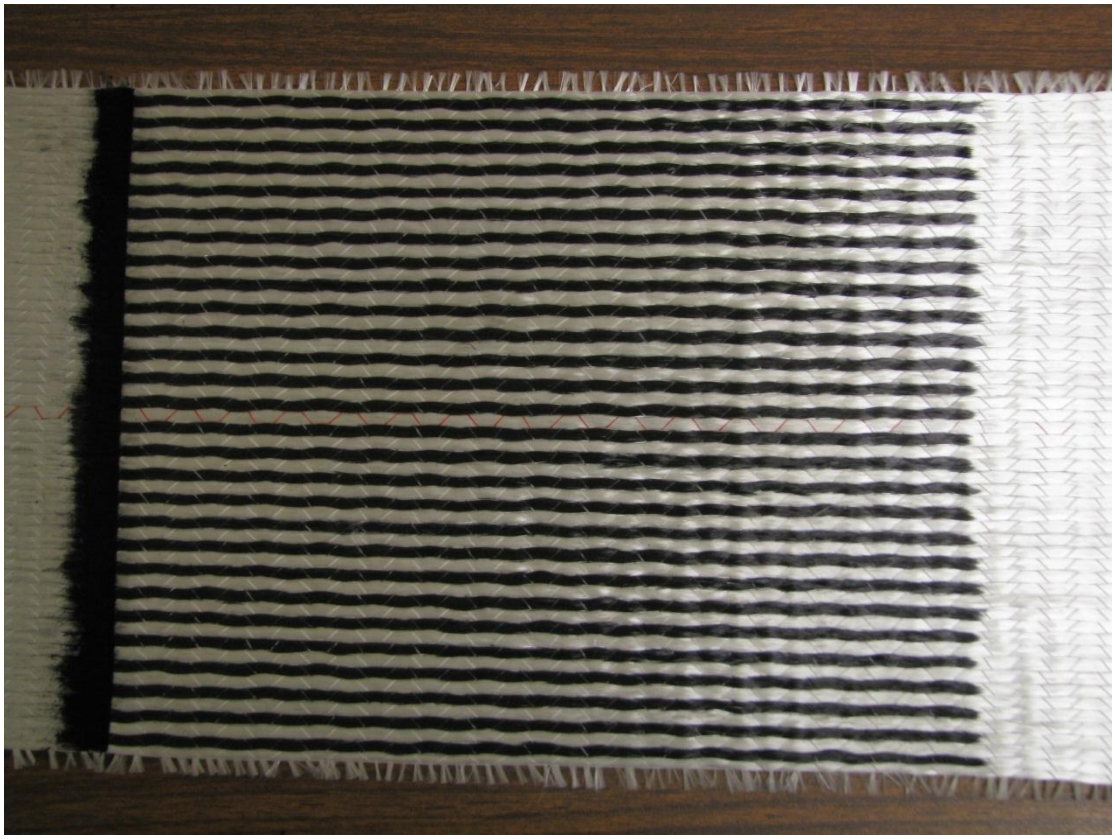

Figure 2. Painted UD fabric.

The laser scanning system consisted of a three-axis motorized linear motion table and a 3D laser scanner (Optix 400L, 3D Digital Corp., see Table 2 for specifications). Figure 3 shows the setup of this measurement equipment. The standard output of the scanner is a point cloud file. Depending on the size of the scanning region, multiple scans may be necessary, resulting in multiple point clouds. In such case, the multiple outputs were registered into a single point cloud file. The effect of the painted pattern was that within the painted region, the painted tows will absorb the laser, while the unpainted tows were laser-reflective, so that they could be captured by the 3D laser scanner and separated by the painted pattern. Figure 4 shows the acquired point cloud of a fabric surface with painted pattern. In this initial work, the pattern was painted on to the fabric surface manually. However, such pattern can be created automatically at the UD fabric production stage, by weaving alternatively arranged bundles of white and black fibers.

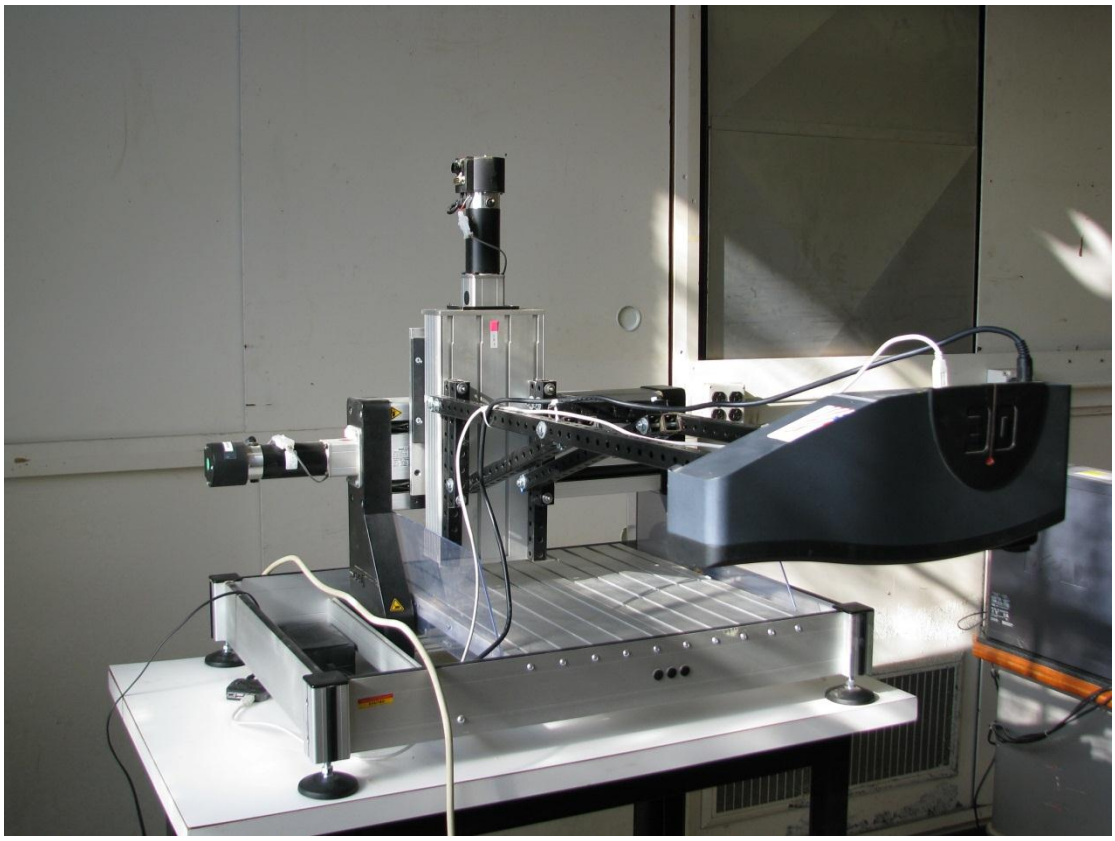

Figure 3. Laser scanning measurement system.

Table 2. Specifications of the 3D laser scanner (Optix 400L, 3D Digital Corp.)

Parameters	***Values***
Resolution (inch)	*0.007*
Standard deviation (inch)	*±.0008*
Depth of field (inch)	*12~36*
Point density	*Up to 1000 x 1000*
Field of view (deg)	*30*

4.2 Extraction of individual fiber tows

The point cloud obtained from the scanning process was separated into sub point clouds, with each representing an individual fiber tow. An algorithm has been developed to

automate this extraction process. The algorithm consisted of three stages: point cloud re-orientation, rough segmentation and noise filtering.

4.2.1 Determination of UD fabric orientation

The 3D point cloud could be separated by series of planes that are parallel to the local orientation of the fiber tows. By projecting the 3D point cloud on to the plane perpendicular to the nominal normal direction ($\vec{n}_0$) of the fabric surface, this 3D problem was simplified to the determination of the separation lines for the projected point cloud within two dimensional space. The fabric's nominal normal direction is calculated by

$$\vec{n}_0 = \sum_{i=1}^{m} \vec{n}_i / m \tag{1}$$

where $\vec{n}_i$ is the local normal direction at the point i, and m is the total number of points within the cloud. The following analysis was done within the projection plane.

Generally, for a piece of projected UD fabric, each fiber tow may have its own orientation, and the value varies within a small range throughout its length. However, a common representative orientation can be found, which is within the overall range of local orientation of the individual fiber tows. This representative direction was utilized for the raw segmentation process.

A randomized search band technique was developed to determine the representative fabric orientation. As shown in Figure 4, a search band was defined by the positioning point p, the direction α, and the band width b. Inclusion test was applied to determine the group of points that were within a particular search band. The included points were projected onto the center line of the search band, and the distances between the neighboring projected points

were calculated. These distances were compared against a threshold value t. The number of distances greater than t was recorded as Nt. Thus, for a particular search band, Nt was a function of the direction α. A number of M points within the cloud were randomly selected as the positioning point of the searching band. The objective was find the solution of α_{rep}, for the optimization problem:

$$\text{minimize } \sum_{i=1}^{M} Nt_i(\alpha), \text{ subject to } \alpha \in [-90^0, 90^0]. \quad (2)$$

The reason for picking multiple positioning points was that solving the optimization problem at a single position could result in erroneous solution. For example, in Figure 4, a search band in 45^0 with positioning point A and band width less than the fiber tow width will result in $Nt = 0$. Although the objective of minimizing $Nt(\alpha)$ is fulfilled at this single point, the solution 45^0 deviates significantly from the actual fabric orientation. By summing up the Nt 's at different positions, this type of error could be prevented. The second reason of using multiple positioning points is that the goal here is to find a global optimal orientation across the whole fabric, rather than a local orientation specific to any single fiber tow.

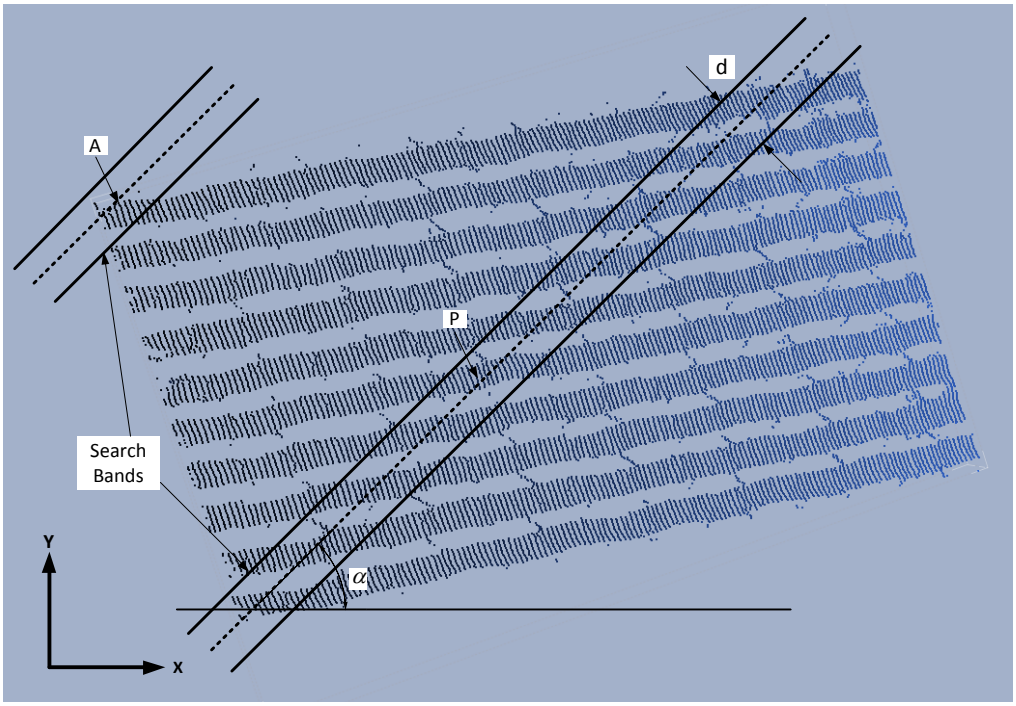

Figure 4. Acquired point cloud and search bands.

The 200mm width UD fabric (SAERTEX, other properties as specified in Table 1.) was utilized as the measurement target in this study. For this specific UD fabric material, the following values of the parameters were selected in the searching process of the representative fabric angle: band width $b = 0.15inch$; in-band threshold distance $t = 0.05inch$. Within the range of $[-90^0, 90^0]$, a series of direction angles spaced by 0.1 degree were utilized as candidate fabric directions. The $\sum_{i=1}^{M} Nt_i(\alpha)$ value was calculated for all the candidate directions, with $M = 200$. The representative fabric direction is the direction that generates the minimum the objective function in (2). After the calculation of fabric direction α_c, the point cloud was turned by $-\alpha_c$, so that the fabric direction coincides with the Y-axis (Figure 5).

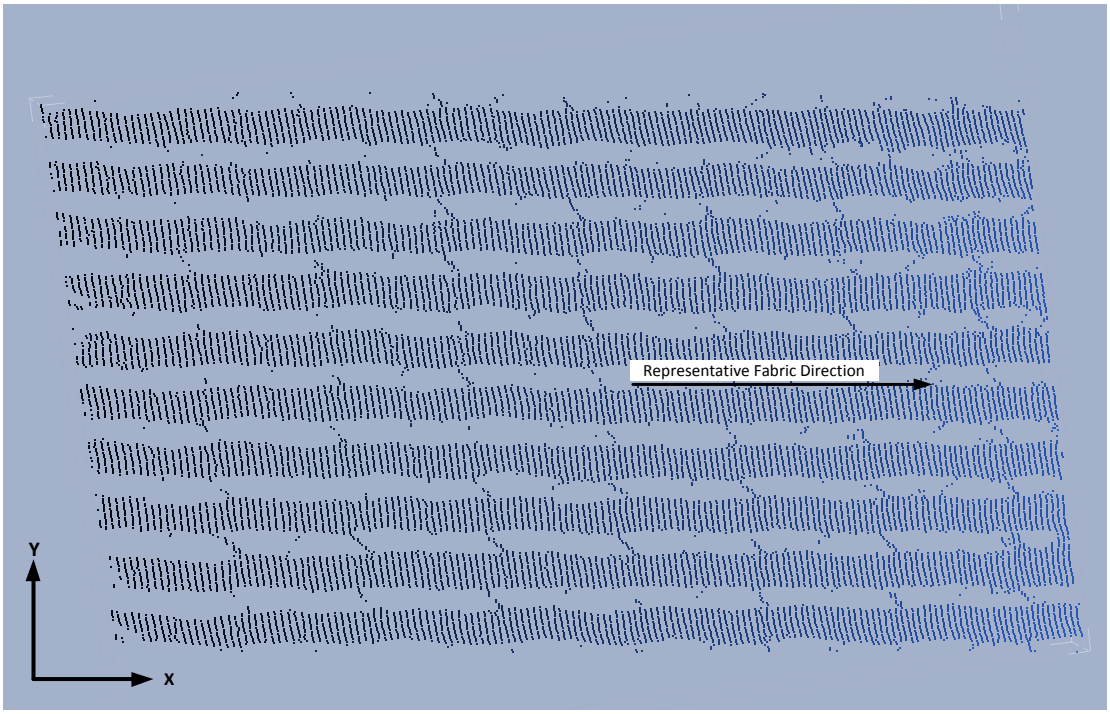

Figure 5. Re-Oriented point cloud

4.2.2 Fiber tow separation and noise reduction

The identification of the representative fabric direction facilitated the fiber tow separation process, because the directions of the separation boundaries generally follow the fabric direction. Here, fiber tow separation and noise reduction was achieved by a two-stage segmentation method sequentially applied to the point cloud, starting from the bottom edge. The first stage is raw segmentation. For the extraction of the first fiber tow, the lines $y = Y_{\min}$ and $y = Y_{\min} + 1.4 \times towwidth$ were used as lower and upper raw segmentation bounds, where $Y_{\min}$ was the minimum y coordinate value within the point cloud, and *tw* was the tow width of the fabric.

It can be seen in Figure 5 that noise points existed between the fiber tows, where was painted in black at the fabric preparation stage. Comparing with the points representing the

fiber tows, the noise points were of low density (number of points per unit area), because of the low reflectivity of the laser in the painted region. This relatively low density feature was utilized in the second stage, the fine segmentation process. Figure 6 shows a point cloud for a single fiber tow. ABCD was a rectangular box with fixed dimension and flexible position. The point density within the box, i.e. per area point quantity d, was a function of the position of the box: $d = d(x, y)$. With a fixed X coordinate, when this box traveled along Y direction, from raw lower segmentation bound to the raw upper segmentation bound, d will vary with the pattern shown in Figure 7. The reason for obtaining this pattern was that the box ABCD traveled from a noise zone to the fiber tow zone, and then to another noise zone. The local fiber tow zone was characterized by the sequence of Y coordinates with relatively high point density. Thus, an appropriate threshold value of point density t_d could be set, and by searching this threshold value from both the forward and reverse direction of Y, the local fine segmentation bound could be identified.

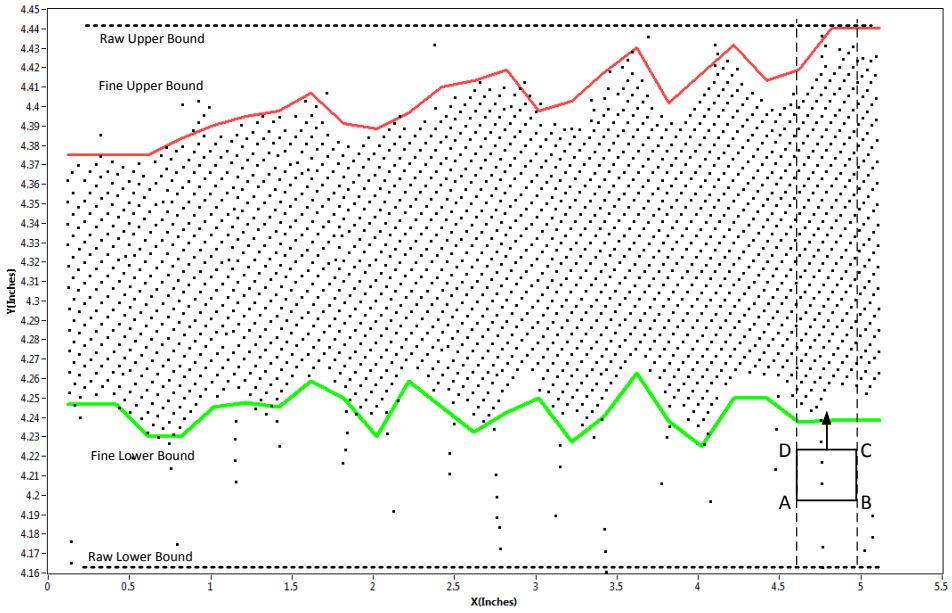

Figure 6. Single fiber tow segmentation.

By repeating the above procedure at different X coordinates, the corresponding local fine segmentation bounds can be found. These local bounds were connected to form the fine lower and upper bounds for the segmentation and noise reduction of a particular fiber tow.

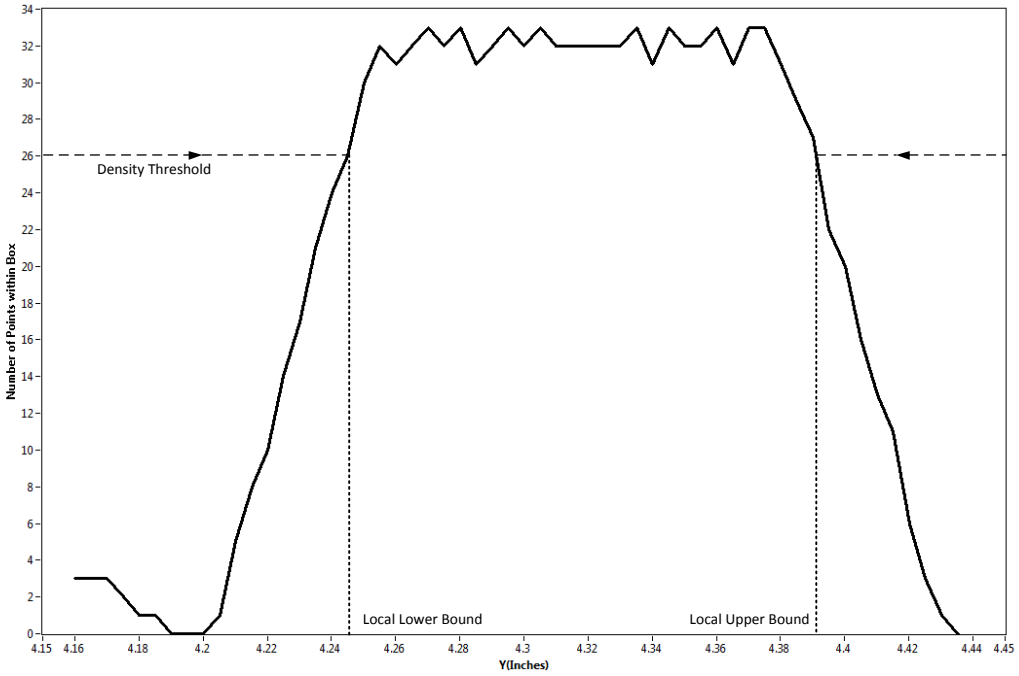

Figure 7. Determination of local segmentation bounds.

(This plot corresponds to the slice profile bounded by AD and BC in Figure 6.)

It can be seen in Figure 6 that the fine segmentation bounds changed their directions adaptively according to the shape of the fiber tow. The maximum Y coordinate of the fine upper bound was utilized for the raw lower segmentation bound for the next fiber tow to be separated from the remaining point cloud. This procedure was repeated until all of the individual fiber tows were extracted from the initial point cloud. The following parameters were used in the fiber tow extraction and noise reduction processes: box width, $AB = 0.2inch$; box height, $BC = 0.05inch$; horizontal box spacing, $\triangle h = 0.2inch$; vertical box spacing,

$\triangle v = 0.005 inch$; within box point density threshold, $t_d = 26$. Figure 8 shows the extracted tows from the point cloud in Figure 5.

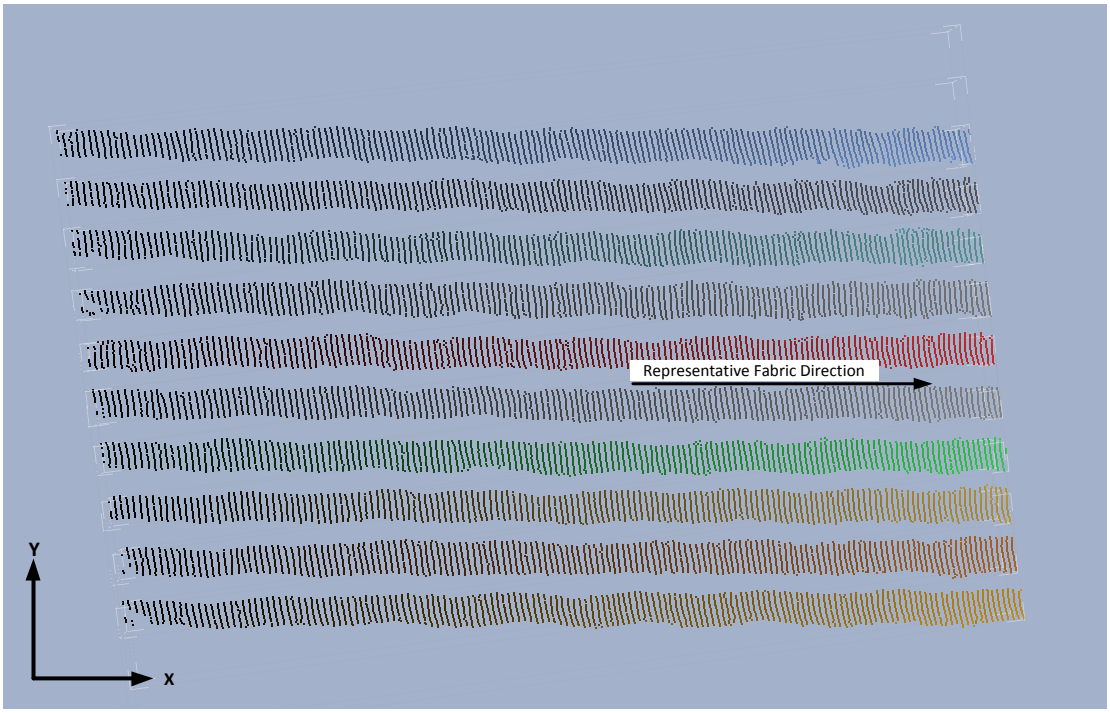

Figure 8. Extracted point clouds for individual fiber tows.

4.3 Calculation of out-of-plane and in-plane deformations

4.3.1 Out-of-plane deformation

In order to analyze the deformations among the fiber tows quantitatively, 3D spline curves were utilized to represent the skeleton of the fiber tows. These curves directly show the out-of-plane deformation of the fabric. It is seen in Figure 8 that the individual tows were of ribbon shape, running along the positive X direction. Due to this feature, the following method was developed to determine the local representative points for the curve fitting process. As shown in Figure 9, starting at the point with minimum X coordinate value, a series of planes parallel to the YZ plane were utilized to divide the point cloud. These planes

were equally spaced by distance d, so that each pair of neighboring planes formed a bin with width d. One representative point (c) was determined at each bin. In the i^{th} bin, let Ai be the collection of all the points within the i^{th} bin, then:

$$Xc_i = Min(X_{Ai}) \tag{3}$$

$$Yc_i = \frac{Median[Min(Y_{Ai}), Min(Y_{Ai+1}), Min(Y_{Ai+2})] + Median[Max(Y_{Ai}), Max(Y_{Ai+1}), Max(Y_{Ai+2})]}{2} \tag{4}$$

$$Zc_i = Median(Z_{Ai}) \tag{5}$$

After the identification of the control points, 3D spline curve was fitted to represent the out-of-plane deformation of the fiber tow.

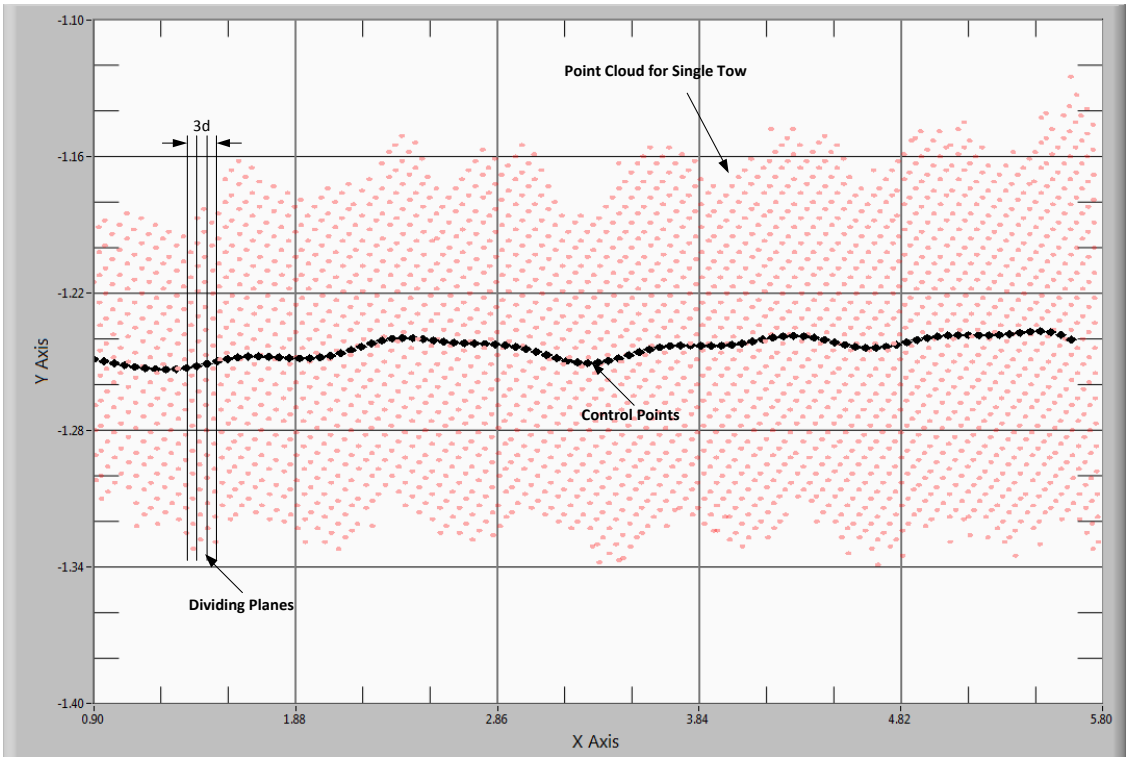

Figure 9. Determination of control points for a single fiber tow.

4.3.2 In-plane shear deformation

In-plane shear angles were calculated between any adjacent pair of fitted fiber tow curves. As shown in Figure 10, a and b were neighboring fiber tow curves; A_0 and B_0 were the starting points of the tows, respectively. $A_1, A_2, ..., A_k$, and $B_1, B_2, ..., B_k$ were nodes on a and b, such that the length of A_0A_i was equal to the one of B_0B_i ($i \in \{1, 2, ..., k\}$). At point A_i, the local shear angle was calculated as

$$\gamma = \pi / 2 - \measuredangle(\overrightarrow{T_{A_i}}, \overrightarrow{A_iB_i}) \tag{6}$$

where $\overrightarrow{T_{A_i}}$ was the tangent direction at A_i.

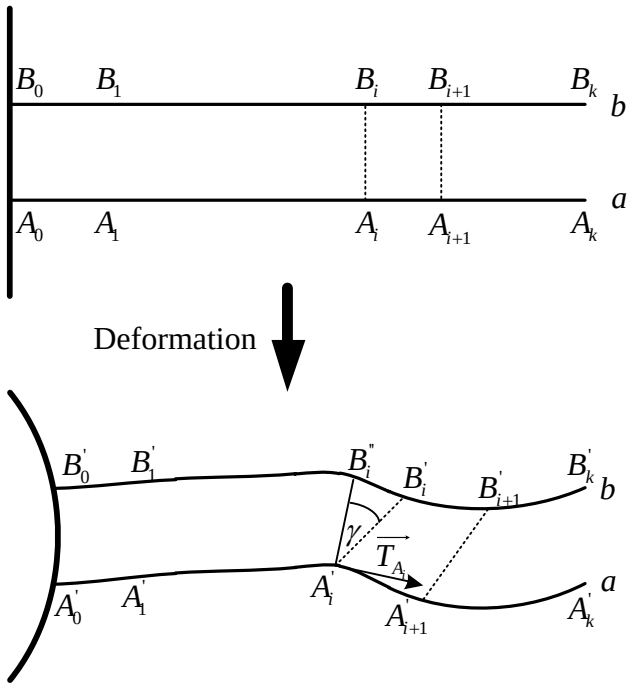

Figure 10. Calculation of in-plane shear angles.

5. Measurement Capabilities

5.1 Measurement accuracy and precision

Picture frame test is one of the most widely applied experiment procedure to characterize the shear behavior of the fabrics. According to Lomov [15], two assumptions are commonly made when analyzing the result from such test: 1) the shear deformation of the fabric sample is homogeneous, and 2) the average shear angle of the fabric is the same as the shear angle of the frame. Based on these two assumptions, the data on the difference of the measured average shear angle of the fabric and the shear angle of the frame could be used to analyzed to evaluate the accuracy and precision of the measurement method.

Figure 11 shows the picture frame tool utilized in this study. By turning the handle, the position of hinge A changed in the groove, which leaded to the change of the shear angle of the frame. The shear angle of the frame was traced by the digital protractor. The UD fabric sample was clamped on to the frame after the shear angle of the frame was adjusted to 0°. Laser scanning was performed when the shear angle of the framed was at 0°, 2.5°, 5°, 7.5° and 10°. This test procedure was repeated five times, with each one using a new UD fabric sample. The data correspond to the center $4\times 4 inch^2$ region of the UD fabric was processed to obtain the shear angle distribution. The differences of the average shear angles of the fabric, measured by the laser scanning method, and the shear angles of the frame were recorded and plotted as shown in Figure 12.

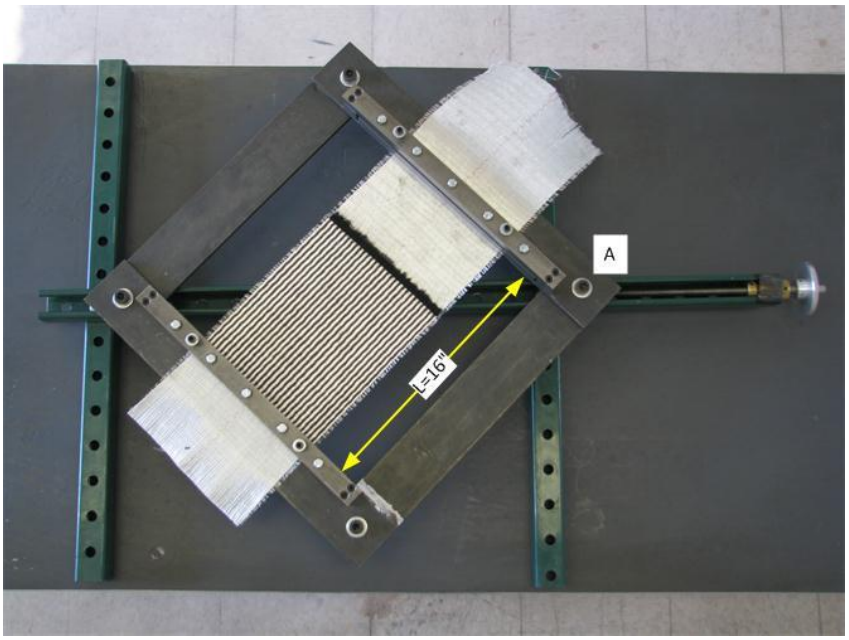

Figure 11. Picture frame device.

Figure 12. Difference of the average shear angle of the fabric, measured using laser scanner, and shear angle of the frame. Error bars indicate the standard deviation in five tests.

Note that the average shear angle of the fabric was consistently greater than the shear angle of the picture frame. This could be explained by the mechanism shown in Figure 13. When the picture frame was sheared, ideally, the fiber tows should be straight and located at the position defined by the head and tail clamping points. However, the fiber tows bent at the clamping regions. Such resistant bending effect reduced the shear angles at the clamping regions, and therefore increased the shear angles in the center part of the fabric. Similar observation was reported in "large sample configuration" case by Lomov et al. [12]. The standard deviation of the difference obtained from the five repetitions was comparable with the DIC method [12, 15].

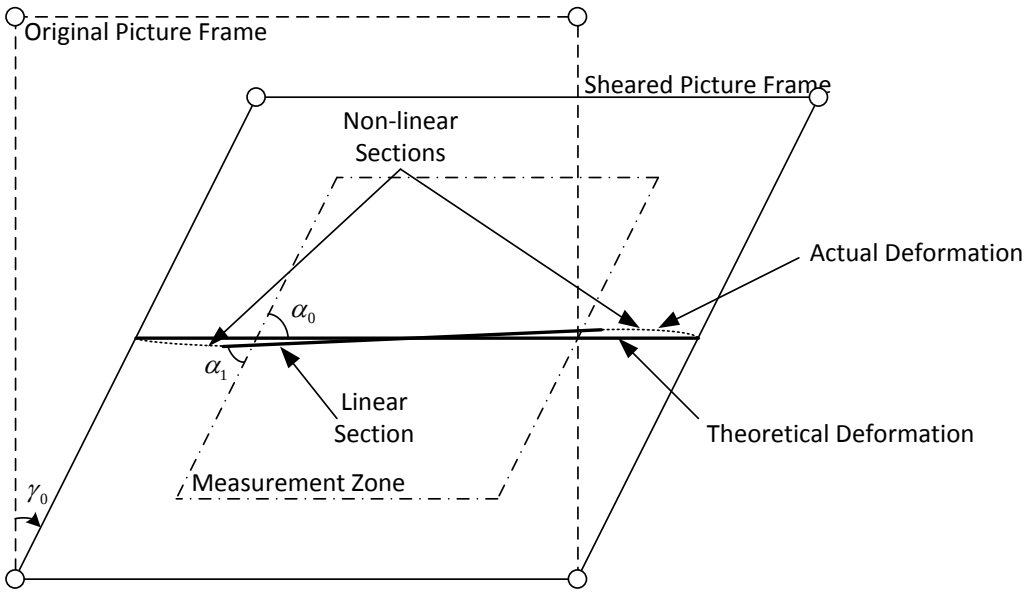

Figure 13. Deformation of fiber tows in picture frame test.

In order to verify the accuracy of the laser scanning method, digital protractor was utilized to measure the shear angle in the center part of the fabric. This direct measurement data was compared with the data obtained from the laser scanning method. As can be seen

from Table 3, the two methods show great consistency, indicating the adequacy of the accuracy of the laser scanning method.

Table 3. Comparison of measurement results between laser scanning and digital protractor methods.

Picture Frame Angle (deg)	*Laser Measurement (deg)*	*Protractor Measurement (deg)*	*Difference (deg)*
0	*0*	*0*	*0*
2.5	*3.15*	*2.96*	*0.19*
5	*6.274*	*6.32*	*-0.046*
7.5	*9.252*	*9.14*	*0.112*
10	*12.202*	*12.36*	*-0.158*

5.2 Measurement of deformations on 3D-shaped fabric

A mold was built for the measurement experiment. It has convex span-wise shape and concave chord-wise shape (See Figure 14 a and b for detailed dimensional specifications.). This surface was designed to resemble the actual surface of spar cap mold used in megawatt wind turbine blade manufacturing. Although the experiment mold was of shorter span, the curvatures chosen for both span-wise and chord-wise directions were more drastic than the mold in industry applications, in order to exaggerate the shearing effects.

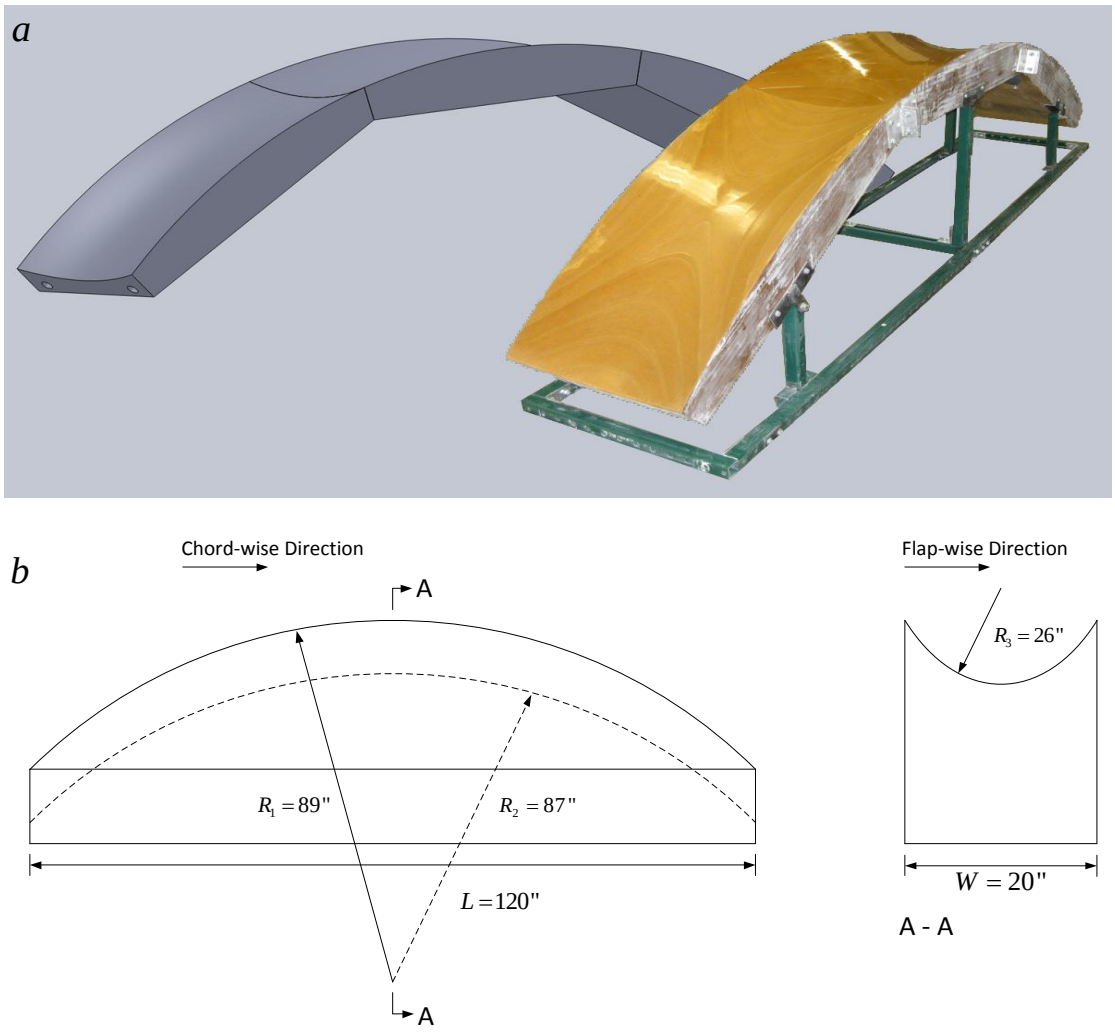

Figure 14. (a) 3D mold used in experiment; (b) mold dimensions.

As shown in Figure 15, the layup started at the constraint position. The UD fabric was smoothed along the chord-wise direction. The region with painted pattern prior to the layup was measured with the laser scanning system. The extracted individual fiber tows are shown in Figure 16 and in-plane shear angle distribution is shown in Figure 17.

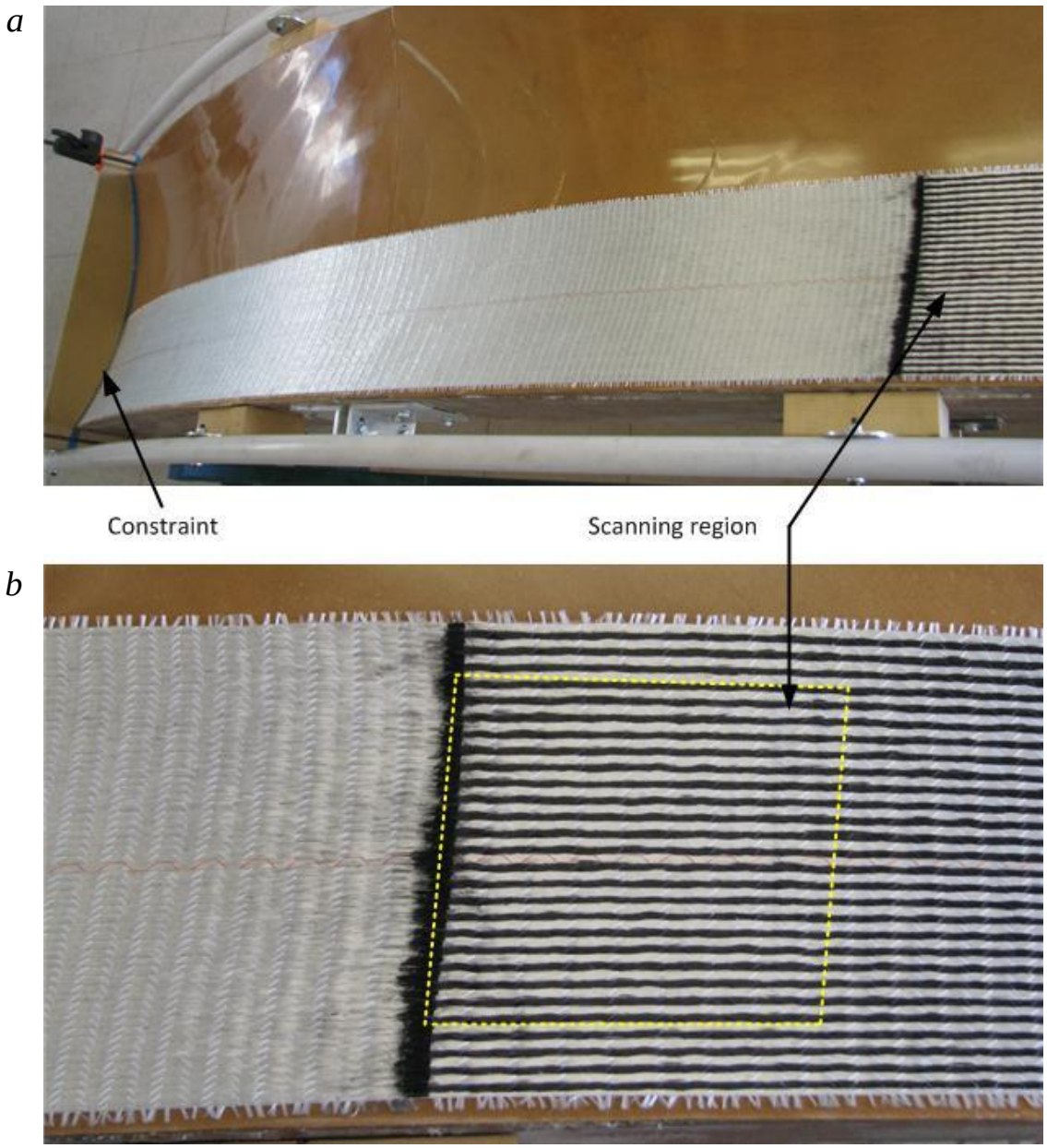

Figure 15. (a) Layup of 3D shaped fabric; (b) zoomed-in of painted region, the zone bounded by dashed lines is the measurement region.

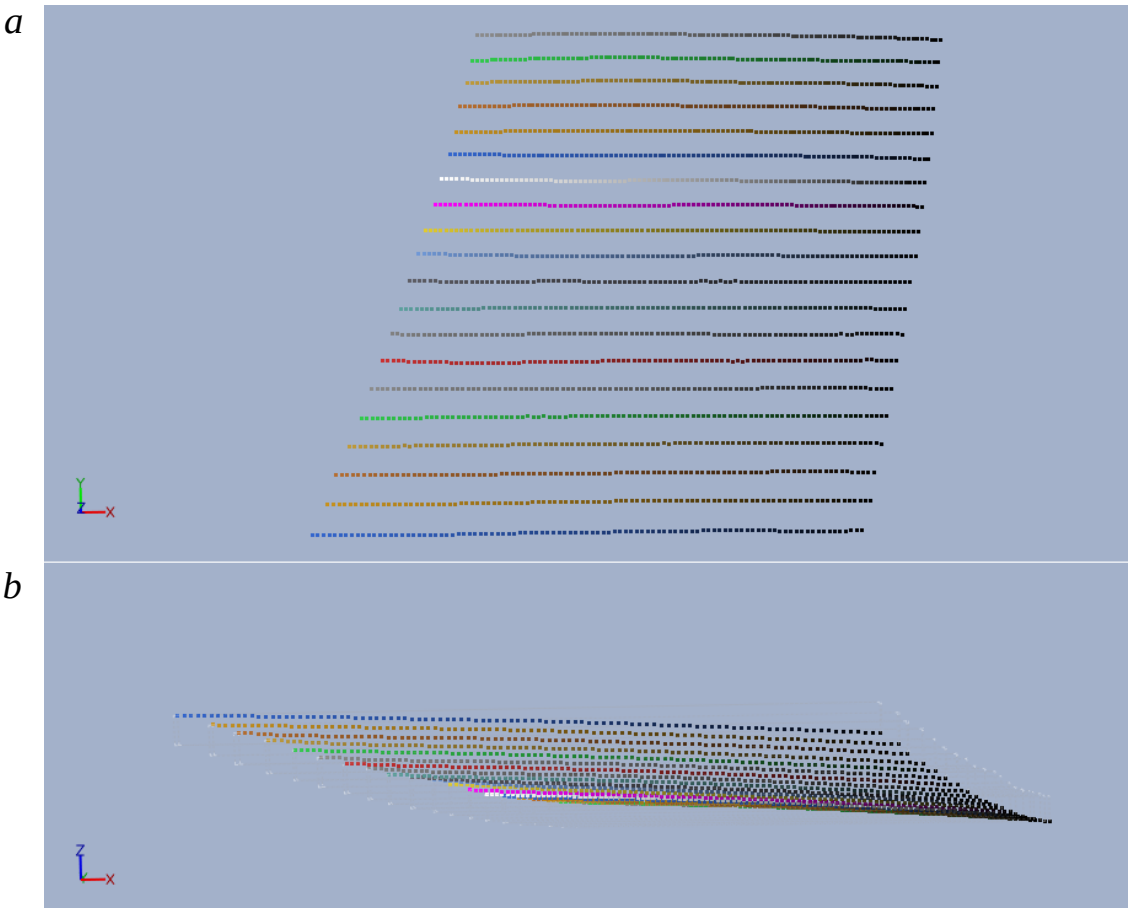

Figure 16. Extracted fiber tows (a) top view; (b) side view.

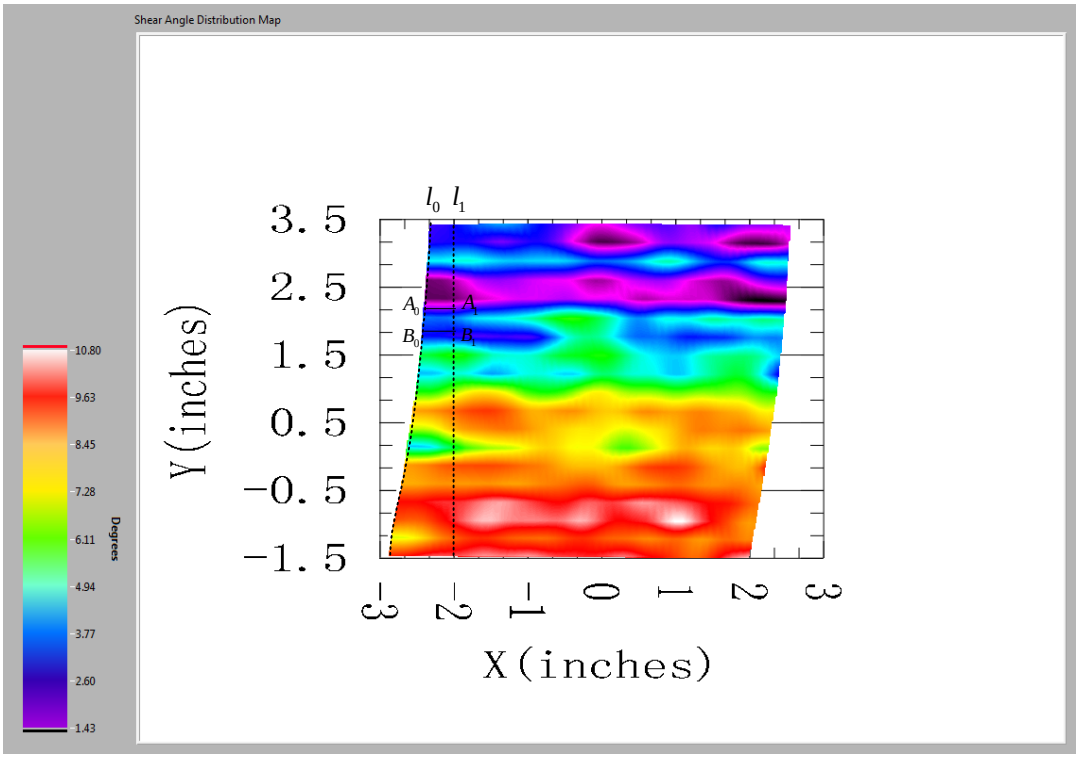

Figure 17. Measured in-plane shear angle distribution.

This direct local shear angle measurement was subsequently compared with an approximate analytical method of calculation of the shear angle. The shear angles along the curve l_1, which was the intersection between the plane of $x=-2$ and the fabric surface was verified. As can be seen in Figure 17, A_1 and B_1 are intersections of fiber tow a with l_1, and b with l_1, respectively. The shear angle between fiber tows a and b at location $x=-2$ was calculated as:

$$\gamma_{ab} \approx \frac{\pi}{2} - arc\tan\left(\frac{2\times w}{B_c B_1 - A_c A_1}\right) \tag{7}$$

where w was the constant fabric tow spacing distance; B_cB_1 was the curve length of fiber tow b, between the constraining point B_c and the point B_1; A_cA_1 was the curve length of fiber tow a, between the constraining point A_c and the point A_1. Because

$$B_cB_1 = B_cB_0 + B_0B_1 \tag{8}$$

where B_0 was the intersection between the painted starting line and fiber tow b, and

$$A_cA_1 = A_cA_0 + A_0A_1 \tag{9}$$

where A_0 was the intersection between the painted starting line and fiber tow a, and by the definition of starting line, we have:

$$B_cB_0 = A_cA_0 \tag{10}$$

Therefore, we have:

$$B_cB_1 - A_cA_1 = B_0B_1 - A_0A_1 \tag{11}$$

Thus, (7) was simplified as:

$$\gamma_{ab} \approx \frac{\pi}{2} - arc\tan\left(\frac{2\times w}{B_0B_1 - A_0A_1}\right) \tag{12}$$

Because the coordinates of A_0, B_0, A_1 and B_1 cloud be directly obtained from the output from the laser scanner, it is straightforward to approximately compute the shear angle between the two tows by (12).

The measurement in Figure 17 included twenty fiber tows, resulting in nineteen shear angles along curve l_1. The shear angle value between all the neighboring pairs of fiber tows calculated by (12) were plotted against the direct measurement values in Figure 18. The

agreement between the two methods indicated the adequacy of the laser scanning method on the 3D deformed piece of fabric.

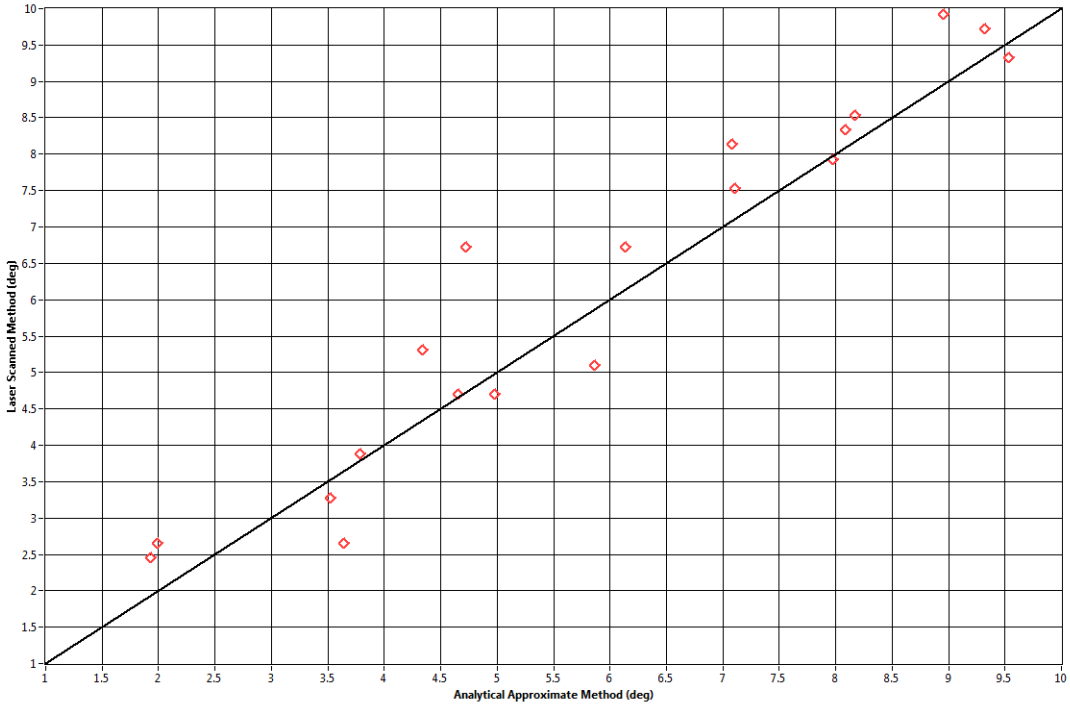

Figure 18. Plot of approximate analytical method against direct measurement data.

6. Conclusions

In this study, modified laser scanning system and analysis techniques were developed, with the capability of measuring the in-plane shear and out-of-plane deformations of UD fabrics at the resolution of between-tows level. Measurement capabilities were verified in both the picture frame test experiment and the draping experiment performed on a double curvature mold. Picture frame test data showed that this new measurement methodology achieved the same level of accuracy and precision in the case of measuring shear deformations of the 2D-shaped fabric, comparing with the existing DIC method. The

data from the 3D mold draping experiment demonstrated the capability of measuring in-plane shear deformations on a 3D-shaped fabric.

The measurement methodology developed in this research will have two fundamental impacts on the current layup procedure within the composite material manufacturing process. Firstly, the automated point cloud re-orientation, separation, noise-reduction and computation of deformations of fabrics realized in this research provide solution for a real-time fabric deformation checking module. This module is critical for a feedback control system employed in automated fabric layup, with the capability of monitoring and controlling the fabric distortions in real-time. Such a system is highly desirable, yet does not exist in the composite manufacturing industry. Secondly, the fine resolution and capability of measuring 3D-shaped fabrics achieved by this measurement methodology allows for further study on the relationship between in-plane shear and out-of-plane deformations at unit cell level. This relationship is essential for extending the capability of existing commercial fabric draping software packages to predict the out-of-mold deformations, which is required for more precisely validating the feasibility of a layup process plan.

Reference

[1] Potter K. In-plane and out-of-plane deformation properties of unidirectional preimpregnated reinforcement. Composites Part A. 2002;33:1469-77.

[2] Prodrodromou AG, Chen J. On the relationship between shear angle and wrinkling of textile composite preforms. Composites Part A. 1997;28(A):491-503.

[3] McBride TM, Chen J. Unit-cell geometry in plain-weave fabrics during shear deformations. Composites: Part A. 1997;57:345-51.

[4] Mohammed U, Lekakou C, Bader MG. Experimental studies and analysis of the draping of woven fabrics. Composites Part A. 2000;31:1409-20.

[5] Potter K. The influence of accurate stretch data for reinforcements on the production of complex mouldings. Part 1: deformation of aligned sheets and fabrics. Composites. 1979; July:161-167.

[6] Dong L, Lekakou C, Bader MG. Solid-mechanics finite element simulations of draping fabrics: sensitivity analysis. Composites Part A. 2000;31:639-52.

[7] Sih G. Advanced technology for design and fabrication of composite materials and structures: Dordrecht: Kluwer; 1995.

[8] Campbell FC. Manufacturing technology for aerospace structural materials: Elsevier; 2006.

[9] Nalla AR, Fuqua M, Glancey J, Lelievre B. A multi-segment injection line and real-time adaptive, model-based controller for vacuum assisted resin transfer molding. Composites Part A. 2007;38:1058-69.

[10] Dunkers JP, Flynn KM, Parnas RS, Sourlas DD. Model-assisted feedback control for liquid composite molding. Composites Part A. 2002;33:841-54.

[11] Lin H, Wang J, Long AC, Clifford MJ, Harrison P. Predictive modelling for optimization of textile composite forming. Composites Science and Technology 2007;67:3242-52.

[12] Lomov SV, Boisse P, Deluycker E, Morestin F, Vanclooster K, Vandepitte D, et al. Full-field strain measurements in textile deformability studies. Composites Part A. 2008;39:1232-44.

[13] Long AC, Rudd CD, Blagdon M, Smith P. Characterizing the processing and performance of aligned reinforcements during preform manufacture. Composites Part A. 1996;27(A):247-53.

[14] Zhu B, Yu TX, Tao XM. Large deformation and slippage mechanism of plain woven composite in bias extension. Composites: Part A. 2007;38:1821-8.

[15] Lomov SV, Willems A, Verpoest I, zhu Y, Barburski M, Stoilova T. Picture frame test of woven composite reinforcements with a full-field strain registration. Textile Research Journal. 2006;76(3):243-52.

[16] Potluri P, Ciurezu DAP, Ramgulam RB. Measurement of meso-scale shear deformations for modelling textile composites. Composites Part A. 2006;37:303-14.

CHAPTER 4. EXPERIMENTAL STUDIES AND ANALYSIS OF THE LAYUP OF UNIDIRECTIONAL FABRICS

A paper to be submitted to *Composites: Part A*

Fanqi Meng[1], Matthew C. Frank, Frank E. Peters[2]

Abstract

This paper investigates the manual layup of unidirectional fiberglass fabric. The mold used in this study was of non-developable three-dimensional shape, which includes the typical geometric changes that occur within megawatt scale wind turbine blades, but over a shorter span to facilitate efficient experimentation.

Due to the geometries of the mold, in-plane shear deformation occurred and some local values of the shear angles were exceeding the shear locking limit of the fabric material. It was observed that, under such conditions, waves (out-of-mold deformations) emerged on the fabric surface.

A theoretical analysis was conducted to understand the relationships among the geometry of the mold, in-plane shear angle distribution, out-of-mold deformation, and material properties of the fiberglass fabric. The results of the experiments also revealed the effect of the position of the starting constraint on the drapability of the fabric. These results provide important links between in-plane and out-of-mold deformations on the draped fabric surface, which are critical for the development of automated and optimized process planning tools for the layup of unidirectional fabrics.

[1] Primary researcher and author
[2] Author for correspondence

1. Introduction

Layup is a common manufacturing process where layers of fabric panels are placed into the mold and smoothed to conform to the mold geometry. This process is typically performed prior to the Vacuum Resin Transfer Molding (VRTM) in the manufacture of advanced composite parts. In order to achieve certain desired aerodynamic and strength characteristics, a large number of composite components are designed of complex geometries. The manufacture of these components requires layup over the molds of complex geometries, which makes it a challenging task. Typically, the molds are of three-dimensional (3D) and non-developable shapes (singly curved surfaces are referred to as developable), which induces the in-plane shear (IPS) deformation within the fabric surface, when the fabric ply is smoothed to conform to the mold surface.

Unidirectional (UD) fabric is one of the primary reinforcement materials for the manufacture of 3D structures. It offers better opportunities to optimize the strength to weight ratio of a component than offered by other types of fabrics, because the UD fabric allows the designer full freedom to set the directions of all fabric layers independently [1]. The UD fabric is characterized by the feature that the majority of tows run in one direction only. This relatively simple structure of UD fabrics results in limited capability in shear deformation. Comparing with bi-axial fabrics, the shear locking limits (SLL) for common types of UD fabrics are much less, which makes the layup process more challenging [2].

Computer-based layup simulation models have been widely applied as feasibility verification tools for the layup process. Typically, these models involve iterative methods on the computation of the unit cell shapes in order to predict the overall draped shape of the fabrics onto specific 3D tool surfaces. These simulation algorithms vary from purely

kinematic approach [3], to more sophisticated finite element analysis methods [4]. Some of these approaches have been integrated into commercial software packages (e.g. FiberSIM and QuickForm). These simulation tools are powerful in the evaluation of given layup plans. For feasible layup plans, where the in-plane shear angles of the draped fabric are within the SLLs, these simulation tools are able to provide accurate in-plane shear angle values and deviation of fiber orientation over the draped fabric surface. For unfeasible layup plans, however, the predicted results by these simulation tools are error prone. This is because a common assumption shared among these simulation methods is that the fabric is always conforming to the tool surface. This assumption ignores other deformation modes that could possibly emerge for the unfeasible case, when the local shear angles are approaching SLLs of the material.

Since current simulation tools are not able to accurately predict the layup process when local in-plane shear angles are beyond the shear locking limit, an alternative way to learn the behaviors of the fabrics under such conditions is by direct measurements in layup experiments. In the work by McBride and Chen [5], as well as Prodromou and Chen [6], the wrinkling mechanism was identified at the unit cell level by conducting bias tension tests and picture frame tests, respectively. They claimed that the in-plane shear deformation resulted in a continuously changing unit cell structure. If the fabric deformation was continued, local shear and in-plane compressive forces build up. This was compensated in the form of buckling or out-of-plane deformation. Neither of these tests are suitable to be utilized to infer the fiber tow behavior in the layup process, where the fiber tows are only partially constrained (as opposed to completely constrained in the bias tension and picture frame

tests). The unconstrained edges will provide the flexibility to allow the generation of other deformation modes.

In addition to the 2D material property testing type of experiments, researchers were also trying to understand the wrinkling mechanism from 3D deformation experiments, such as the forming process. In the work by Potter [7] and Lin et al. [8], the shape of the fabric material was initially flat. Then it was directly pressed by the punch tool into the die, without any draping or layup procedure involved. Mohammed et al. [9] conducted a forming experimented with a semispherical shaped lower male die, onto which the fabric material was placed. Then the upper female die was dropped upon the setup. This experiment was repeated for four different types of fabric materials, wrinkling was observed for three of them. For the unwrinkled part obtained from the forming process, the shear angle distribution from can be directly measured by some optical methods [10]. This distribution information is helpful for verifying the accuracy of the layup simulation models. In addition, by varying the forming process parameters, such as temperature and forming speed, or material types, it is possible to find an optimal combination of process conditions and material to produce wrinkle free parts. Such forming experiments, however, do not provide a quantitative link between the local shear angle and the emergence of wrinkling, because for a wrinkled region, it is impossible to measure the shear angle accurately.

The objective of this study is to explore different deformation modes and understand the mechanisms of the deformation and the relationship among these deformation modes within the layup process using UD fabrics.

2. Experiment

2.1 Material

Unidirectional fiberglass (SAERTEX U14EU920, see Table 1 for specifications) was utilized.

Table 1. Properties of experiment UD fabric

Parameter	***Value***
Fabric width (mm)	*500*
Yarn width (mm)	*3.81*
Fabric area density (g/m^2)	*970*
Shear Locking Limit (deg)	*16**

**Value obtained from picture frame test by the authors*

2.2 Equipment and measurement instrumentations

A mold was built for the layup experiment. It has convex span-wise shape and concave chord-wise shape. Figure 1 (a) and (b) shows its detailed dimensional specifications. This surface was designed to resemble the surface of spar cap mold used in megawatt wind turbine blade manufacturing. Although the experimental mold was of shorter span, the curvatures chosen for the span and chord directions were more drastic than the mold utilized in industry applications, in order to simulate the layup conditions and facilitate the identification of the fabric wrinkling problems.

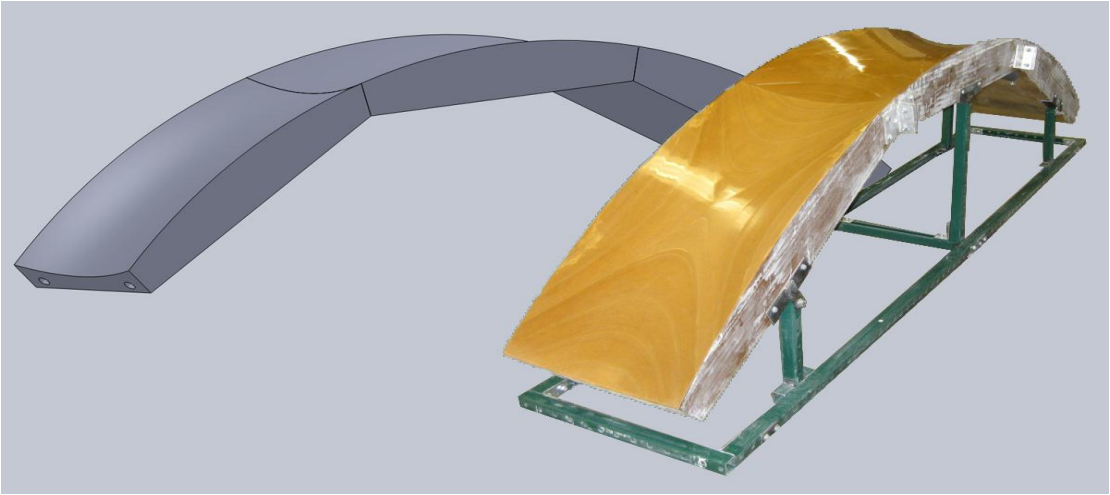

Figure 1. (a) 3D mold used in the experiment

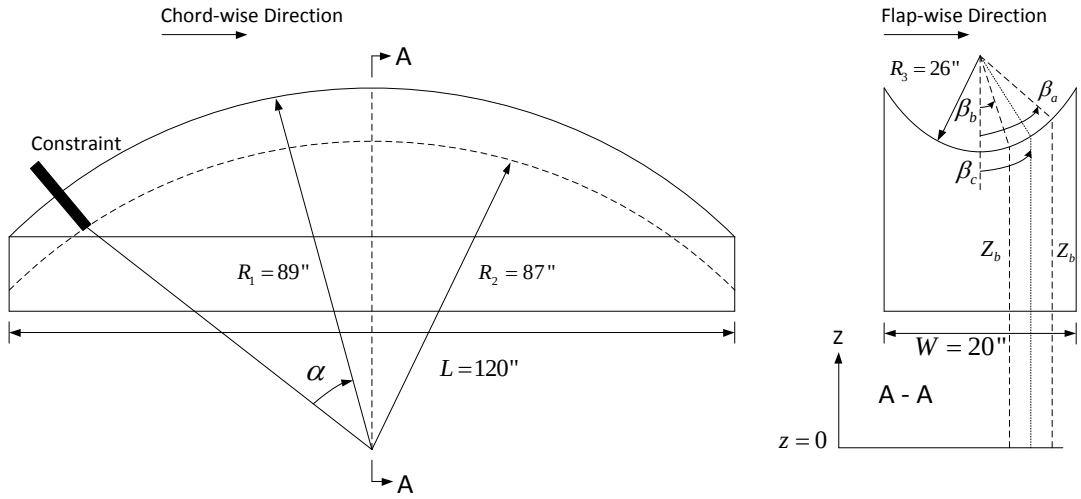

Figure 1 (b) Mold dimensions

An innovative laser scanning methodology developed by the authors [10] was utilized to capture three dimensional profiles of the mold surface, the fabric surface after layup, as well as the in-plane shear angle distributions.

2.3 Experiment procedure

As shown in Figure 2, a piece of UD fabric will be cut from the roll of the experiment material, with the length of 140 inches to cover the mold surface from -45 degree to 45

degree. This piece of fabric will be initially clamped with a constraining device at the -45 degree position, where all the fiber tows will be adjusted so that they are parallel to the local tangent direction of the centerline of the mold, and the center tow is positioned right on the centerline of the mold. Then the fabric will be smoothed along the direction of the centerline of the mold, until the 45 degree position was reached.

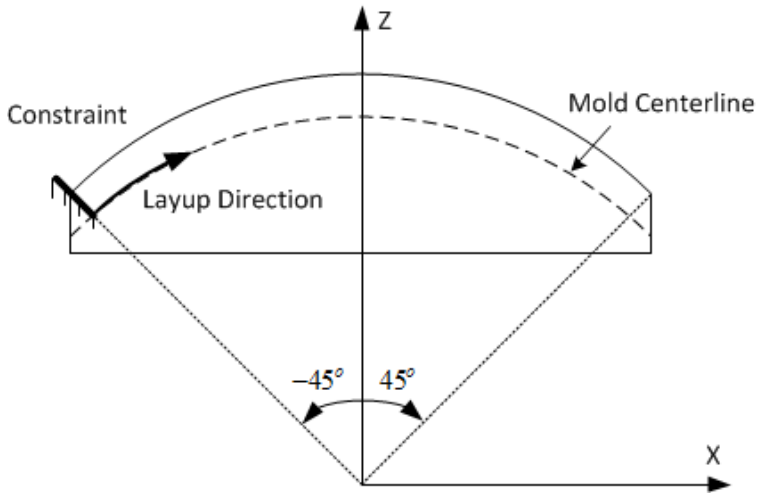

Figure 2. Layup plan

In order to collect data on the position and deformation of the fabric, the fabric was prepared prior to the layup. In the specific region of interest that is to be measured, a black line orthogonal to the fabric tow direction was drawn to serve as a starting line. Starting from this line and along the fabric direction, every other fiber tow was painted black. Such painted pattern is shown in Figure 3. The purpose of creating this pattern was that within the region, the unpainted tows were laser-reflective, so that they could be captured by the 3D scanner. Meanwhile, these unpainted tows were separated by the black pattern. Thus, later in the data processing stage, they could be individually extracted from the acquired 3D point cloud.

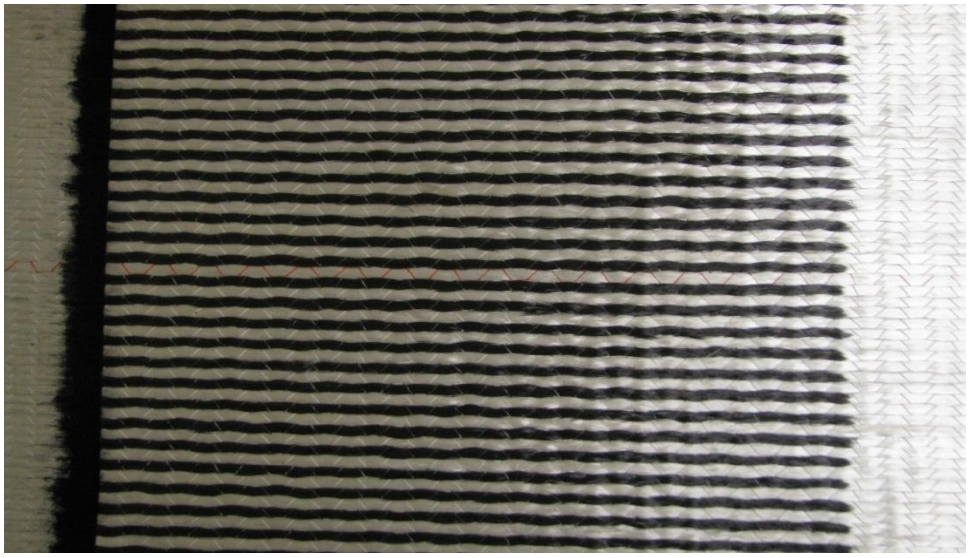

Figure 3. Fabric painting prior to the layup process

After preparation, the layup plan was implemented. The fabric piece was smoothed in a geodesic manner from this constraint toward the other end of the mold. As the smoothing progressed across the mold, out-of-mold (OOM) deformations (waves) occurred. These waves could not be further smoothed, because such operation would result in wrinkling of the fabric piece. Therefore, all the wave zones were left intact to allow the fabric to naturally bend and reach the mold surface again. The smoothing operation was continued when the fabric piece naturally returned to the mold surface after the wave zones. Figure 4 shows the fabric surface after layup. The region with waves was measured by the 3D laser scanner. This contactless device ensured that the shape draped fabric piece, especially the region of OOM deformation was not interrupted during the measurement process.

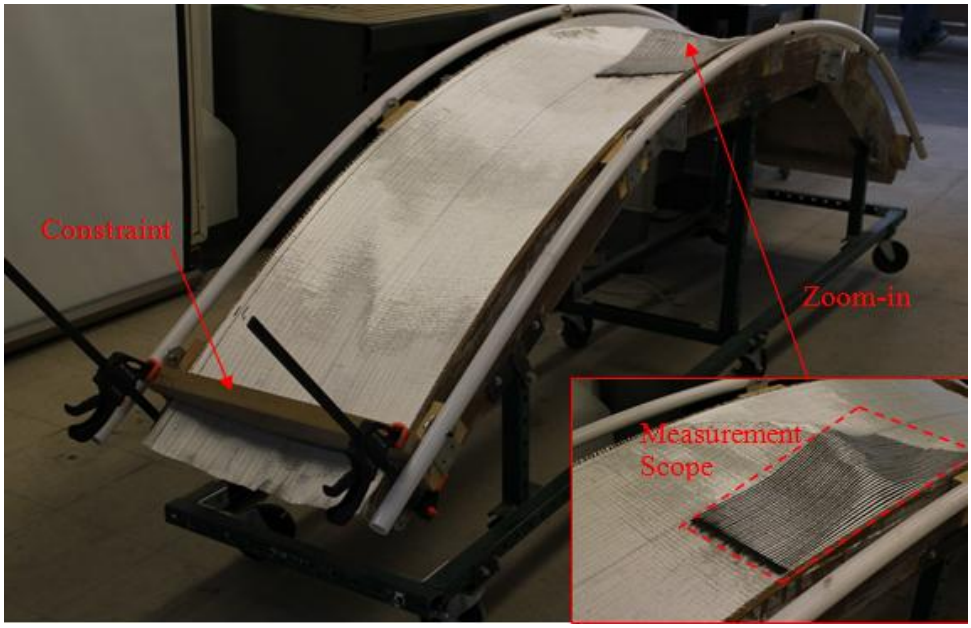

Figure 4. UD fabric layup result

3. Results

3.1 OOM deformation and its relationship with IPS deformation

There is a distinction between the out-of-plane (OOP) and the OOM deformations of fiber tows in the context of layup onto 3D mold surfaces. OOP deformation is inherent to the process of layup, when the mold is 3D, and the fiber tows are conformed to follow certain curved path of the mold. In layup simulations, the amount of OOP deformation at a given fabric node can be approximated by accounting for the angular difference between the actual tow trajectories and the tow trajectories projected on the plane, which is tangent to the mold surface at the given point [11]. OOM deformation happens when the fiber tow does not conform to the mold shape, and presents a waved shaped with respect to the mold surface. This type of deformation typically results in extra amount of fabric material covering a region of the mold surface, which can significantly increase the likelihood of the generation

of wrinkling defects when the vacuum is applied in the subsequent VRTM process. In addition, the shape of the OOM and the IPS distribution within the OOM region cannot be predicted by common simulation methods, and therefore, experimental measurements were made with the laser scanning technique [10] to quantify the deformation modes in this OOM region.

Because the mold geometry is symmetric about its centerline, and the layup direction followed this centerline, the resulted layup fabric surface was highly symmetric about the centerline, despite some local minimal deviations due to hand smoothing operations. Therefore, the measurement scope was limited to half of the OOM region (as shown in Figure 4), in order to facilitate the efficiency of the experimentation while providing sufficient data to characterize the relationship between different deformation modes over the entire OOM region. Figure 5 shows the raw point cloud data acquired by the measurement system, where the point cloud data representing the mold surface was acquired prior to the layup process. The distance between the mold surface and the fabric surface along the local normal direction of the mold surface was calculated, and is shown in Figure 6. The nominal fabric thickness was utilized as the threshold value. If the measured distance is less than the threshold value, the fabric is regarded as conformed to the mold surface, while being greater than this threshold value is considered as an OOM region. It can be seen in Figure 6 that a single OOM region was formed, which was bounded by the two dotted curves, Boundary I and Boundary II, respectively. The maximum positional deviation between the fabric and the mold surface was 2.35 inches within this OOM region.

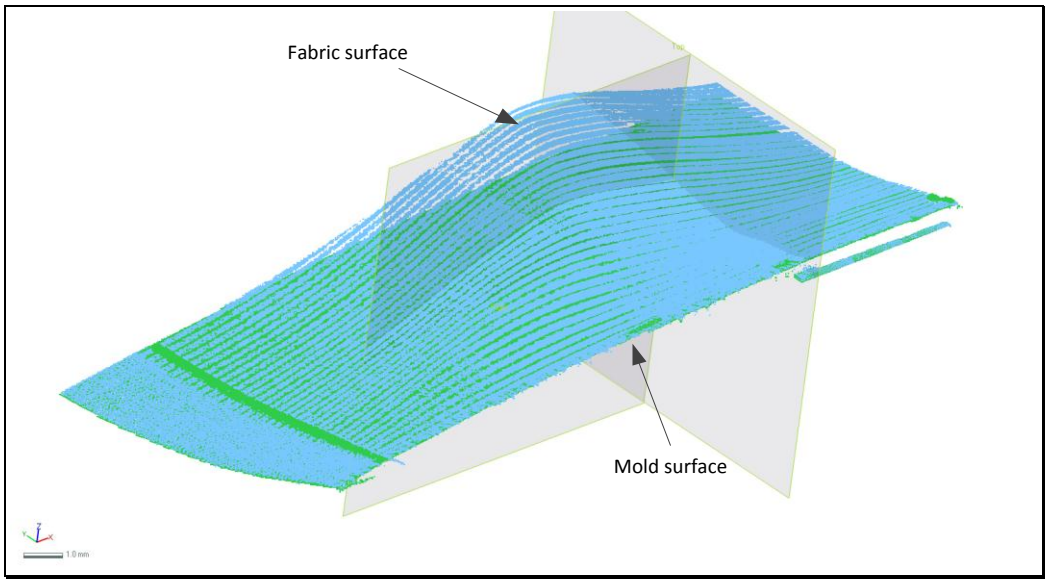

Figure 5. Point cloud representation of mold and fabric surfaces

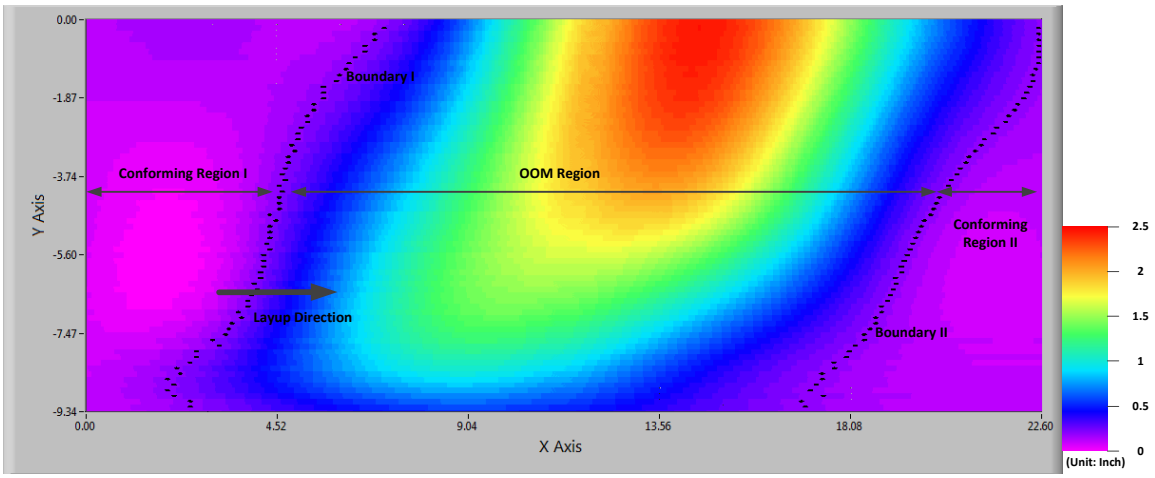

Figure 6. Positional deviation between fabric and mold surfaces

Positions of the individual tows were extracted from the point cloud, in order to find the IPS deformation within the measurement scope. Figure 7 shows that 34 tows were extracted within the measurement scope. These tows formed 33 tow pairs, where each tow pair consisted of two adjacent tows. Tow pair 1 was designated as the pair near the edge of the mold, and the index increased toward the center of the mold. The IPS angle values between each tow pair was calculated and are shown in Figure 8. Figure 9 shows numerically

the IPS angle values at the boundaries of the OOM region. It is seen in Figure 8 that the IPS angle reaches the shear locking limit (as given in Table 1) between the tow pairs near the edge of the mold (Location A). Also, within the OOM region, this location has the minimum distance from the starting constraint along the layup direction. Therefore, it can be inferred that the OOM is initiated at Location A, and the initiation is due to the reaching of shear locking limit of the fabric material. Similar effects were also reported in Prodromou and Chen [5], where OOP deformation occurrence was observed when the local IPS was beyond the shear locking limit, due to the build-up of the local in-plane compressive forces.

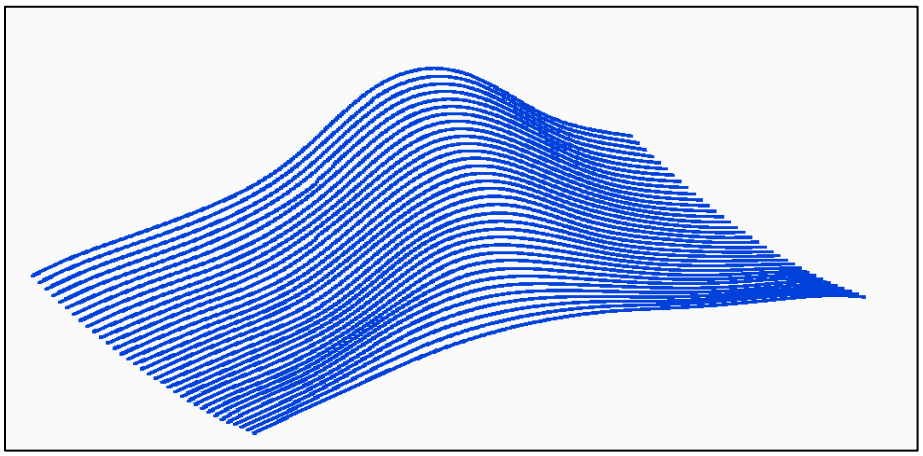

Figure 7. Extracted individual tows from point cloud

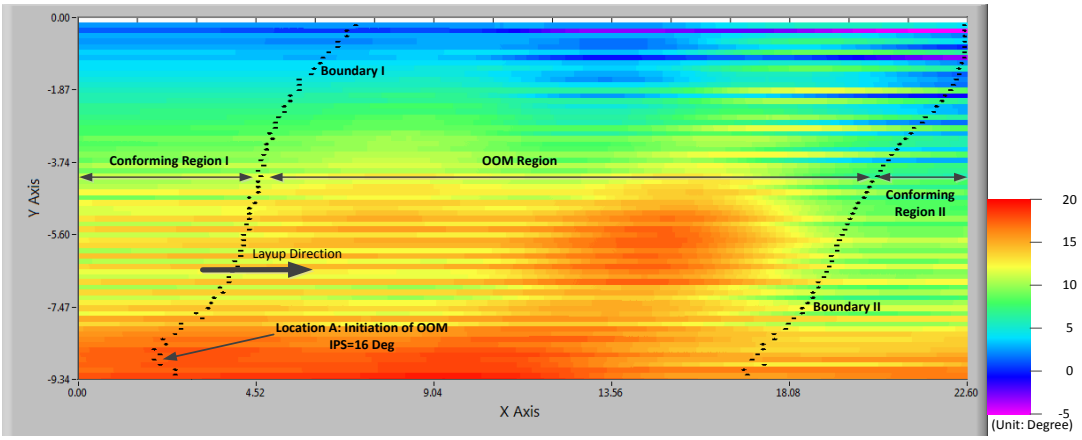

Figure 8. IPS angle distribution

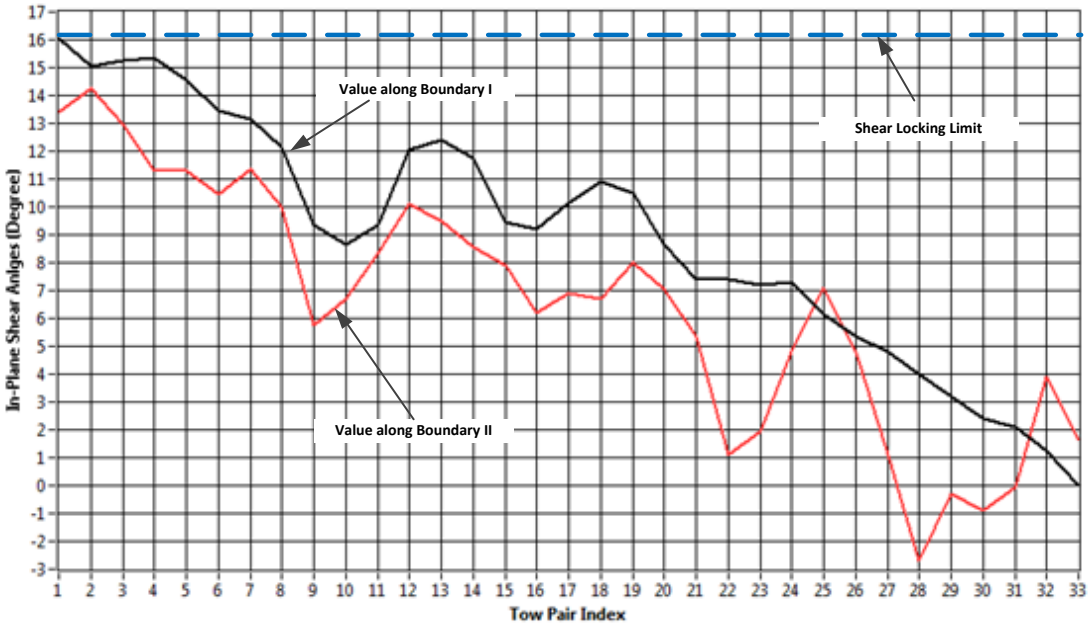

Figure 9. IPS angle values at OOM boundaries

As described in the experimental procedure, the smoothing operation stopped when OOM was generated. The stop location for each tow pair is given as Boundary I in Figure 8. It can be seen from Figure 9 that along Boundary I, the IPS angle values for tow pairs 1~4 reaches the shear locking limit, whereas IPS angle values for the rest of the tow pairs are significantly below the shear locking limit, and it appears that these tow pairs can be further smoothed until the shear locking limit is reached. This would be true if the mold were to be covered by narrower UD tapes placed in parallel along the layup direction, as used in [12]. The fact is for a single piece of UD fabric, the tows are cross-linked by stitching lines and loosely spaced tows in the perpendicular direction (Figue 10). As a result of this structure, further smoothing the tow pairs with IPS angle values below the shear locking limit at Boundary I will cause the tow pairs 1~4 passively conforming to the mold surface. This will increase the IPS angle values beyond the shear locking limits and result in bucking of the

fabric surface. Therefore, it is impossible to further the smoothing operation beyond Boundary I without damaging the fabric surface.

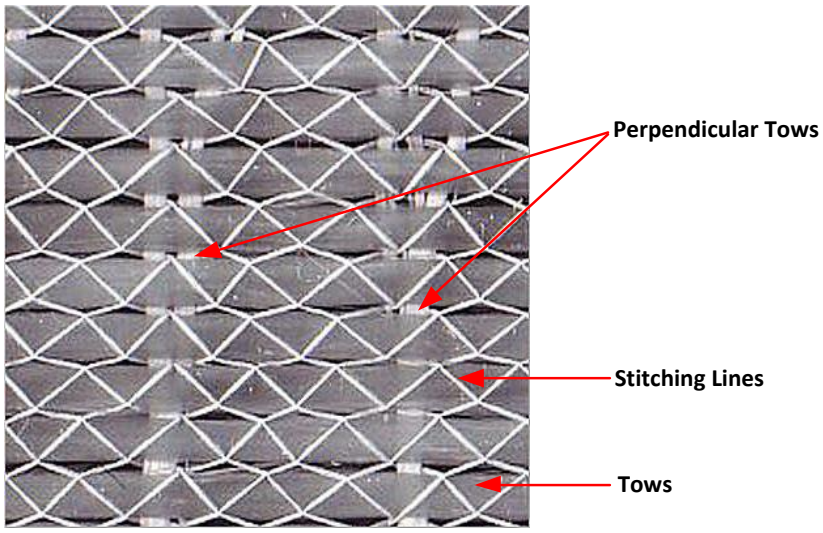

Figure 10. Structure of UD fabric

It is also seen in Figure 9 that comparing the beginning (Boundary I) with the ending (Boundary II) of the OOM, there is generally a reduction on the IPS angle values.

3.2 Model assisted analysis of the relationship between mold shape and IPS distribution

A significant structural difference between the biaxial fabric and the UD fabric is that UD fabric is non-woven, due to insufficient number of tows in the transvers direction. In practical layup applications, UD fabric only allows smoothing along its tow direction, because smoothing along the transverse direction will cause tow splitting, and result in a defective layup surface. According to this structural feature, and the corresponding smoothing operation in the layup process for UD fabrics, a volume conservation unit cell shear deformation model (Figure 11) is proposed, where Δl_i is the shear distance, the tow

spacing w is assumed to be constant, and α_i is the corresponding shear angle at the unit cell. A kinematic simulation program in LabVIEW was developed based on this unit cell deformation model. Utilizing the fabric material property listed in Table 1, the layup mold geometry given in Figure 1, and the layup plan specified in Figure 2 as inputs, this program generated the layup results of tow position and the IPS angle distribution, which are given in Figure 12 and Figure 13, respectively.

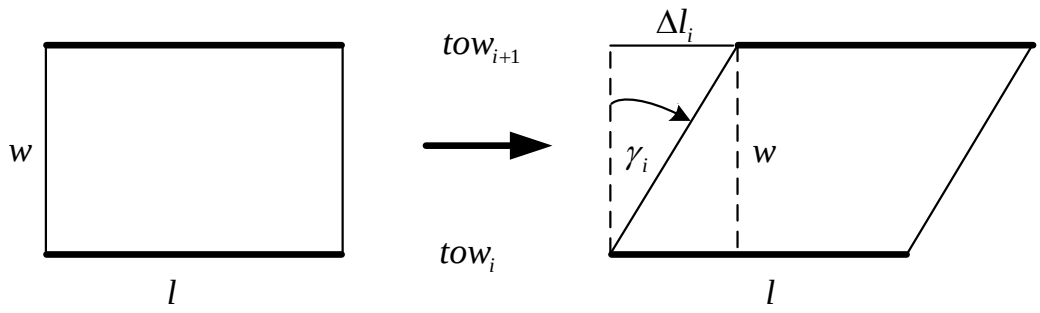

Figure 11. Volume conservation unit cell deformation model

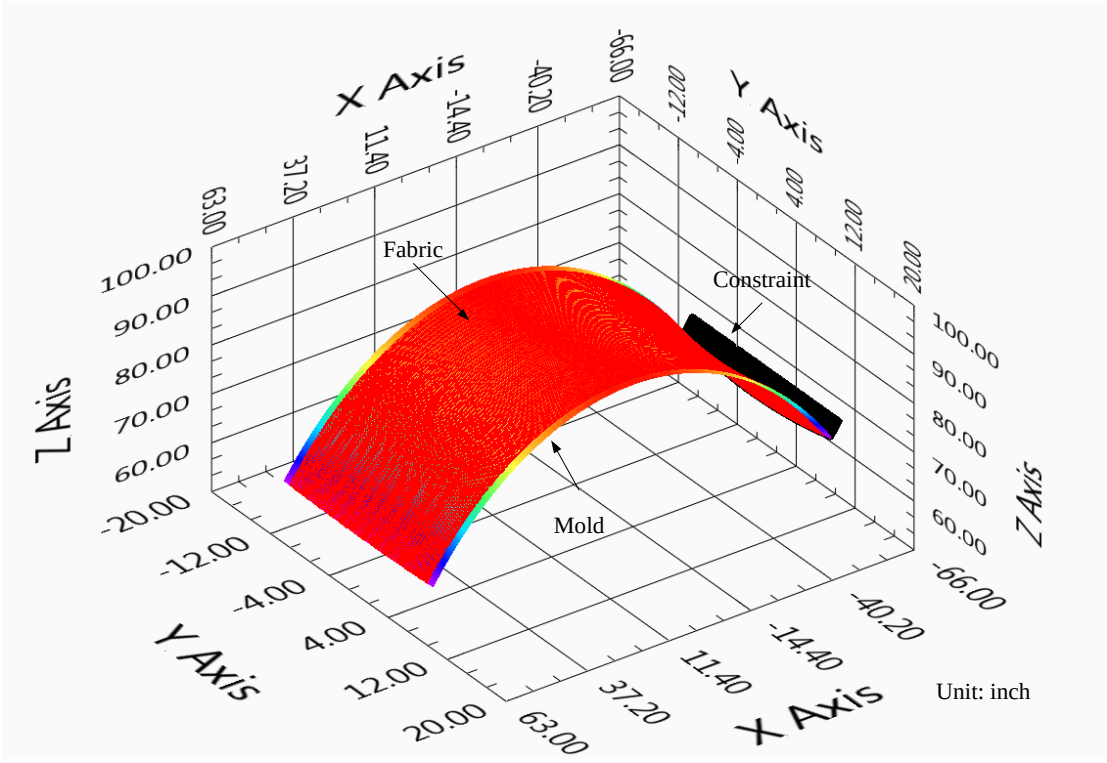

Figure 12. Layup simulation result – fabric tow position

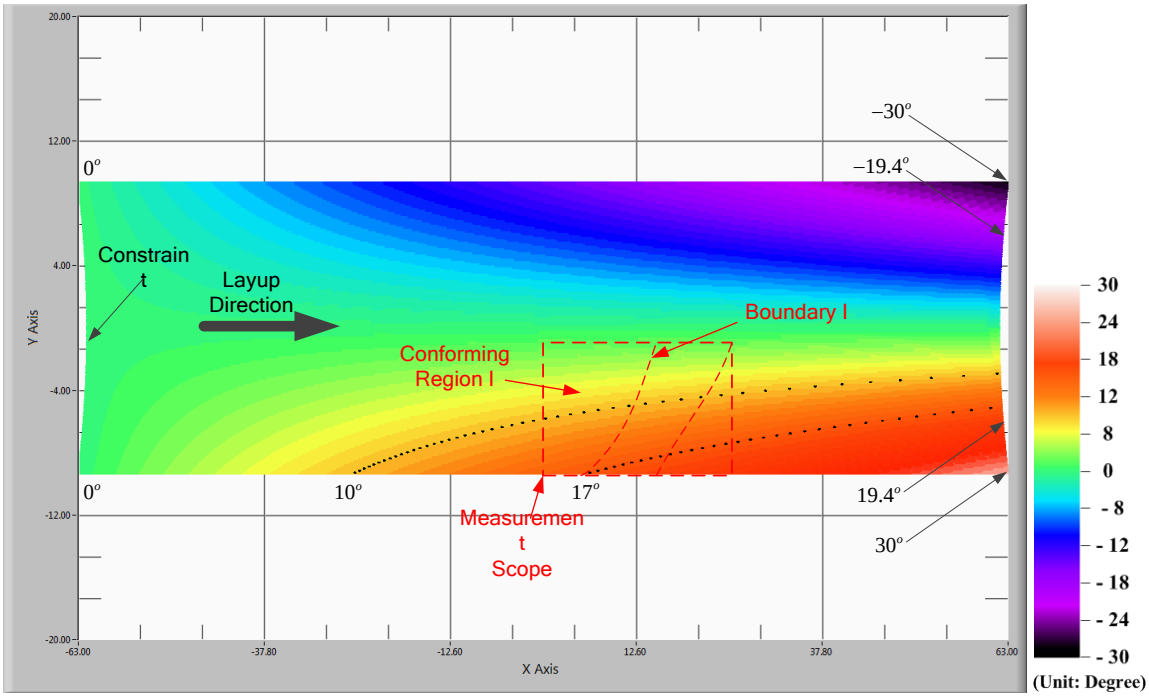

Figure 13. Layup simulation result – IPS angle distribution

As shown in Figure 12, the simulation method assumes that the fabric always conforms to the mold surface, even in the region where IPS angle is out of the range of the SLLs, which is contradictory to the experiment result shown in Figure 4. This shortage is shared by almost all of the commercial layup simulation software packages. It is valuable, however, to utilize these simulation tools to identify if the SLL is reached for a given fabric, mold shape and layup plan combination, so that the feasibility of the layup process can be determined. It is seen in Figure 13 that the maximum predicted IPS angle is 30^o, which is greater than the SLL specified in Table 1. Therefore, the layup process is unfeasible, and the IPS angle simulation is only valid within the region from the starting constraint to Boundary I where the OOM is initiated.

Because the Conforming Region I is within this valid simulation region, and it is also included in the measurement scope (Figure 4), a correlation analysis was conducted to validate the simulation method based on the proposed volume conservation unit cell deformation model. Five hundred locations were randomly selected within the Conforming Region I. The IPS angle values from the model simulation were plotted against the value obtained from measurement at each location, as shown in Figure 14. It is seen in the plot that the simulation data and the measurement data are highly correlated, showing the adequacy of the proposed simulation method.

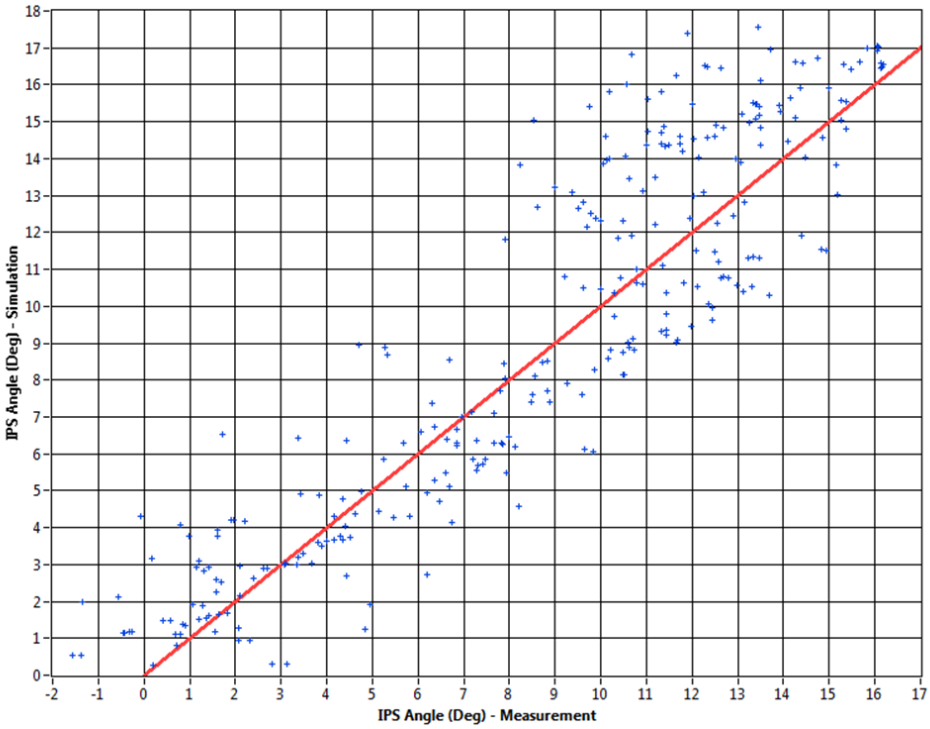

Figure 14. Plot of simulated against measured IPS angle values

Under the volume conservation model assumption, tow length information can be utilized to calculate the approximate (sometimes exact) IPS angle at a given unit cell. This approach will allow the analysis of the relationship between the mold geometry, the start

location of layup, and the resulted IPS angle distribution. As shown in Figure 15, Tow_a and Tow_b are neighboring tow curves; A_0 and B_0 are the starting nodes of the tows, where constraint is applied. $A_1, A_2, ..., A_k$, and $B_1, B_2, ..., B_k$ are nodes on Tow_a and Tow_b, such that the length of A_0A_i was equal to the length of B_0B_i ($i \in \{1, 2, ..., k\}$). At node A_i, the local shear angle is calculated as:

$$\gamma = \pi / 2 - \measuredangle(\overrightarrow{T_{A_i}}, \overrightarrow{A_iB_i}), \quad (1)$$

where $\overrightarrow{T_{A_i}}$ is the tangent direction at node A_i, P_i is the plane orthogonal to $\overrightarrow{T_{A_i}}$ at node A_i, and B_i' is the intersection between P_i and Tow_b. Thus, the IPS angle between the tow pair at P_i can be approximately calculated as:

$$\gamma_{ab} \approx \tan^{-1}\left(\frac{\Delta l}{w}\right) = \tan^{-1}\left(\frac{B_i'B_i}{w}\right) = \tan^{-1}\left(\frac{B_0B_i - B_0B_i'}{w}\right) = \tan^{-1}\left(\frac{A_0A_i - B_0B_i'}{w}\right). \quad (2)$$

Because w is a known constant under the volume conservation model, Equation (2) shows that the tangent value of the IPS angle value between a given pair of neighboring tows at a given node is approximately proportional to the difference of the cumulative tow lengths between the constraint and the orthogonal plane at the given node. Note that if P_i is also orthogonal to the local tangent direction of Tow_b at B_i', then (2) becomes an exact equation.

For the mold geometry and the layup plan shown in Figure 1 and Figure 2, any orthogonal plane will be aligned with the radial direction, and can therefore be designated as P_α, which forms α angle with the constraint. Suppose a and b are an arbitrary pair of neighboring tows. The cumulative length difference between them at P_α is:

$$\Delta l_\alpha = \alpha \times \left(R_a - R_b \right), \tag{3}$$

where

$$R_a - R_b \equiv Z_a - Z_b = R_3 \left(\cos \beta_b - \cos \beta_a \right) = -R_3 \sin\left(\frac{\beta_b + \beta_a}{2} \right) \sin\left(\frac{\beta_b - \beta_a}{2} \right). \tag{4}$$

Also, from the model assumption,

$$w = \left(\beta_a - \beta_b \right) \times R_3 . \tag{5}$$

Lastly, let

$$\beta_c \equiv \frac{\beta_b + \beta_a}{2}, \tag{6}$$

so that β_c designates the position of the tow pair in the flap-wise direction, where $\beta_c = 0$ means the tow pair is along the centerline of the mold, and large β_c value means the tow pair is near the edge of the mold. Combining (2) ~ (6), the IPS angle for tow pair (a,b) at P_α can be calculated as:

$$\gamma\left(\alpha, \beta_c \right) = \tan^{-1}\left(\frac{\alpha R_3 \sin \beta_c \sin\left(\dfrac{w}{2R_3} \right)}{w} \right). \tag{7}$$

Equation (7) provides the explanation to the IPS angle distribution shown in Figure 13. At the constraint, where the layup started, $\alpha = 0$, and therefore the corresponding IPS angle is zero. Along the mold centerline, $\beta_c = 0$, and the resulted IPS angle is also zero. Generally, the absolute value of the IPS angle is larger for the location that is further away from the constraint and closer to the edge of the mold, where the difference in cumulative tow length between the corresponding neighboring pair of tows gets greater. Note that only

for layup on special mold geometries such as the one utilized in this study allows the expression of IPS angle in explicit analytical form as given in Equation (7).

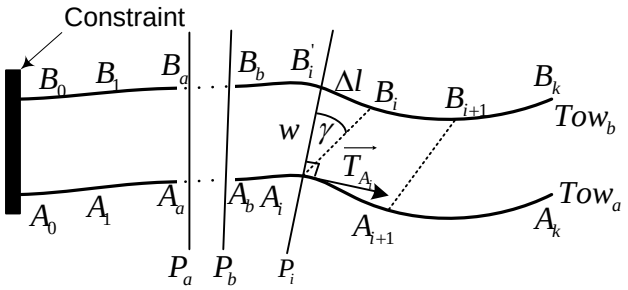

Figure 15. Approximate approach of IPS angle calculation

4. Discussion

4.1 OOM deformation prescription

The OOM deformation generated during the experiment was due to excessive IPS deformations, as analyzed in the previous section. This passively generated OOM deformation in turn reduces the IPS deformation (Figure 9). Although the reductions in IPS angle magnitudes among all the tow pairs are neither consistent, nor sufficient to guarantee that the IPS angle values will be within the shear locking limits beyond this OOM deformation region, this leads to a potential solution of introducing active planned OOM deformations with certain shape and deployment location to an unfeasible layup process to make it feasible. Suppose in Figure 15, γ is close to the shear locking limit, and it is desired to reduce this value to γ' ($\gamma' < \gamma$), by inserting a OOM deformation between the orthogonal planes, P_a and P_b. From Equation (2),

$$\gamma = \tan^{-1}\left(\frac{A_0A_i - B_0B_i'}{w}\right) = \tan^{-1}\left(\frac{A_0A_a + A_aA_b + A_bA_i - B_0B_a - B_aB_b - B_bB_i'}{w}\right). \quad (8)$$

Thus,

$$\gamma' = \tan^{-1}\left(\frac{A_0A_i - B_0B_i'}{w}\right) = \tan^{-1}\left(\frac{A_0A_a + A_aA_b' + A_bA_i - B_0B_a - B_aB_b' - B_bB_i'}{w}\right), \quad (9)$$

and

(9) – (8) gives

$$\left(A_aA_b' - B_aB_b'\right) = w\tan(\gamma' - \gamma) + \left(A_aA_b - B_aB_b\right). \quad (10)$$

Equation (10) shows quantitatively the needed length difference between P_a and P_b, in order to decrease the IPS angle to γ' at P_i. Because $A_aA_b' - B_aB_b' < A_aA_b - B_aB_b$, at least one of the two tows will not conform to the mold surface, which means a OOM deformation is needed between P_a and P_b. There are infinitely many combinations of A_aA_b' and B_aB_b' that satisfy (10), and the design of the OOM tow curves should consider some important factors: 1) continuity with the tow sections adjacent to the OOM deformation region; 2) aspect ratio of the OOM curve must be within the manufacturing tolerance; 3) maximum positional deviation between the fabric and the mold surface should be within the manufacturing tolerance. This method of actively planning for OOM deformations can be integrated to the design of composite structures with complex geometries, in order to facilitate the manufacturability.

4.2 Alternative starting position of the layup

In Equation (7), α is the angle between the constraint and the orthogonal plane. According to the original layup plan shown in Figure2, its maximum value is:

$$\alpha_{MAX} \equiv \alpha_{stop} - \alpha_{constra\,\mathrm{int}} = \left(45^o - (-45^o)\right) = 90^o, \tag{11}$$

where α_{stop} corresponds to the stop angle of the layup process. This large maximum value of α leads to the large values of IPS angles ($\pm 30^o$) at the ending position of the layup, as shown in Figure 13. The optimal alternative layup process is starting (constraint) position of the layup process is at 0^o, and then smoothing the fabric toward 45^o and -45^o on front and back sides of the constraint respectively, in order to minimize α_{MAX} ($\alpha_{MAX} = 45^o$ for this case). As given in Figure 16, the simulated IPS angle distribution shows that the maximum IPS angle value is only 15.66^o, which is less than the shear locking limit of the fabric. This suggests that the layup is feasible. A layup experiment was conducted following the alternative plan. Figure 17 shows that no OOM deformation was generated, which confirms the feasibility of the alternative layup plan.

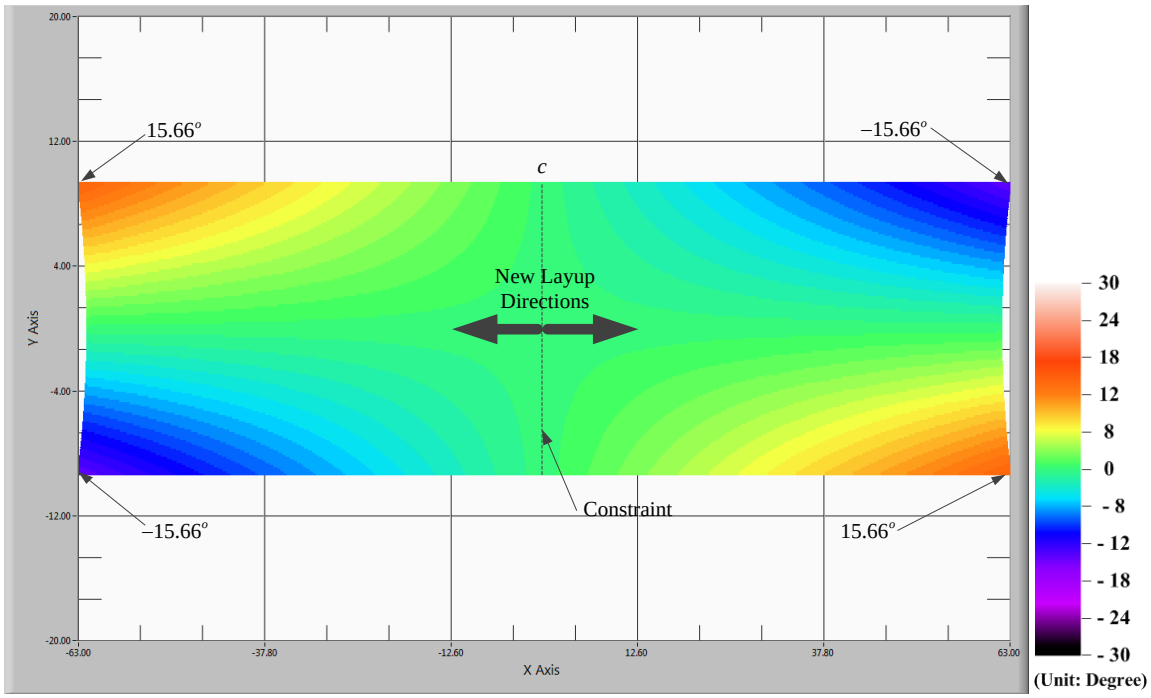

Figure 16. Simulated IPS angle distribution following an alternative start position

Figure 17. Implementation of the alternative layup plan

5. Conclusion and Future Work

In this work, a layup experiment was conducted using UD fabric draped over a 3D undevelopable mold surface. A set of measurement data on the IPS and OOM deformations of UD fabric was collected using a modified laser scanning technique. These data allowed the analyses to understand the interaction between the two deformation modes. It was found that the when local IPS angle value reached the shear locking limit, the OOM deformation was initiated. This OOM deformation in turn decreased the magnitude of the IPS deformation.

A volume conservation unit cell model based simulation method was proposed and validated utilizing the measurement data. Under this model, it was mathematically shown that the IPS angle at a given unit cell can be computed by utilizing the layup constraint position, and the tow lengths from the constraint. This technique enabled an analytical explanation for the IPS angle distribution for the given mold geometry and layup plan.

Two interesting findings from this work were further discussed and explored to provide some insight on the development of improved layup techniques. While the presented attempts are specific to the fabric material, mold geometry utilized in this study, the next phase of the research will extend the scope of this work to provide some generalized solutions for improving the process of fabric layup.

References

[1] Olsen HB, Craig JH. Automated composite tape layup using robotic devices. Proceedings of the IEEE international conference on robotics and automation, Los Alamitos, CA 1993.

[2] Lee SM. Handbook of composite reinforcements: Wiley-VCH; 1992.

[3] Potter K. The influence of accurate stretch data for reinforcements on the production of complex mouldings. Part 1: deformation of aligned sheets and fabrics. Composites 1979; July:161-167.

[4] Dong L, Lekakou C, Bader MG. Solid-mechanics finite element simulations of draping fabrics: sensitivity analysis. Composites Part A 2000;31:639-52.

[5] McBride TM, Chen J. Unit-cell Geometry in plain-weave fabrics during shear deformation. Composites Science and Technology 1997;57:345-351.

[6] Prodromou AG, Chen J. On the Relationship between the shear angle and wrinkling in textile composite preforms. Composites Part A 1997;28(A):491-503.

[7] Potter K. In-plane and out-of-plane deformation properties of unidirectional preimpregnated reinforcement. Composites Part A 2002;33:1469-1477.

[8] Lin H, Wang J, Long AC, Clifford MJ, Harrison P. Predictive modelling for optimization of textile composite forming. Composites Science and Technology 2007;67:3242-52.

[9] Mohammed U, Lekakou C, Bader MG. Experimental studies and analysis of the draping of woven fabrics. Composites Part A 2000;31:1409-20.

[10] Meng F, Frank M, Peters F. Measurement, analysis and process planning for the layup of fabrics in wind turbine blades. Proceedings of the American Wind Energy Association Conference, Atlanta, GA 2012.

[11] Hancock SG, Potter KD. The use of kinematic drape modeling to inform the hand layup of complex composite components using woven reinforcements. Composites Part A 2006; 37; 413-422.

[12] Campbell FC. Manufacturing technology for aerospace structural materials: Elsevier; 2006.

CHAPTER 5. PRE-SHEARING PLANNING FOR THE LAYUP OF UNIDIRECTIONAL FABRICS

A paper to be submitted to *Composites: Part A*

Fanqi Meng[1], Matthew C. Frank, Frank E. Peters[2]

Abstract

This paper presents the methodology of pre-shearing planning for the manipulation of unidirectional fabrics prior to the layup process, with the purpose of obtaining optimal IPS angle distribution on the draped fabric, for a given three dimensional mold geometry-fabric property-layup process plan combination.

The pre-shearing pattern is obtained quantitatively utilizing the shear angle distribution map obtained from kinematic drape simulation of commonly applied naïve/direct layup approach. It will be shown that the pre-shearing can make an unfeasible layup process feasible, or, at least, it can increase the drapability of the unidirectional fabric, reducing the effort on the smoothing operation during the layup process.

As a layup process feasibility verification tool, traditional drape simulation software only provides binary answers of feasible or unfeasible by comparing extreme shear angle values against the shear locking limit of the fabric material. The pre-shearing method augments these simulation tools by predicting the optimal shear angle distribution that will be obtained after the improvements, and by giving the fabric manipulation plans to achieve the improvements.

[1] Primary researcher and author
[2] Author for correspondence

The pre-shearing method simplifies the hardware requirements for layup process automation by shearing the fabric on two dimensional fabric surface prior to the layup process, which would otherwise needs multiple axes actuator and specially designed end effectors to manipulate the fabric during/after it is placed into a three dimensional mold with complex geometry.

1. Introduction

In the manufacture of advanced composite components, manual placement and smoothing operations dominate the layup process of the unidirectional fabrics, especially when the mold geometry is complex [1]. Although some defects such as local wrinkling or fiber tow deviation from the specification could be corrected in manual layup, lacking of repeatability in smoothing patterns and loads will result in random and unpredictable locations of defects. Handling these types of defects relies heavily on the skills and experience of the operators. As a result, the dimensional variability of the manufactured composite parts will be large due to the non-consistent smoothing and corrective operations.

Previous research had been done on the development of automated and robotic machine system to perform the lay-up process, in order to reduce the dimensional viability and the likelihood of introduction of the defects. Ruth and Mulgaonkar [2] proposed a robotic work cell for the automation of the layup process, capable of doing ply acquisition, transfer, placement, stacking and smoothing operations. The entire process was planned by mimicking the hand layup sequence typically performed by an operator. Vision system was applied to determining the plies' positions and orientations, and providing visual guidance during ply placement on the mold. A similar automated layup system was presented in [3], where an

electrostatic gripping device (EGD) was utilized to overcome some of the disadvantages of the conventional fabric handling techniques. Vacuum-assisted large scale gripping system was introduced by Jarvis [4], which was capable to handle the full sized fabric plies in the manufacture of high performance aircraft propeller blades. Adaptive end-effector was designed in the work by Kordi et al. [5], which featured local passive and active degrees of freedom to adapt the fabric geometry to the mold geometry, so that better smoothing result can be achieved. Zhang and Sarhadi [6] proposed an integrated CAD/CAM system for automated composite manufacture, where the application of non-crimp fabric dramatically simplified the layup process. The high drapability of this fabric material allowed the preforms to be laid up flat and then conformed to the required 3D geometry as they are placed into the mold. This significantly reduced the complexity of automating the layup operation and removes 3D tools from the process. The process planning is therefore simplified to solving a tool surface coverage problem. These early studies on the automation of the layup process emphasized the positional accuracy of fabric placement and mold surface coverage. However, they ignored the in-plane shear (IPS) deformation which can be introduced when a two-dimensional (2D) is conformed to a 3D non-developable mold surface. Excessive degree of in-plane deformation will lead to wrinkling problem, causing significant reduction in material strength for the infused composite structure.

In the industrial composite manufacturing, three types of automated machines that can perform the layup process are widely applied [7]. The first type is the automated tape laying (ATL) machine, which lays down narrow tapes to large flat parts, such as wing skins. The second type is filament winding machine, which are suitable for making relatively long, round, convex shells of constant wall thickness, such as pressure vessels and pipes. The third

type is fiber tow placement machine, which places individual tows to the mold surface. Because these systems place individual narrow tapes/tows that are hardly cross-linked, the IPS deformation problem is circumvented. However, due to the input material difference, none of the above techniques can be directly applied to the layup of a wide (e.g. 20 inches ~ 50 inches) piece of unidirectional fabric ply onto a three dimensional (3D) mold with complex geometry.

The IPS deformation presents the biggest challenge for the automation of the layup process. Computer-based draping models have been developed to predict the IPS deformation since early 1970s. Typically, draping simulations involve iterative methods on the computation of the unit cell shapes in order to predict the overall draped shape of the fabrics onto specific 3D tool surfaces. These methods vary from purely kinematic approach [8], to more sophisticated finite element analysis approach [9]. Some of these approaches have been integrated into commercial software packages (For example, FiberSIM, QuickForm). Although these simulation models can be utilized as tools for the feasibility evaluation of layup process plans, only binary answers of feasible or unfeasible could be provided. A feasible plan corresponds to the situation where the IPS angle value is within the shear locking limits (SLLs) for every location of the fabric, while an unfeasible plan corresponds to the situation where the IPS angle value is beyond the SLLs for some locations of the fabric. Generally, for unfeasible layup plans, these simulation tools cannot automatically suggest alternative layup plans or fabric preparation schemes to improve the IPS angle distribution. It usually requires extensive experience and trail-and-error efforts for the process engineers to improve a fabric layup plan to reach the desired shear deformation pattern, resulting in excessive lead time in the manufacturing of composite structures.

The present paper considers how a manipulation plan can be developed, for unidirectional (UD) fabrics, utilizing the output from kinematic drape simulation, to pre-process the fabric prior to the implementation of the laying the fabric down to the mold. A methodology to generate the manipulation plan will be introduced, which will augment the computer drape simulation tools by generating plans on how to improve the simulated shear angle distribution, and by predicting the optimized shear angle distribution that can be achieved after the improvements.

As argued by Hancock and Potter [1], the degree of IPS deformation can be loosely interpreted as the energy or the effort needed for local manipulation on the fabric during the layup process. Therefore, it is desirable to optimize the shear angle distribution, by minimizing the extreme shear angle values, so that the effort needed for local smoothing and manipulation can be reduced. Such optimization could potentially simplify the hardware requirements for layup process automation by shearing the fabric on two dimensional fabric surface prior to the layup process, which would otherwise needs multiple axes actuator and specially-designed end effectors to manipulate the fabric during/after it is placed into a three dimensional mold with complex geometry.

2. Overview of the Solution Approach

Kinematic drape simulation will be initially applied to the given combination of mold geometry, UD fabric material and layup plan, assuming the UD fabric has zero IPS deformation prior to the layup process. From the simulated overall IPS deformation distribution map after the layup, the deformation values for each neighboring pair of tows can be obtained.

Next, the IPS deformation values for each neighboring pair of tows will be optimized. The objective is to minimize the maximum absolute magnitude of the deformation values. However, if this minimized value is out of the SLLs, the objective will be switched to push the position of reaching SLLs downstream the layup direction to the furthest position measured from the starting position of the layup.

Based on the unit cell deformation model, the relationship between the change in the magnitude of IPS deformation and the change of the relative positions of the neighboring pair of tows can be established. The change in the magnitude of IPS deformation is obtained by comparing the original shear angle deformation with the one after optimization. This change will determine the relative positional differences that have to be manipulated for each of the neighboring pair of tows.

The relative positional differences are to be manipulated prior to the layup process, which is equivalent to embedding some designed IPS deformation pattern during the fabric preparation step (pre-shearing the fabric), so that the IPS deformation obtained after the layup process has superior properties over the one would be obtained from the layup without fabric preparation (the direct/naïve layup approach). The overall solution approach is summarized in Figure 1.

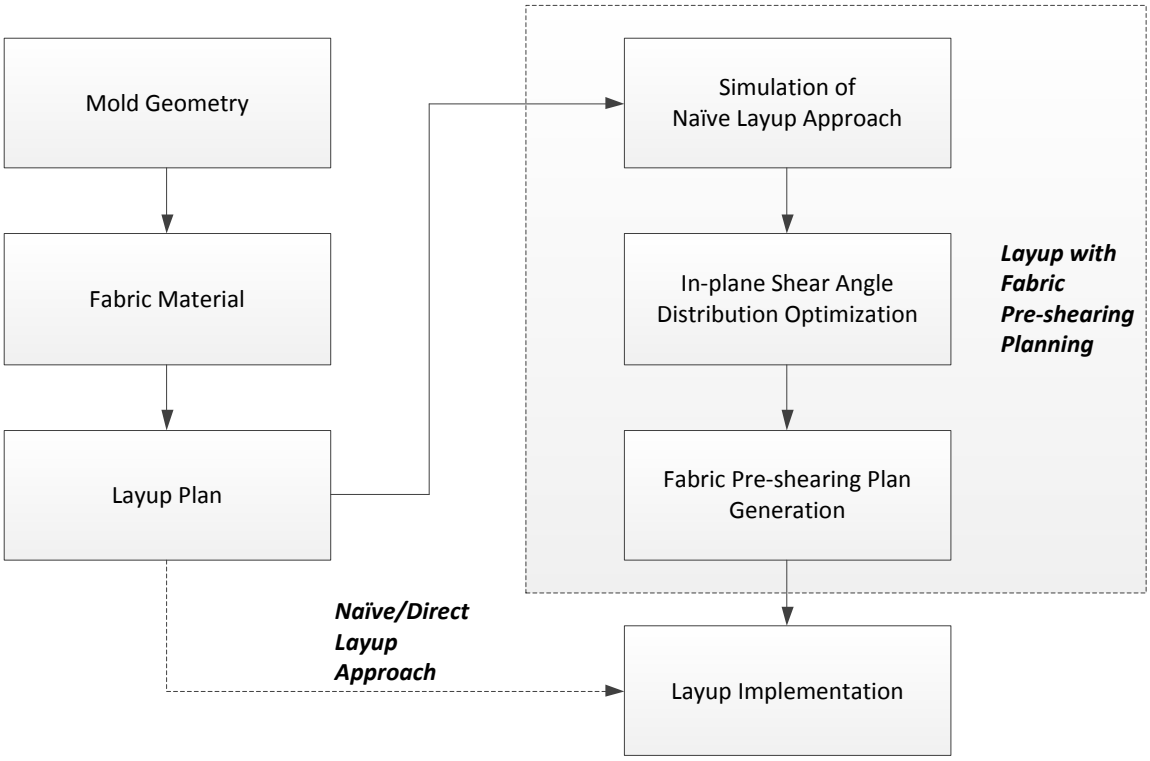

Figure 1. Overview of the solution approach

3. Mold Geometry, Fabric Material and Layup Plan

For the purposes of validation of the simulation model, and verification of the pre-shearing method, a mold was built. It has convex span-wise shape and concave chord-wise shape (See Figure 2 (a) and (b) for detailed dimensional specifications.). This surface was designed to resemble the actual surface of spar cap mold used in megawatt wind turbine blade manufacturing. Although the experiment mold was of shorter span, the curvatures chosen for both span-wise and chord-wise directions were more drastic than the actual mold used in industry applications, in order to exaggerate the shearing effects.

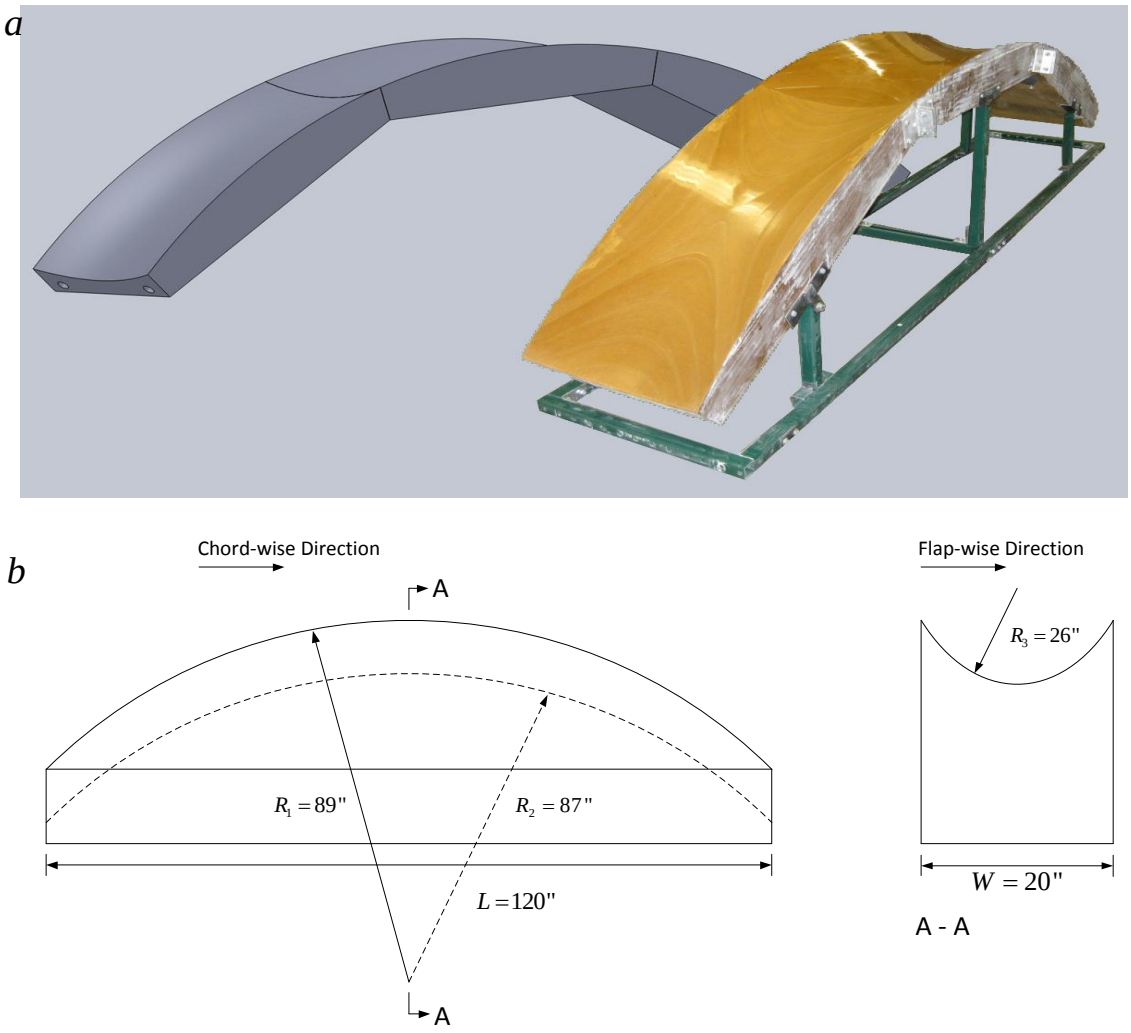

Figure 2. (a) 3D mold used in experiment; (b) mold dimensions.

A piece of 20 inches wide UD fabric (number of tows:138; tow spacing: 0.1395") was utilized for the layup process. Following the general steps of naïve method, the starting line (constraint) was selected at the starting edge of the chord-wise direction, and the fabric was oriented so that the center tows follow the centerline of the mold. Then the fabric was smoothed toward the ending edge of the mold in chord-wise direction. Figure 3 illustrates the layup plan. It is important to emphasize that the methodology provided in this paper is a

generic solution, not specific to this mold, fabric and layup plan combination. However, this combination is frequently referred to as a representative example to illustrate important ideas.

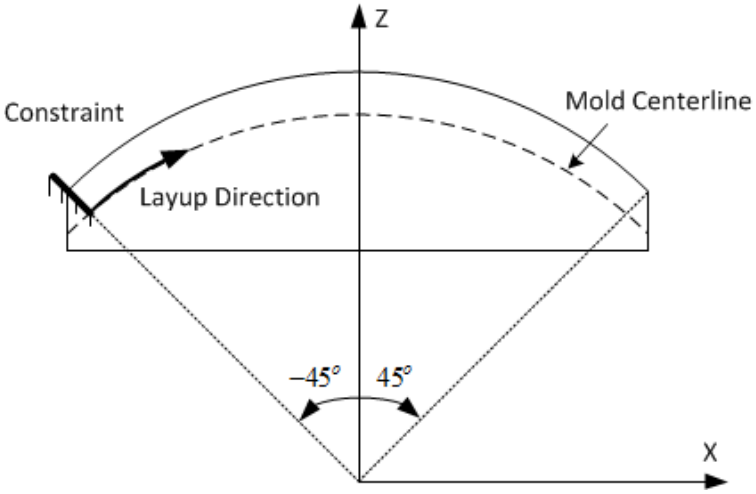

Figure 3. Layup plan

4. Detailed Methodology

4.1 Unit cell deformation model for unidirectional fabrics

The true shear unit cell deformation model (see Figure 4) is utilized in the development of the methodology. Different from the pin-jointed shear model, which is usually applied in the picture-frame testing experiments, the true shear model assumes that the volume of the unit cell conserves during the shear deformation [10]. This model was also validated in [11], where UD fabric was utilized in the layup over a 3D mold.

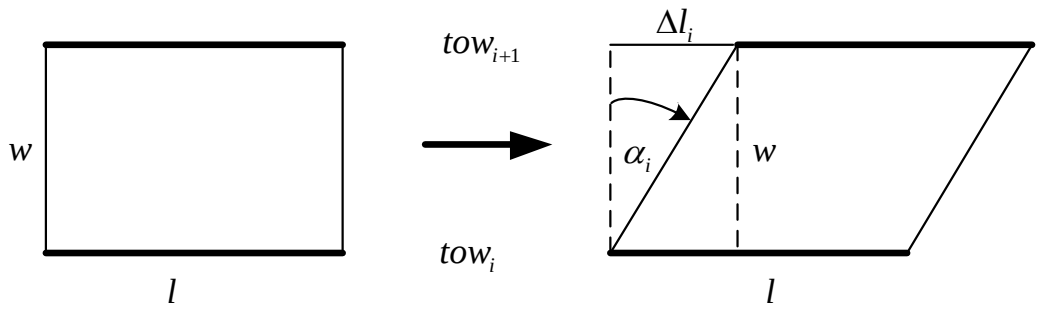

Figure 4. Volume conservation unit cell deformation model

4.2 Layup simulation

A kinematic simulation program in LabVIEW was developed by the authors, based on the true shear unit cell deformation model. This program simulates the typical operation steps of the layup process: firstly, the fabric is placed at the starting line where the fabric initially contacts the mold surface; secondly, a single fabric tow is matched to certain designated curve on the mold surface, (in practice, a marked curve or a laser projected curve on mold surface is typically utilized); lastly, the fabric is smoothed from the starting line outward toward fabric ply edges. Given mold geometry, fabric properties and process parameters, this program is able to predict IPS angle distribution over the draped fabric surface.

4.3 Naïve layup approach

Naïve (or direct) layup refers to the approach where the implementation strictly follows the layup plan, regardless of the IPS angle distribution to be obtained. This layup approach is widely used in industrial composites manufacturing applications.

The naïve layup approach was simulated for the mold-fabric-layup plan combination given in Section 3. Figure 5 shows the fabric position on the mold surface, while Figure 6 shows the shear angle distribution over the fabric surface (top view). It can be seen from Figure 6 that along the layup direction curve, the IPS deformation gets larger in magnitude, and the value is reaching 30^o at the ending edge of the mold. If given that the shear locking limit of this fabric is 10^o, then this naïve layup plan is unfeasible, because the shear angle value between the bottom tow pair reaches 10^o at $x = -27$ inches, which is before the ending

position of the layup at $x = 63$ inches. The next sub-sections will introduce the method of pre-shearing planning, which solves this feasibility problem.

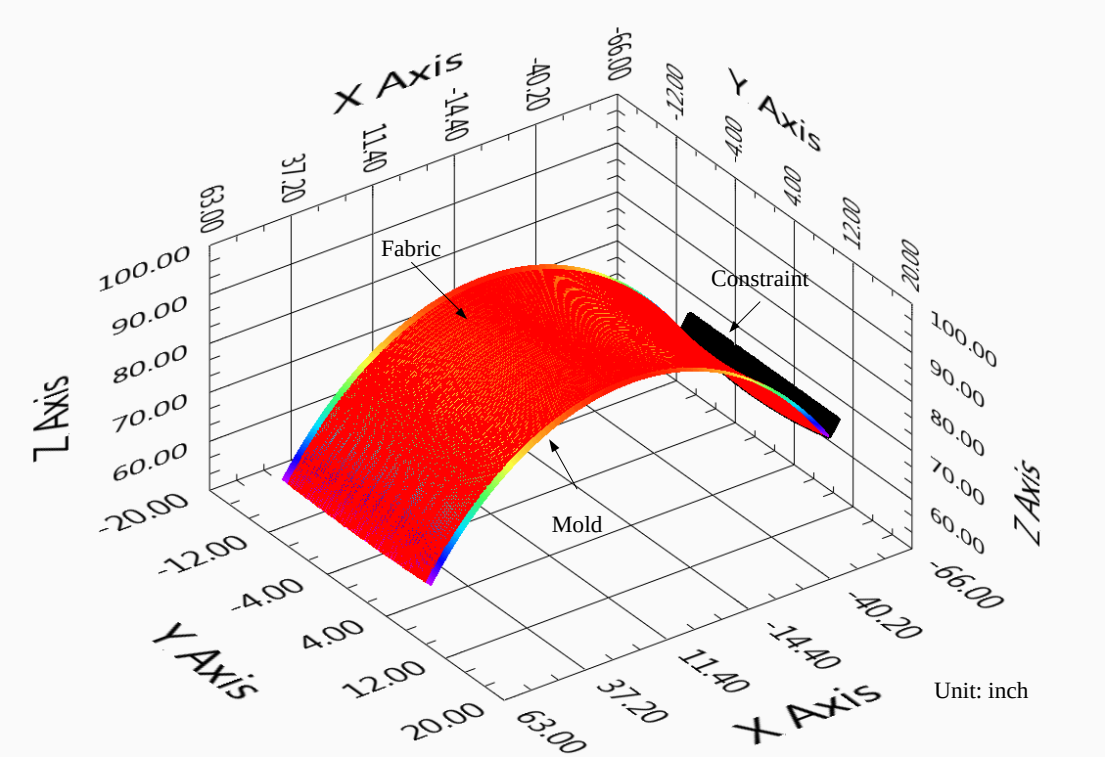

Figure 5. Naïve layup simulation – fabric position

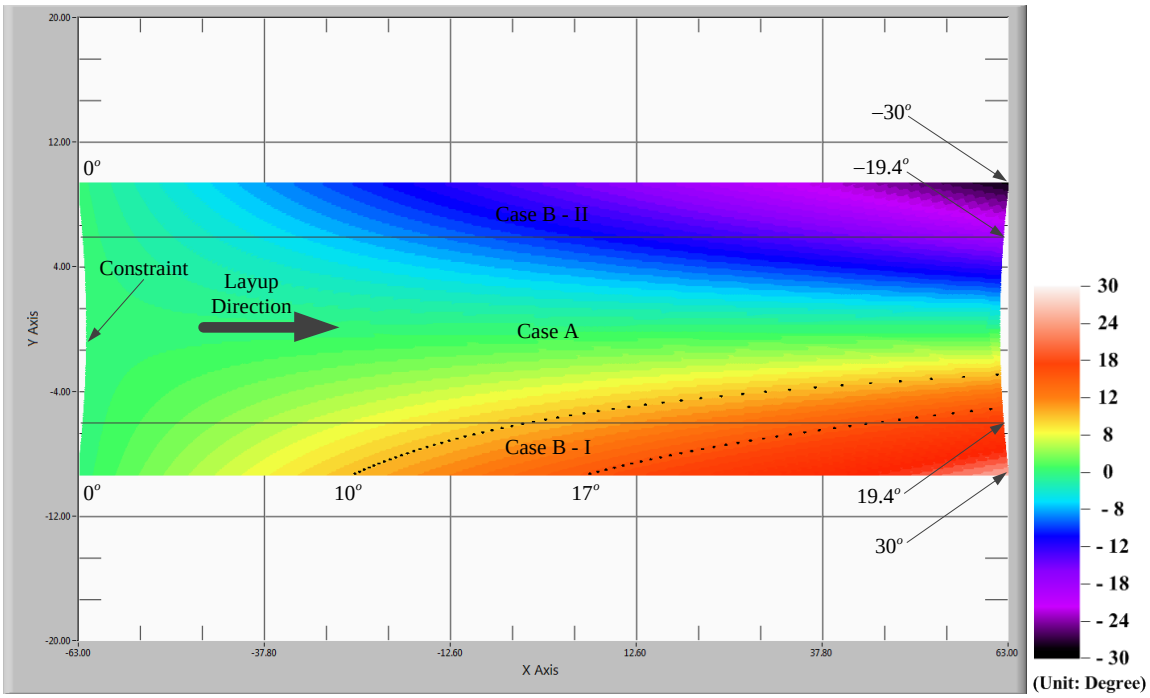

Figure 6. IPS distribution for naïve layup (top view)

4.4 Pre-shearing planning

Pre-shearing is the process introducing shear deformations to the UD fabric prior to the layup process. The objective is to embed certain shear angle values in the fabric, so that when the fabric is placed into a 3D mold, the shear angles introduced by conforming to the non-developable mold geometry can be locally balanced with the embedded shear angles.

In industry applications, the layup process almost always starts with a 2D shaped fabric panel, so in this paper, it is assumed that the original fabric panel is of 2D shape, with zero IPS deformation, and that the pre-shearing process does not introduce any out-of-plane deformation or any change in fiber direction. Under this assumption, the pre-shear angle value between any neighboring pair of tows (tow_i and tow_{i+1}) is a constant α_i, and this value has to be within the range of $[-\alpha_{SLL}, \alpha_{SLL}]$, where α_{SLL} is the shear locking limit of the fabric material (Figure 7). It can be seen from Figure 1 that geometrically,

$$\Delta l_i = w \times \tan \alpha_i \,. \tag{1}$$

Thus, the determination of α_i is equivalent to the determination of Δl_i , within the range of $\left[-w \times \alpha_{SLL}, w \times \alpha_{SLL}\right]$.

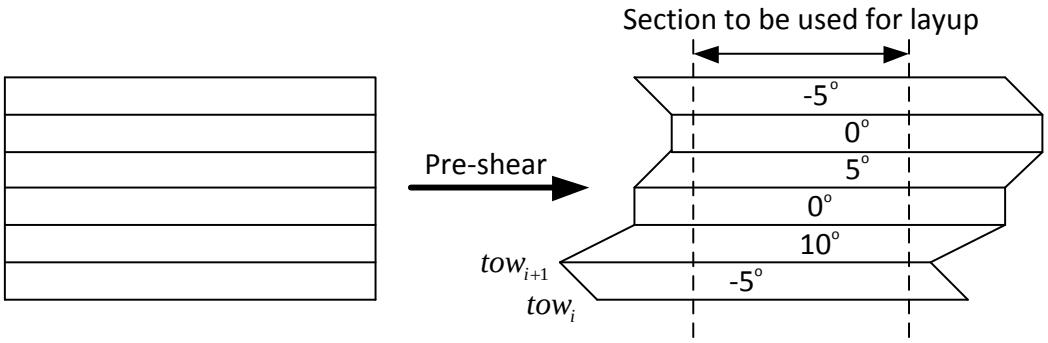

Figure 7. Pre-shearing of UD fabric

4.4.1 Effect of pre-shearing on layup result at unit cell level

Figure 8 shows the effect of pre-shearing at unit cell level, where $\alpha_{Ni,j}$ is the shear angle at the j^{th} pair of node ($N_{i,j}$ and $N_{i+1,j}$) on the i^{th} pair of neighboring tows, which would be obtained be following the naïve layup approach. Similarly, $\alpha_{APi,j}$ corresponds to the shear angle to be obtained from the layup if pre-shearing method is utilized. Geometrically, at the j^{th} pair of node,

$$\Delta l_i = -\left[\left(\tan \alpha_{Ni,j}\right) \times w - \left(\tan \alpha_{APi,j}\right) \times w\right] = w \times \left(\tan \alpha_{APi,j} - \tan \alpha_{Ni,j}\right), \forall j \tag{2}$$

and therefore,

$$\tan \alpha_{APi,j} = \tan \alpha_{Ni,j} - \frac{\Delta l_i}{w} \,. \tag{3}$$

Negative sign in (2) indicates that the pre-shearing direction in opposite to the layup direction. (2) shows that Δl_i makes the same amount of linear change in the tangent value of

shear angles at all neighboring pair of nodes, while (3) indicates that in order to determine the value of Δl_i, the pairwise tow length difference for the corresponding tow pair, both the shear angle distribution obtained from naïve layup and the desired shear angle distribution for the layup with pre-shearing should be considered.

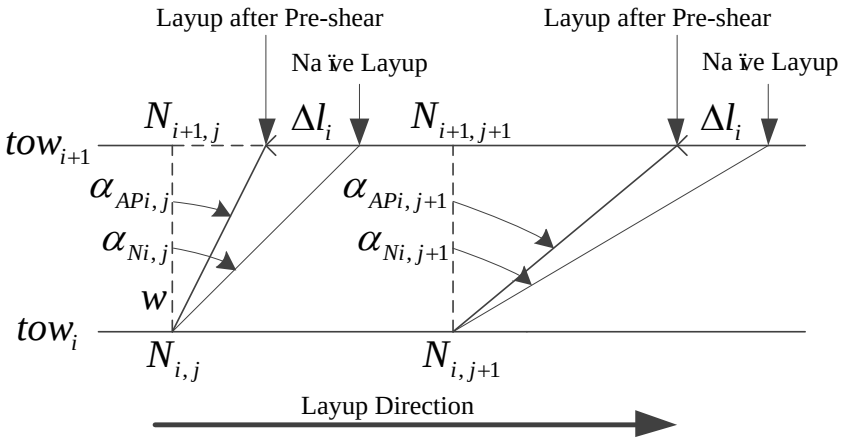

Figure 8. Effect of pre-shearing on unit cell deformation

4.4.2 Algorithm: pre-shearing planning

An algorithm is developed, with the general objective of achieving optimal IPS angle distribution for the layup process, via the determination of appropriate values of Δl_i's, the pairwise tow length differences. To begin the presentation of the algorithm, critical parameters are defined as follows:

$\underset{j}{Min}\{\tan\alpha_{Ni,j}\}$: the minimum tangent value among naïve shear angles at the $1^{st} \sim j^{th}$ nodes, for the i^{th} tow pair.

$\underset{j}{Max}\{\tan\alpha_{Ni,j}\}$: the maximum tangent value among naïve shear angles at the $1^{st} \sim j^{th}$ nodes, for the i^{th} tow pair.

$\underset{j}{R}\{\tan\alpha_{Ni,j}\} = \underset{j}{Max}\{\tan\alpha_{Ni,j}\} - \underset{j}{Min}\{\tan\alpha_{Ni,j}\}$: the range of tangent value among naïve shear angles at the $1^{st} \sim j^{th}$ nodes, for the i^{th} tow pair.

Case A: $\underset{j}{R}\{\tan\alpha_{Ni,J}\} \le 2\times\tan\alpha_{SLL}$. The specific objective for this case is to minimize the maximum absolute pairwise IPS angle. In this case, the range of the tangent of naïve shear angles is within twice of the tangent of shear locking limit, therefore, the interval $\left[\underset{j}{Min}\{\tan\alpha_{Ni,J}\}, \underset{j}{Max}\{\tan\alpha_{Ni,J}\}\right]$ can be shifted into the acceptable interval of $\left[-\tan\alpha_{SLL}, \tan\alpha_{SLL}\right]$. The optimal distance to be shifted is $-\left(\underset{j}{Max}\{\tan\alpha_{Ni,J}\} + \underset{j}{Min}\{\tan\alpha_{Ni,J}\}\right)/2$, so that the resulted interval $\left[-\left(\underset{j}{Max}\{\tan\alpha_{Ni,J}\} - \underset{j}{Min}\{\tan\alpha_{Ni,J}\}\right)/2, \left(\underset{j}{Max}\{\tan\alpha_{Ni,J}\} - \underset{j}{Min}\{\tan\alpha_{Ni,J}\}\right)/2\right]$ has minimum absolute extreme values (see *proof A* in the Appendix). This shifted interval corresponds to the interval of the tangent of the shear angle values obtained from the layup after pre-shearing, and the pairwise tow length difference for the i^{th} pair is determined as:

$$\Delta l_i = -\frac{\underset{j}{Max}\{\tan\alpha_{Ni,J}\} + \underset{j}{Min}\{\tan\alpha_{Ni,J}\}}{2}\times w \qquad (4)$$

Case B: $\underset{j}{R}\{\tan\alpha_{Ni,J}\} > 2\times\tan\alpha_{SLL}$. In this case, the range of the tangent of naïve shear angles is outside twice of the tangent of shear locking limit, therefore, the interval $\left[\underset{j}{Min}\{\tan\alpha_{Ni,J}\}, \underset{j}{Max}\{\tan\alpha_{Ni,J}\}\right]$ cannot be shifted into the acceptable interval of $\left[-\tan\alpha_{SLL}, \tan\alpha_{SLL}\right]$, and therefore, the specific objective for this case is to move the location where SLL is initially reached downstream along the layup direction as far as possible from

the start location. A cumulative range checking method, as shown in Figure 9, was developed to determine the value of Δl_i for this case.

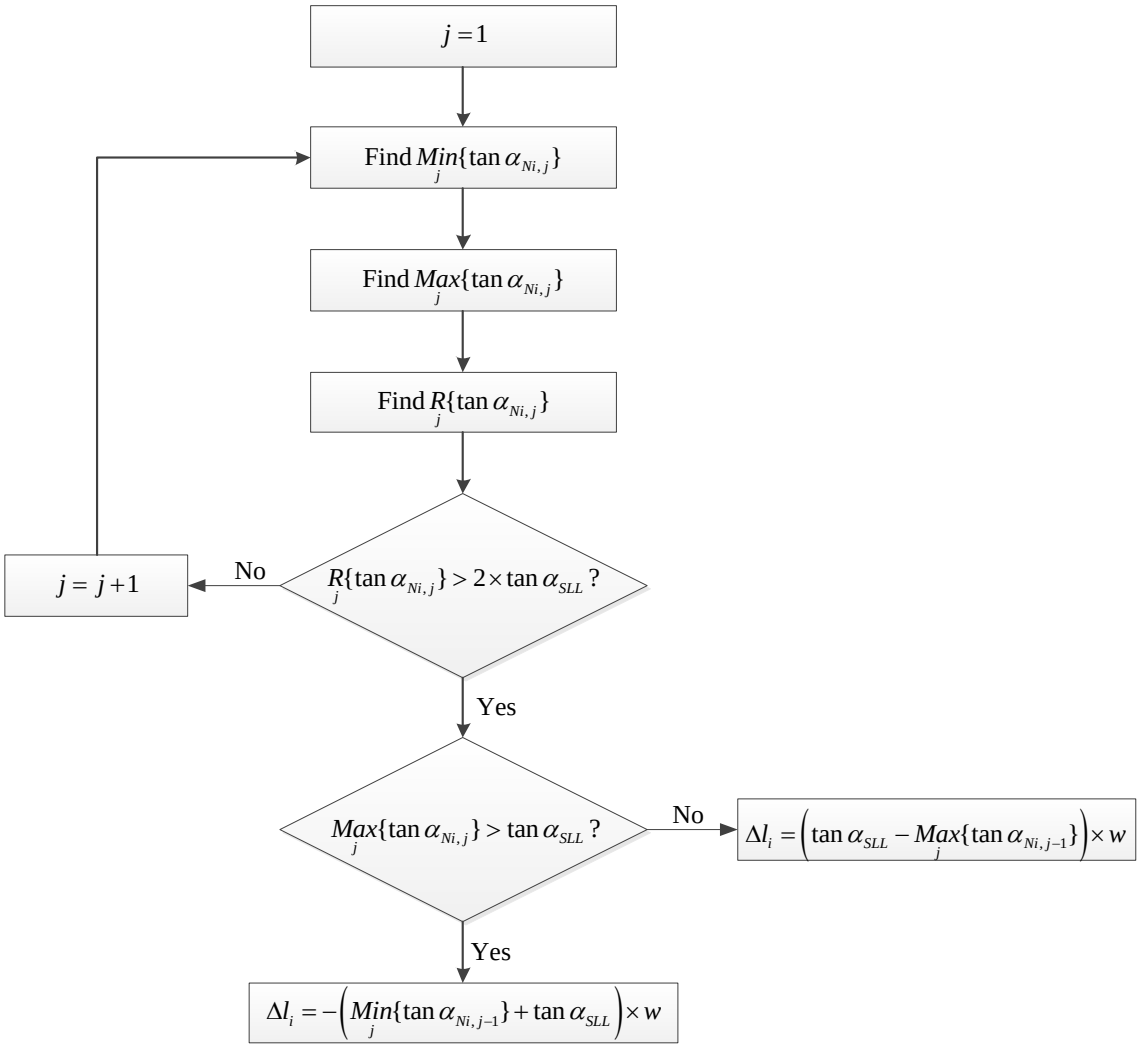

Figure 9. Cumulative range checking method for pre-shearing

Starting from the first node ($j=1$), this method calculates $\underset{j}{R}\{\tan\alpha_{Ni,j}\}$ with increasing j value continuously, until the K^{th} node is reached, where $\underset{j}{R}\{\tan\alpha_{Ni,K}\} > 2\times\tan\alpha_{SLL}$. It can be proved (see *proof B* in the Appendix) that only two sub-

cases exist under this condition. Case B-I is $\underset{j}{Max}\{\tan\alpha_{Ni,K}\} > \tan\alpha_{SLL}$, where the pre-shearing length is determined as:

$$\Delta l_i = -\left(\underset{j}{Min}\{\tan\alpha_{Ni,K-1}\} + \tan\alpha_{SLL}\right)\times w. \quad (5)$$

Case B-II is $\underset{j}{Min}\{\tan\alpha_{Ni,K}\} < -\tan\alpha_{SLL}$, where the pre-shearing length is determined as:

$$\Delta l_i = \left(\tan\alpha_{SLL} - \underset{j}{Max}\{\tan\alpha_{Ni,K-1}\}\right)\times w. \quad (6)$$

As shown in Figure 10, the purpose of pre-shearing for Case B is to push the happening location of the problem ($\underset{j}{Max}\left\{\left|\tan\alpha_{Ni,j}\right|\right\} > \tan\alpha_{SLL}$) as far as possible downstream the layup direction.

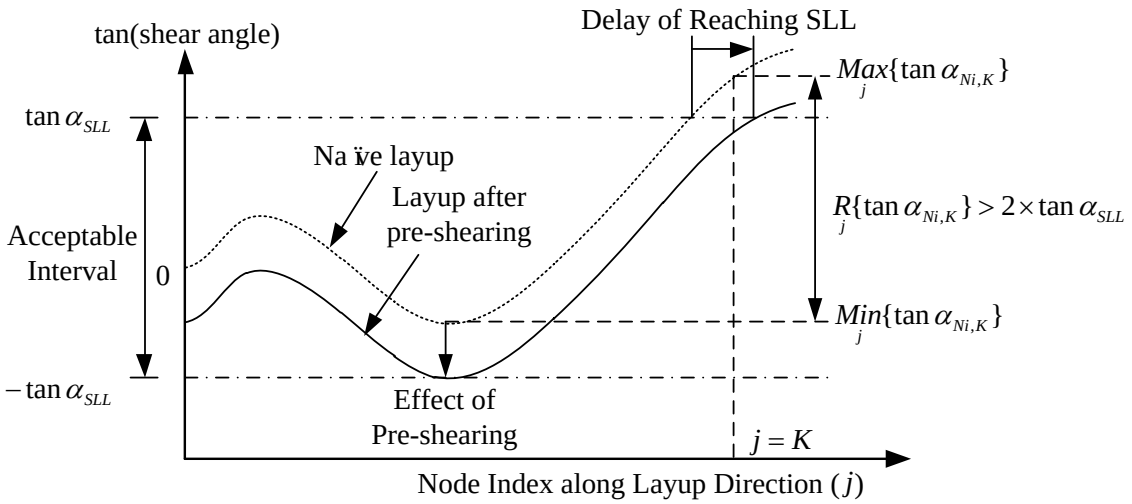

Figure 10. Effect of pre-shearing on IPS deformation in Case B

4.4.3 Pre-shearing pattern determination

Algorithm I provides the relative distance (Δl_i) between neighboring pair of tows that has to be manipulated prior to the layup process. The pre-shearing distance for each tow (l_i) can be calculated by accumulating these relative distances:

$$l_i = \begin{cases} 0 & (i=1) \\ \sum_{k=1}^{i-1} \Delta l_k & (i \geq 2) \end{cases} . \tag{7}$$

These l_i values determine the shape of the pre-sheared UD fabric (see Figure 11).

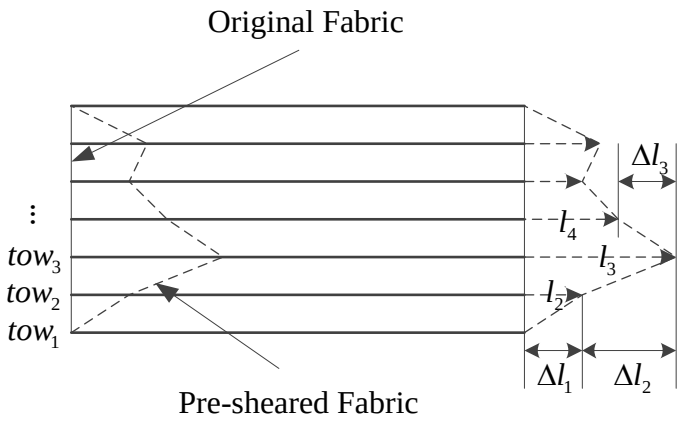

Figure 11. Pre-shearing pattern determination

5. Implementation

The pre-shearing method was implemented for the fabric-mold-layup process combination given in Section 2. Two scenarios are considered here, with fabrics of different SLLs.

5.1 Scenario I – improved after pre-shearing

In this scenario, it is assumed that the SLL of the fabric material is 10^o. Algorithm I was applied to the shear angle distribution simulated for the naïve approach given in Figure 6, and the fabric pre-shearing pattern was generated, as shown in Figure 12, which gives the needed pre-shearing length (l_i) as a function of tow index i ($i = 0,1,...,137$). Layup with this pre-sheared fabric resulted in the shear angle distribution given in Figure 13.

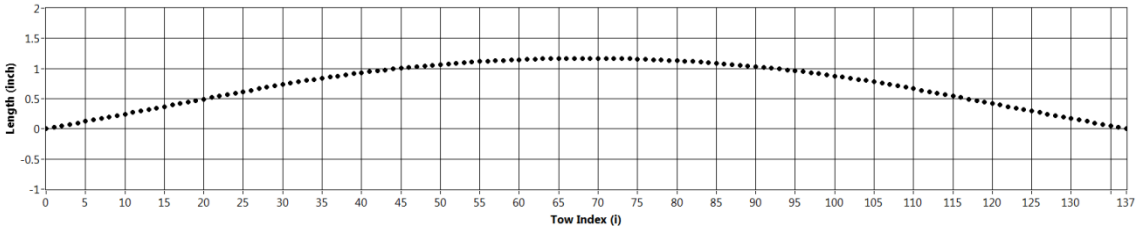

Figure 12. Pre-shearing length for the fabric

(fabric SLL = 10^o)

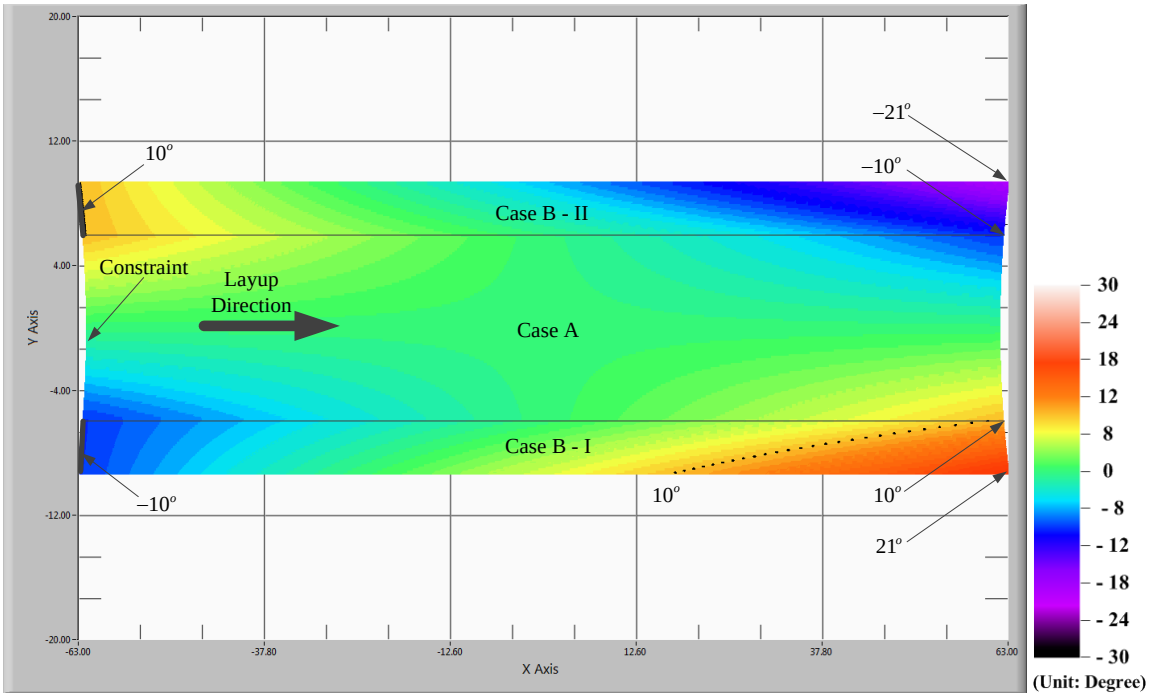

Figure 13. IPS distribution for layup with pre-shearing

(top view; fabric SLL = 10^o)

A comparison between Figure 6 and Figure 13 shows that, the pre-shearing method significantly improved the shear angle distribution for the layup process. In Figure 6, the region of Case A consists of all of the tow pairs satisfying the condition $\underset{j}{R}\{\tan\alpha_{Ni,J}\} \le 2\times\tan\alpha_{SLL}$. In this scenario, the SLL for the fabric is 10^o, so it can be calculated accordingly that all the tow pairs in Case A have the shear angle range within in

19.4^o. Within the region of Case A, pre-shearing guarantees that resulted shear angle values are within the SLLs. Outside the region of Case A, pre-shearing makes the absolute values of shear angle equal to SLL, at the beginning position of the layup, where constraint is applied. In the region of Case B-I of Figure 13, the beginning location for shear angle value to be greater than SLL is at $x = 15$ inches, whereas the corresponding location is at $x = -27$ for the naïve layup. This difference shows that, for case B, the pre-shearing method can push the emergence position of unfeasible region downstream along the layup direction, although it cannot eliminate the unfeasible region. The overall maximum amplitude of the shear angle values in Figure 13 is 21^o, which is 9^o less than the values from naïve layup. This reduction shows that the drapability of the fabric has been improved with the pre-shearing method. This result can also be interpreted as an increment in the drapability of the UD fabric.

5.2 Scenario II – feasible after pre-shearing

The SLL of the fabric is assumed to be 17^o for this scenario. After the application of Algorithm I, the optimal shear angle distribution and the needed pre-shearing profile were generated, as shown in Figure 14 and Figure 15 respectively.

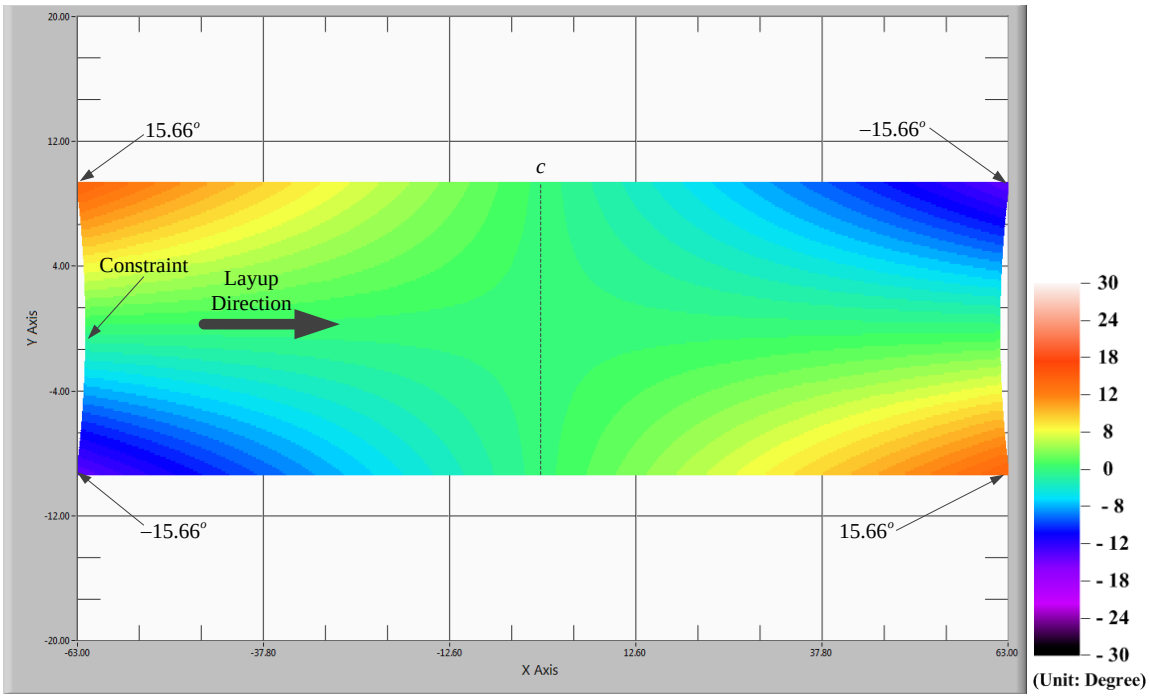

Figure 15. IPS distribution for layup with pre-shearing

(top view; fabric SLL = 17^o)

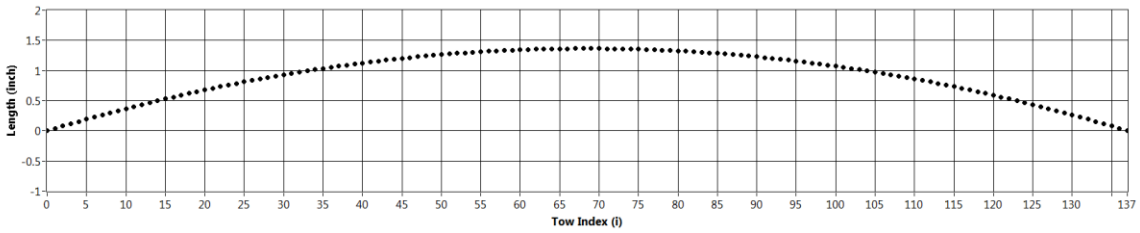

Figure 14. Pre-shearing profile for the fabric

(fabric SLL = 17^o)

It can be seen in Figure 15 that the layup with the fabric pre-sheared according to the pattern shown in Figure 14 will be feasible, because the extreme absolute shear angle value is 15.66^o, which is less than the SLL of 17^o. A comparison between Figure 15 and Figure 6 reveals that for this particular mold shape, the layup from one edge of the mold toward the

other edge with a pre-sheared fabric is equivalent to the layup from the center of the mold toward both edges with the original non-deformed fabric (see Figure 16).

Experiments were conducted to verify the effectiveness of the pre-shearing method. One piece of UD fabric with 138 tows and zero initial IPS deformation was firstly laid onto the mold following the layup plan show in Figure 4. The result of this naïve layup is shown in Figure 16, where it can be observed that out-of-mold (OOM) deformation was generated in the center region of the mold. The initiation location of the OOM deformation correspond to the location where the IPS deformation is reaching the SLL of 17^o, as predicted by the simulation result given in Figure 6. This OOM deformation cannot be further smoothed to conform to the mold surface, otherwise split and wrinkle will be introduced to the fabric. The generation of the OOM deformation confirmed experimentally that the naïve layup approach was not feasible.

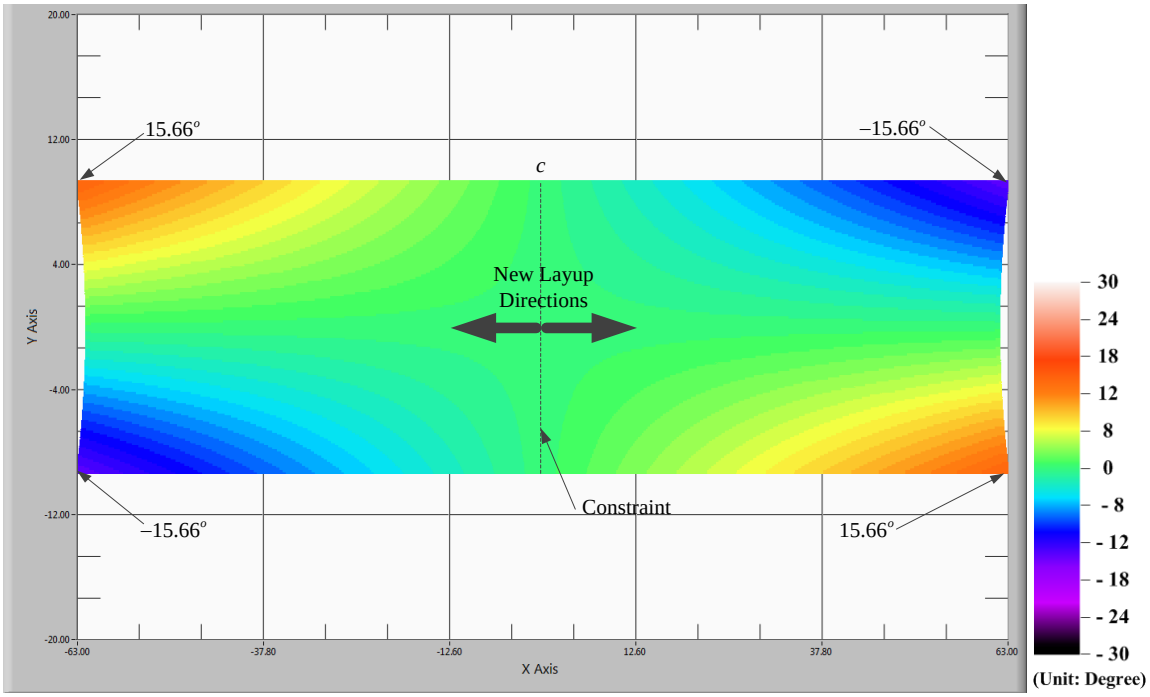

Figure 15. IPS distribution for layup without pre-shearing, following an alternative start position (top view; fabric SLL = 17^{o})

For the second experiment, the layup started in the middle of the mold, and the fabric was smoothed toward both ends of the mold, as illustrated in Figure 15. Figure 17 shows the result of the implementation of this alternative layup plan. It can be observed that the fabric conformed to the mold surface completely without any OOM deformation, which demonstrated that this alternative plan was feasible.

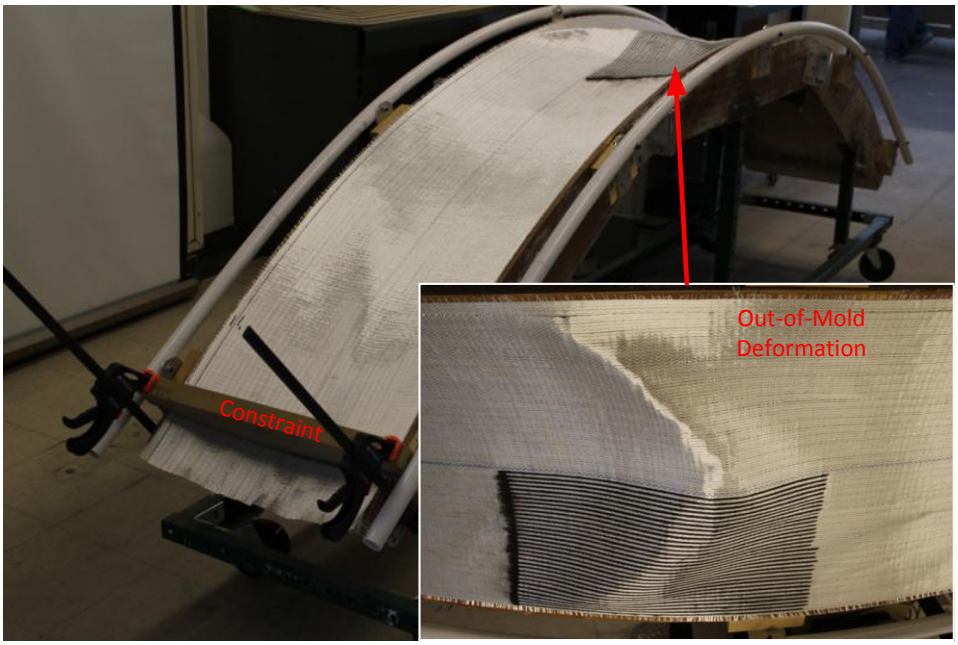

Figure 16. Implementation of naïve layup

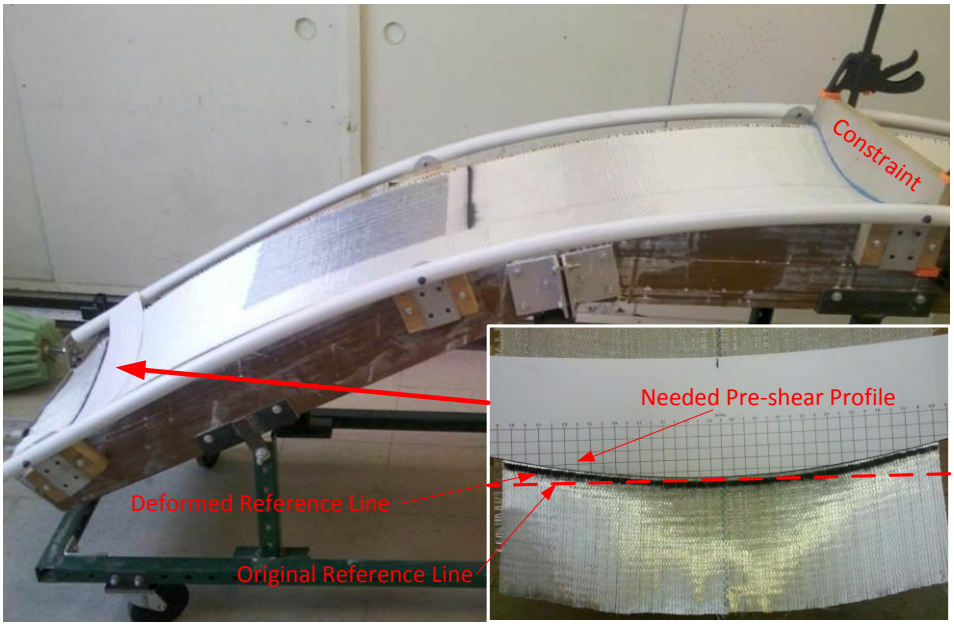

Figure 17. Implementation of alternative layup

A straight reference line perpendicular to the tow direction was drawn on the fabric prior to the layup process to track the IPS deformation of the fabric near the left edge of the mold. It is seen in Figure 17 that the deformed reference line after layup has almost the same shape as the pre-shear profile given in Figure 14. It can be inferred that if the fabric was pre-sheared according to the profile shown in Figure 14, the original layup plan described in Figure 4 will become feasible.

Although the second experiment have shown the equivalency between the result of alternative layup and the result that can be achieved by following the original layup plan with pre-shearing the fabric, the latter solution is more general. The equivalency is due to the symmetric mold geometry about the center line, which leads to symmetric IPS deformation pattern after optimization (as shown in Figure 15). This symmetric pattern intuitively suggests the alternative layup method. For a more complex, non-symmetric mold shape, the

equivalent relationship generally does not exist, where the pre-shearing method is the only solution.

6. Discussion

This section will discuss how the fabric pre-shearing method can be implemented in practice, and how this technique can be integrated with existing automated systems in the manufacturing of composite structures.

6.1 Fabric pre-shearing methods

The fabric can be pre-sheared utilizing the mechanism given in Figure 18. The system consists of two axes and six clamps. With outer clamps closed and upper and lower clamps open, the fabric can be transferred vertically by the outer clamps. Certain neighboring pair of tows (tow_i and tow_{i+1}) can be placed so that tow_i is within the upper clamps and tow_{i+1} is within the lower clamps. Then the upper and lower clamps are closed, while the outer clamps become open. The relative horizontal motion between the upper clamps and the lower clamps creates the desired shear angle between this neighboring pair of tows. This procedure will iterate for all the neighboring pair of tows, until the given pre-shearing profile (for example, the one shown in Figure 14) is achieved.

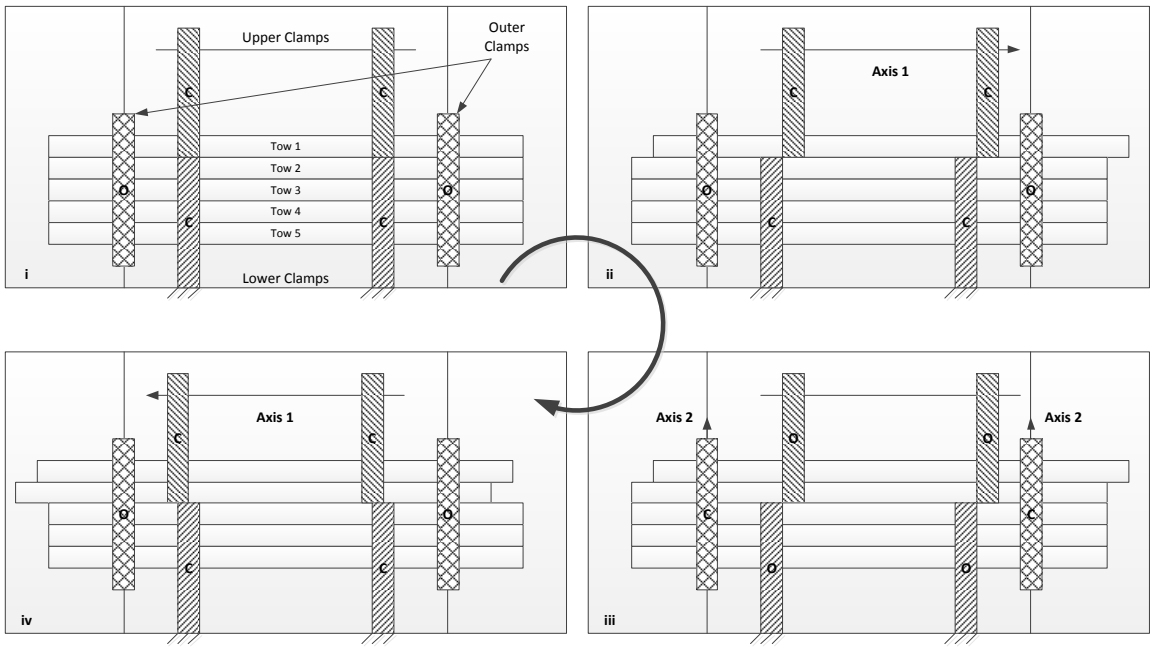

Figure 18. Fabric pre-shearing device

Alternatively, a multi-roller system can be utilized to achieve the desired pre-shearing profile. Figure 19 shows a simplified version for creating the shear angle between one neighboring pair of tows. Six sets of active rollers driven by motors control the dispensing of the fabric. Assuming that there is no relative motion between the rollers and the fabric at their contact points, if the roller sets follow the speed profiles as given in Figure 19, after the time point t_s, the system will dispense the fabric with constant shear angle α for this pair of tows. Here $\alpha = \arctan(w/\Delta l)$, where w is the distance between neighboring pair of tows, and Δl is the displacement difference caused by the two speed profiles within the time interval of $(0, t_s)$. In practice, the α value determined by the pre-shearing profile, and then speed profiles can be chosen accordingly for the roller sets. The simplified mechanism can be easily augmented to adapt to a fabric with larger number of tows by deploying more roller sets, and designating the corresponding appropriate speed profiles.

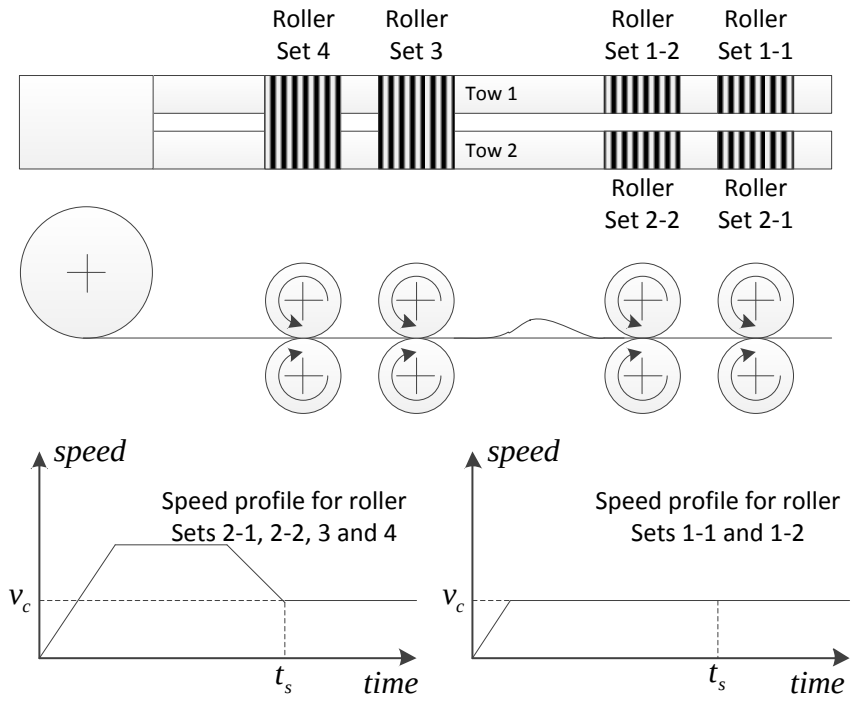

Figure 19. Multi-roller system

6.2 Improvement of traditional automation solutions for fabric placement

It has been reviewed in the introduction section that the IPS deformation is among the biggest challenges for the traditional automation solutions of the layup process, because excessive degree of in-plane deformation will result in wrinkling of the fabric. The method developed in this study is able to reduce the overall extreme shear angle values to be achieved after the layup, by pre-shearing the fabric at the preparation step. With this preparation step integrated, the traditional automation methods of fabric placement and smoothing will be able to handle more complex mold geometry or extended length of UD fabrics. Particularly, if the multi-roller system (Figure 19) is utilized as a fabric dispensing head that travels over the mold, the fabric pre-shearing can be done in real-time, right before it is placed onto the mold surface.

6.3 Hybrid solution of fabric placement and tow placement

A hybrid method combining fabric placement and tow placement provide solution for the layup plans that are still predicted to be unfeasible after pre-shearing planning. The idea is to place individual tows in the unfeasible region to circumvent the "beyond SLL" problem. For the feasible region, fabric is utilized to increase the productivity and efficiency of the overall layup process. Figure 13 shows an extreme case where the SLL of the fabric is only 10^o. 88 tows inside Case A region are with shear angles within the SLLs. Thus, during the implementation, a piece of fabric with 88 tows can be pre-sheared according to the $tow_{26} \sim tow_{113}$ section of the profile given in Figure 12, and then placed in to the Case A region in Figure 13. The tows outside Case A region can be covered by placing 50 individual tows, in order to avoid the problem of exceeding the SLL, as indicated in Figure 13.

7. Conclusion and Future Work

This article presented an algorithm through which the shear angle distribution obtained from kinematic simulation of the naïve layup approach can be utilized to generate fabric pre-shearing plan prior to the layup process. It has been demonstrated via simulations and experiments that the pre-shearing method is effective in the optimization of the shear angle distribution that can be obtained from the layup process.

The fabric pre-shearing method developed in this work can be applied in several aspects in the composite manufacturing industry. Firstly, as an add-on optimization package for the existing layup simulation software, the method presented in this work is able to automatically suggest the optimal shear angle distribution, and how this optimal result can be achieved via pre-shearing the fabric by following the pre-shearing profile generated from the

package. Secondly, the pre-shearing method virtually increased the drapability of a given UD fabric, so that design with more complex geometric features are allowed without switching to more expensive fabrics with better shear tolerance. This is particularly important for the aerospace and wind turbine designers, who can be given looser material and manufacturing constraints, so that better aerodynamic characters can be achieved. Lastly, as discussed in the article, the pre-shearing method can be implemented efficiently by different types of automated machineries. If integrated with the pre-shearing function, the capability of traditional automated fabric placement and smoothing machines can be significantly extended to perform layup on molds with more complex geometries.

The authors are currently developing an in-process fabric manipulation method, to further mitigate the IPS angle during the layup process, so that the shear deformation can be controlled within the SLLs. Preliminary results have shown that this new method, in compliment to the pre-shearing method presented in this paper, will provide a complete solution to the feasibility problems caused by excessive IPS deformation in the layup process.

References

[1] Hancock SG, Potter KD. The use of kinematic drape modeling to inform the hand layup of complex composite components using woven reinforcements. Composites Part A 2006;37:413-422.

[2] Ruth D, Mulgaonkar P. Robotic layup of prepreg composite plies. Proceedings of the IEEE international conference on robotics and automation, Cincinnati, Ohio 1990.

[3] Sarhadi M. Automated lay-up of non-rigid fabrics. Proceedings of the Manufacturing Technology Update, IEE; June 1993.

[4] Jarvis SDH, Wilcox K, Chen XQ, McCarthy R and Sarhadi M. Design of a handling device for composite ply lay-up automation. Proceedings of the international conference on advanced robotics, Pisa, Italy 1991.

[5] Kordi MT, Hüsing M, Corves B. Development of a multifunctional robot end-effector system for automated manufacture of textile preforms. Proceedings of IEEE/ASME international conference on advanced intelligent mechatronics 2007, pp.1–6.

[6] Zhang Z, Sarhadi M. An integrated CAD/CAM system for automated composite manufacture. Journal of materials processing technology 1996; 61(2): 104-9.

[7] Campbell FC. Manufacturing technology for aerospace structural materials: Elsevier; 2006.

[8] Potter K. The influence of accurate stretch data for reinforcements on the production of complex mouldings. Part 1: deformation of aligned sheets and fabrics. Composites. 1979; July:161-167.

[9] Dong L, Lekakou C, Bader MG. Solid-mechanics finite element simulations of draping fabrics: sensitivity analysis. Composites Part A 2000;31:639-52.

[10] Potter K. In-plane and out-of-plane deformation properties of unidirectional preimpregnated reinforcement. Composites Part A. 2002;33:1469-77.

Appendix

Proof A: Part 1, optimal shifting distance

Let the shifting distance on the tangent value of naïve shear angle be x, then

$\underset{j}{Max}\{\tan\alpha_{APi,J}\} = \underset{j}{Max}\{\tan\alpha_{Ni,J}\} + x$, and $\underset{j}{Min}\{\tan\alpha_{APi,J}\} = \underset{j}{Min}\{\tan\alpha_{Ni,J}\} + x$

Case 1: $\left|\underset{j}{Max}\{\tan\alpha_{APi,J}\}\right| \geq \left|\underset{j}{Min}\{\tan\alpha_{APi,J}\}\right|$

$\underset{j}{Max}\left|\{\tan\alpha_{APi,J}\}\right| = \left|\underset{j}{Max}\{\tan\alpha_{APi,J}\}\right| \geq \left|\underset{j}{Min}\{\tan\alpha_{APi,J}\}\right|$

$\Rightarrow Min\left\{\underset{j}{Max}\left|\{\tan\alpha_{APi,J}\}\right|\right\} = \left|\underset{j}{Min}\{\tan\alpha_{APi,J}\}\right|$, which is achieved when

$\left|\underset{j}{Max}\{\tan\alpha_{APi,J}\}\right| = \left|\underset{j}{Min}\{\tan\alpha_{APi,J}\}\right|$.

$\Rightarrow \left(\underset{j}{Max}\{\tan\alpha_{APi,J}\}\right)^2 = \left(\underset{j}{Min}\{\tan\alpha_{APi,J}\}\right)^2$

$\Rightarrow \left(\underset{j}{Max}\{\tan\alpha_{Ni,J}\} + x\right)^2 = \left(\underset{j}{Min}\{\tan\alpha_{Ni,J}\} + x\right)^2$

$\Rightarrow x = -\dfrac{\underset{j}{Max}\{\tan\alpha_{Ni,J}\} + \underset{j}{Min}\{\tan\alpha_{Ni,J}\}}{2}$

Case 2: $\left|\underset{j}{Max}\{\tan\alpha_{APi,J}\}\right| \leq \left|\underset{j}{Min}\{\tan\alpha_{APi,J}\}\right|$

$\underset{j}{Max}\left|\{\tan\alpha_{APi,J}\}\right| = \left|\underset{j}{Min}\{\tan\alpha_{APi,J}\}\right| \geq \left|\underset{j}{Max}\{\tan\alpha_{APi,J}\}\right|$

$\Rightarrow Min\left\{\underset{j}{Max}\left|\{\tan\alpha_{APi,J}\}\right|\right\} = \left|\underset{j}{Max}\{\tan\alpha_{APi,J}\}\right|$, which is achieved when

$\left|\underset{j}{Min}\{\tan\alpha_{APi,J}\}\right| = \left|\underset{j}{Max}\{\tan\alpha_{APi,J}\}\right|$

$$\Rightarrow \left(\underset{j}{Max}\{\tan \alpha_{APi,J}\} \right)^2 = \left(\underset{j}{Min}\{\tan \alpha_{APi,J}\} \right)^2$$

$$\Rightarrow \left(\underset{j}{Max}\{\tan \alpha_{Ni,J}\} + x \right)^2 = \left(\underset{j}{Min}\{\tan \alpha_{Ni,J}\} + x \right)^2$$

$$\Rightarrow x = -\frac{\underset{j}{Max}\{\tan \alpha_{Ni,J}\} + \underset{j}{Min}\{\tan \alpha_{Ni,J}\}}{2}$$

Proof A: Part 2, optimal shifting distance is pre-shearable

$$\underset{j}{R}\{\tan \alpha_{Ni,J}\} \le 2 \times \tan \alpha_{SLL}$$

$$\Leftrightarrow \underset{j}{Max}\{\tan \alpha_{Ni,J}\} - \underset{j}{Min}\{\tan \alpha_{Ni,J}\} \le 2 \times \tan \alpha_{SLL} \quad \text{(A1)}$$

$\alpha_{Ni,1} = 0$ (Shear deformation is zero at the first node for naïve layup.)

$$\Rightarrow \tan \alpha_{Ni,1} = 0$$

$$\Rightarrow \underset{j}{Min}\{\tan \alpha_{Ni,J}\} \le 0 \le \underset{j}{Max}\{\tan \alpha_{Ni,J}\}$$

$$\Rightarrow 2 \times \underset{j}{Min}\{\tan \alpha_{Ni,J}\} \le 0 \le 2 \times \underset{j}{Max}\{\tan \alpha_{Ni,J}\}, \text{ combining with A1}$$

$$\Rightarrow -\tan \alpha_{SLL} \le -\frac{\underset{j}{Max}\{\tan \alpha_{Ni,J}\} + \underset{j}{Min}\{\tan \alpha_{Ni,J}\}}{2} \le \tan \alpha_{SLL}$$

$$\Rightarrow \quad -\frac{\underset{j}{Max}\{\tan \alpha_{Ni,J}\} + \underset{j}{Min}\{\tan \alpha_{Ni,J}\}}{2} \text{ is a pre-shearable distance}$$

Proof B

For Case B, it is given that

$$\underset{j}{R}\{\tan \alpha_{Ni,J}\} > 2 \times \tan \alpha_{SLL}$$

$$\Leftrightarrow \underset{j}{Max}\{\tan \alpha_{Ni,J}\} - \underset{j}{Min}\{\tan \alpha_{Ni,J}\} > 2 \times \tan \alpha_{SLL} \quad \text{(A2)}$$

Suppose that

$\underset{j}{Max}\{\tan\alpha_{Ni,J}\} \le \tan\alpha_{SLL}$ and $\underset{j}{Min}\{\tan\alpha_{Ni,J}\} \ge -\tan\alpha_{SLL}$

$\Rightarrow \underset{j}{Max}\{\tan\alpha_{Ni,J}\} - \underset{j}{Min}\{\tan\alpha_{Ni,J}\} \le 2\times\tan\alpha_{SLL}$, which is a contradiction to A2

$\Rightarrow$ It is TRUE that $\underset{j}{Max}\{\tan\alpha_{Ni,J}\} > \tan\alpha_{SLL}$ or $\underset{j}{Min}\{\tan\alpha_{Ni,J}\} < -\tan\alpha_{SLL}$.

CHAPTER 6. IN-PROCESS MANIPULATION PLANNING FOR THE LAYUP OF UNIDIRECTIONAL FABRICS

A paper to be submitted to *Composites: Part A*

Fanqi Meng[1], Matthew C. Frank, Frank E. Peters[2]

Abstract

This paper presents a methodology for in-process manipulation planning for the layup of unidirectional composite fabric. The goal is to provide a robust method of modifying an potentially unfeasible layup plan, in order to make it feasible for implementation.

Specifically, the in-process manipulation planning considers the layup process, which is predicted to be unfeasible by common computer layup simulations. By sacrificing a controlled amount of geometric conformity to the given three-dimensional mold, the proposed method modifies the shear angle distribution within the unfeasible region of the fabric layup, such that all shear angles can be held within the fabric's shear locking limits. The fabric's loss of geometric conformity to the mold is represented as out-of-mold deformations, and each of the deformation regions consists of tows with out-of-plane waves with respect to their nominal positions. Obviously, these waves would have to be within quality specifications of the product.

The method of in-process manipulation redefines the position of each individual tow in three-dimensional space, so that the feasibility of the layup process is guaranteed by having all the in-plane shear deformation angles within the shear locking limits, while keeping the loss of the geometric conformity within the manufacturing tolerances.

[1] Primary researcher and author
[2] Author for correspondence

As a design for manufacturability approach, the redefined positions of the tows can be achieved directly during layup using a modified mold surface, which can be obtained by adding three-dimensional patches to the original mold surface, where out-of-mold deformations of the fabric are needed, or a modification of the mold shape entirely. In summary, we propose that although in plane shear beyond the locking limit causes waves, then inverse is true; waves can reduce shear values and avoid the locking limit. To that end, this paper proposes the somewhat provocative idea of prescribed wave creation in order to make an unfeasible layup feasible or, in the least, present the modifications of a mold required for a feasible layup.

1. Introduction

Fiber-reinforced composite materials are gaining increasing popularity where products need to be lightweight, yet strong enough to take harsh loading conditions, and be resistant to environmental corrosions. In the wind energy industry, for example, fiber-reinforced composite dominates the material usage in the manufacturing of wind turbine blades. Nowadays, one trend in blade design is toward larger dimensions. An example is the design of multi-Megawatt offshore wind turbines, where a larger blade area effectively increases the tip-speed ratio of a turbine at a given wind speed, thus increasing its energy extraction [1]. Another design trend is toward the improvement of the shape of the blade, so that better aerodynamic characteristics can be achieved [2].

The emphases on large dimensions and complex geometries significantly increase the difficulty in manufacturing these structures, particularly at the layup stage. Layup is one of the most critical manufacturing processes in the fabrication of Vacuum Resin Transfer

Molded (VRTM) composite structures, where layers of dry fabric panels are placed into the mold. During layup, in-plane shear (IPS) deformation occurs when the fabric panels are smoothed to conform to the three dimensional mold surfaces or offsets of mold surfaces (when laying subsequent layers in multi-layer thick composites). When deforming, the fabric material behaves as a pin-jointed net [3]. If the local in-plane shear angle is beyond the shear locking limits (SLL) of the fabric, buckling or out-of-mold (OOM) deformation will occur [4-6]. The OOM deformation typically results in excessive fabric material covering the region on the tool where it occurs and induces waves or wrinkling when vacuum is applied during the resin transfer stage. This wave or wrinkling defect will significantly or catastrophically reduce the strength and fatigue endurance of the component.

Since the early 1970s, computer-based layup models have been developed to predict the in-plane shear deformation during the layup process. Typically, layup simulations involve iterative methods on the computation of the unit cell shapes in order to predict the overall draped shape of the fabrics onto specific 3D tool surfaces. These methods vary from a purely kinematic approach [7], to more sophisticated finite element analysis methods [8]. Some of these approaches have been integrated into commercial software packages, for example, FiberSIM and QuickForm. Although these simulation models can be utilized as tools for the feasibility evaluation of layup process plans, only binary answers of feasible or unfeasible could be provided. A feasible plan corresponds to the situation where the IPS angle value is within the SLLs for every location of the fabric, while an unfeasible plan corresponds to the situation where the in-plane shear angle value is beyond the SLLs for at least some locations. Generally, these simulation tools cannot automatically suggest alternative layup plans or fabric preparation schemes to improve the IPS angle distribution. It usually requires

extensive experience and trail-and-error efforts for the engineers to improve a fabric layup plan to reach the desired shear deformation pattern, resulting in excessive lead time in the manufacturing of composite structures.

In previous work, the authors presented a methodology for pre-shearing planning for the manipulation of unidirectional fabrics prior to the layup process, with the purpose of obtaining optimized shear angle distribution on the draped fabric a-priori; for a combination of 3D mold geometry, fabric properties and layup process plan [9]. Such a method can minimize the overall extreme shear angle, which in turn reduces the manipulation efforts required during the layup process [10]. However, in the situation where the mold geometry is extremely complex or fabric properties are limited, obtaining a feasible layup plan through this shear angle optimization method is not guaranteed. The experimental layup study conducted by the authors revealed that certain OOM deformations of a neighboring pair of tows of the fabric can reduce the downstream magnitude of the IPS deformation between them [9]. This discovery sheds light on the method of further reducing IPS deformations by sacrificing some controlled amount of geometric conformity to the given 3D mold.

As an extension of that work, this paper presents an in-process manipulation planning tool for the layup of unidirectional fabrics. The goal is to provide a robust method for modifying an existing unfeasible layup plan, thereby making it feasible. “In-process” refers that this method is applied to the fabric during the layup process, as contrary to the previously proposed method of pre-shearing; which is applied prior to laying the fabric in the mold.

2. Overview of the Solution Approach

The in-process manipulation planning considers a layup process that is predicted to be *unfeasible* by common kinematic layup simulations. Typically, the simulation result for an unfeasible layup plan includes regions with IPS deformation values beyond Shear Locking Limit.

The initial step is to separate the simulation result into feasible and unfeasible regions along the fabric panel, based on IPS values. Then, for unfeasible regions, individual tows are manipulated within the fabric surface. The objective is to modify and control the IPS values within the SLLs by applying minimum tow manipulations. Based on the unit cell model, the relationship between the change in the IPS deformation and the change of length difference between neighboring pair of tows can be established.

By capacitance analysis, specific zones within the feasible regions can be selected to accommodate the change of length differences between neighboring tow pairs. Due to this change, the individual fabric tows may have extra length within the accommodation zones, and therefore, these tows cannot conform to the mold surface. Specific wave shapes are then designed for the OOM deformations, so that the standard industry's measure of aspect ratio can be applied to quantify the deformation. By appropriately picking the quantity and sizes of accommodation zones, the aspect ratio of the OOM deformations can be controlled within certain manufacturing quality tolerances; for the given layup schedule and design.

The overall solution approach is summarized in the flow chart of Figure 1.

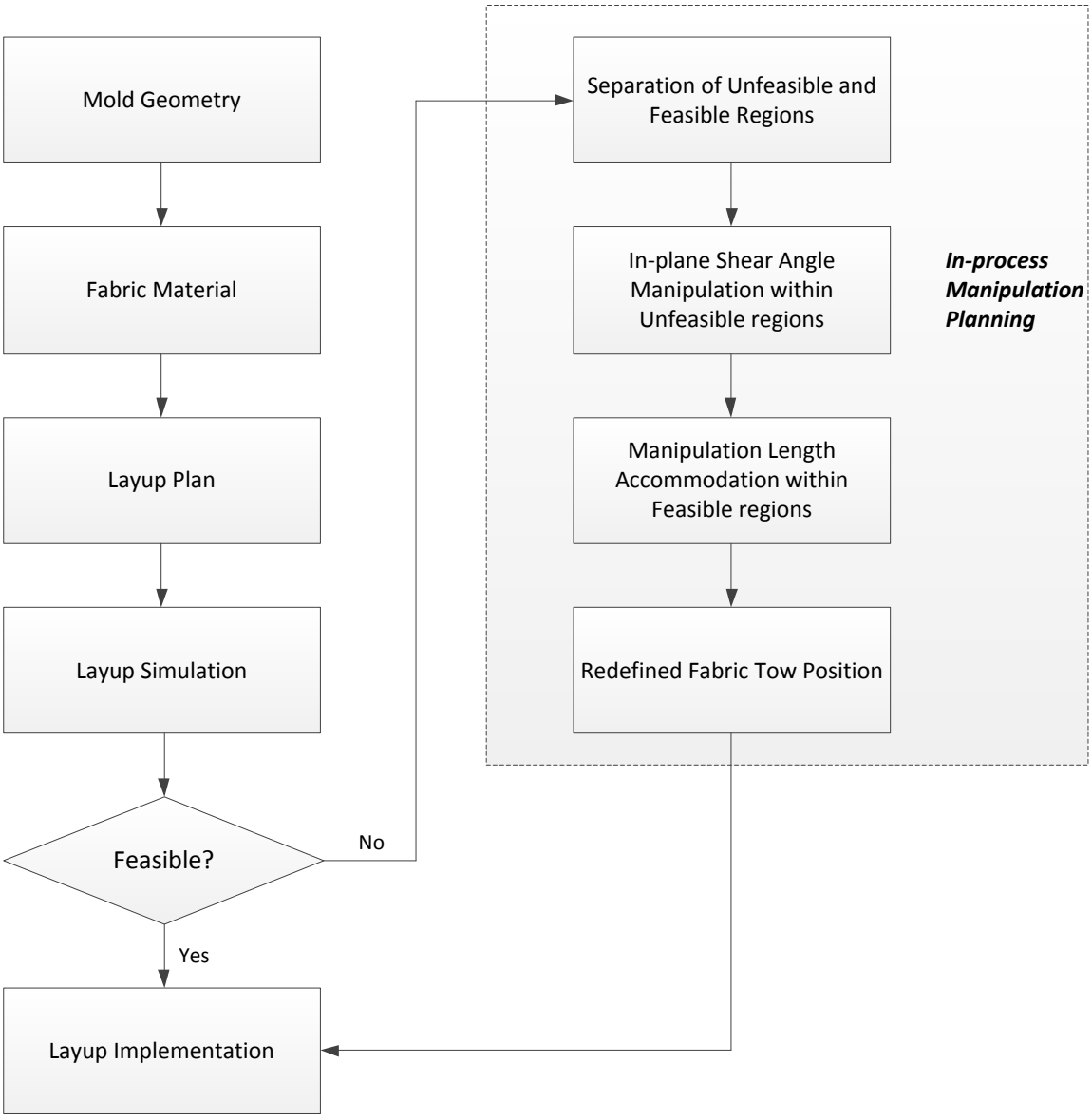

Figure 1. Overview of the solution approach

3. Mold Geometry, Fabric Material and Layup Plan

For the purposes of validation of the simulation model, and verification of the in-process manipulation method, a mold was built. It has convex span-wise shape and concave chord-wise shape (Figure 2). This surface was designed to represent an adapted surface of an actual spar cap mold used in megawatt-scale wind turbine blade manufacturing. Although the

experimental mold is of shorter span, the curvatures chosen for both span-wise and chord-wise directions were more drastic than the actual mold used in industry applications, in order to exaggerate the shearing effects. In a sense, this laboratory mold forces a 3m section of fabric to undergo that typically asked for by a 30m section; allowing wave and wrinkling effects to be exacerbated for easier experimental study.

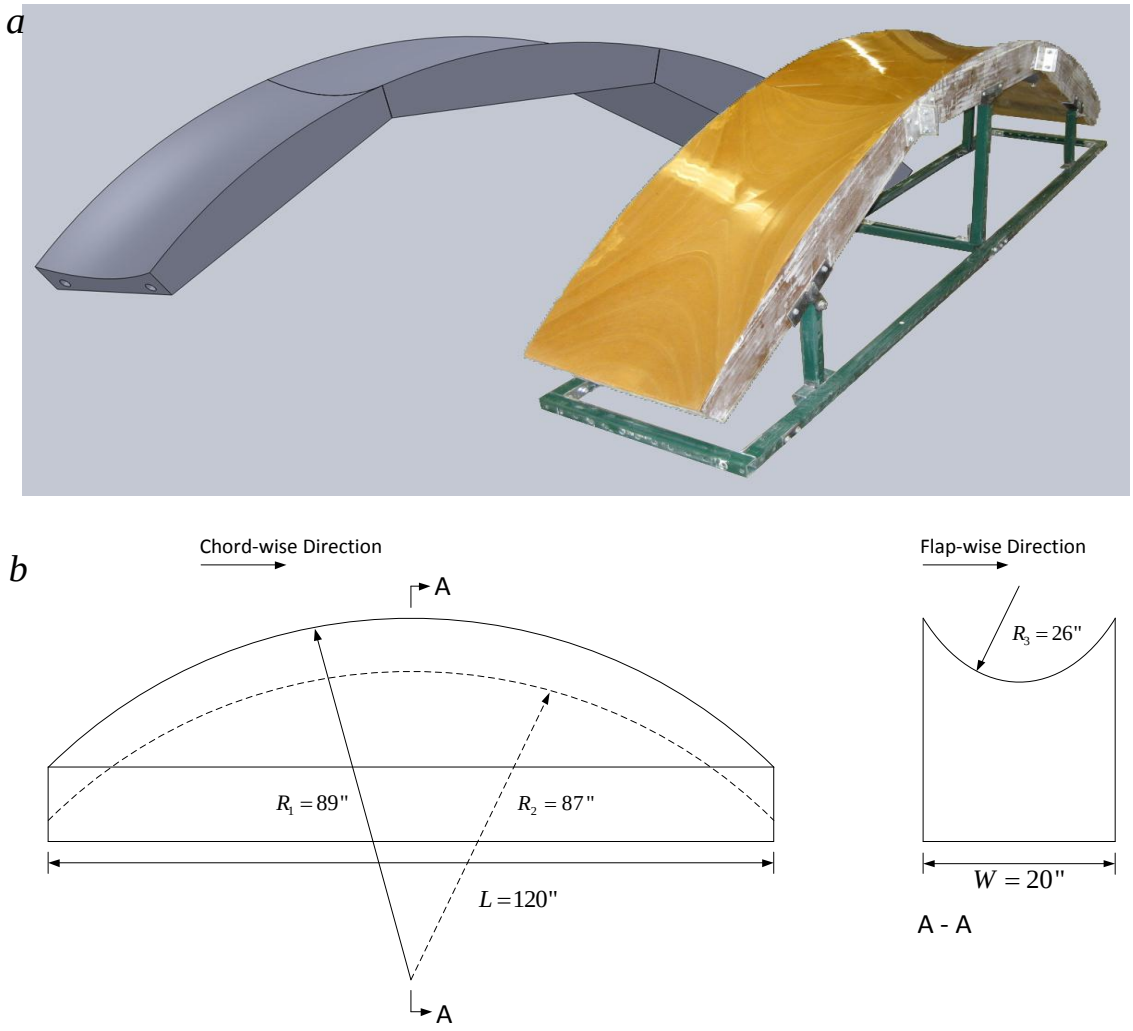

Figure 2. (a) 3D mold used in experiment; (b) mold dimensions.

A piece of 20" wide UD fabric (number of tows: 138; tow spacing: 0.1395") was utilized for the layup process. Following the steps of a typical layup method, the starting line

(constraint) was selected at the starting edge of the chord-wise direction, and the fabric was oriented so that the center tows follow the centerline of the mold. Then the fabric was smoothed toward the ending edge of the mold in chord-wise direction. Figure 3 generally illustrates the layup plan. Note that the methodology provided in this work is a generic solution, not necessarily specific to this mold, fabric and layup plan combination. However, this combination is frequently referred to as a representative example to illustrate important ideas.

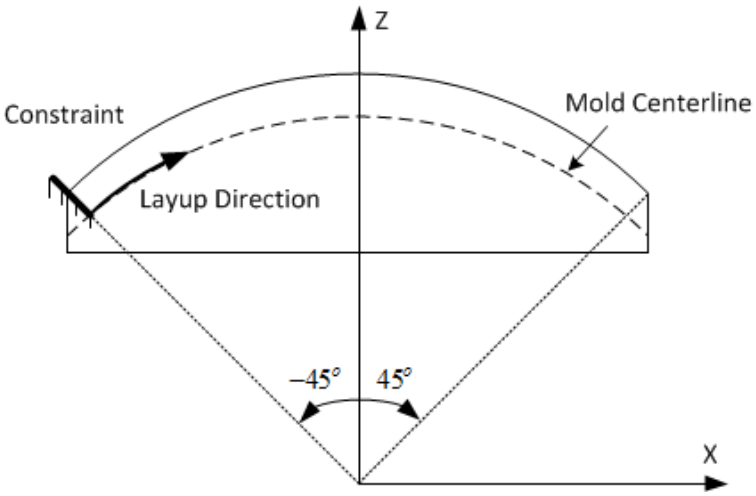

Figure 3. Layup plan

4. Detailed Methodology

4.1 Unit cell deformation model for unidirectional fabrics

The true shear unit cell deformation model (Figure 4) is utilized in the development of the methodology. Different from the pin-jointed shear model, which is usually applied in the picture-frame testing experiments, the true shear model assumes that the volume of the

unit cell conserves during the shear deformation [3]. This model was also validated in [12], where UD fabric was utilized in the layup over a 3D mold.

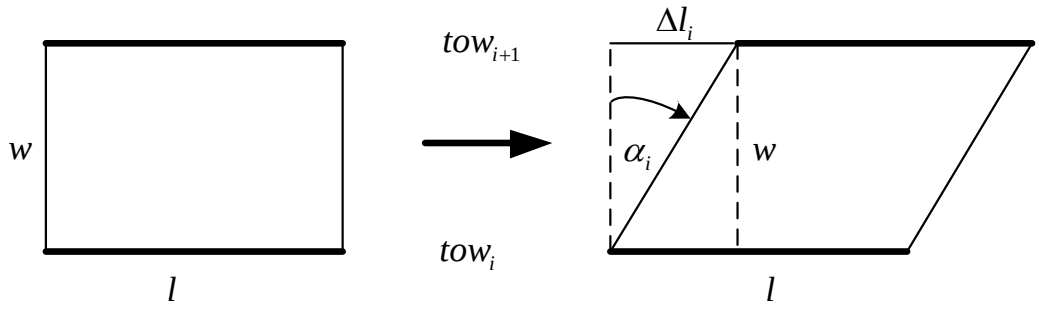

Figure 4. Volume conservation unit cell deformation model

4.2 Layup simulation

A kinematic simulation program in LabVIEW was developed by the authors, based on the true shear unit cell deformation model. This program simulates the typical operation steps of the layup process: firstly, the fabric is placed at the starting line where the fabric initially contacts the mold surface; secondly, a single fabric tow is matched to a certain designated curve on the mold surface, (in practice, a marked curve or a laser projected curve on mold surface is typically utilized); lastly, the fabric is smoothed from the starting line outward toward fabric ply edges. Given mold geometry, fabric properties and process parameters, this program is able to predict IPS angle distribution over the draped fabric surface.

4.3 Naïve layup process

In this work, we will propose using the term *Naïve layup*, referring to a layup approach where the implementation strictly follows the layup plan, regardless of the IPS angle distribution to be obtained. This layup approach is widely used in industrial composites

manufacturing applications; simulation is done to verify a layup only, then specific layup process plans are developed on the manufacturing floor.

The naïve layup approach was simulated for the mold-fabric-layup plan combination given in Section 3. Figure 5 shows the fabric position on the mold surface, while Figure 6 shows the shear angle distribution over the fabric surface (top view). It can be seen in Figure 6 that along the layup direction, the IPS deformation gets larger in magnitude, and the value is reaching 30^o at the ending edge of the mold. If given that the SLL of this fabric is 17^o, then this given layup plan is unfeasible, because the shear angle value between the bottom tow pair reaches 17^o at $x = 6$ inches past the middle of the mold length. The next sub-section will introduce the method of in-process manipulation, which will attempt to provide a solution to an infeasible layup such as this.

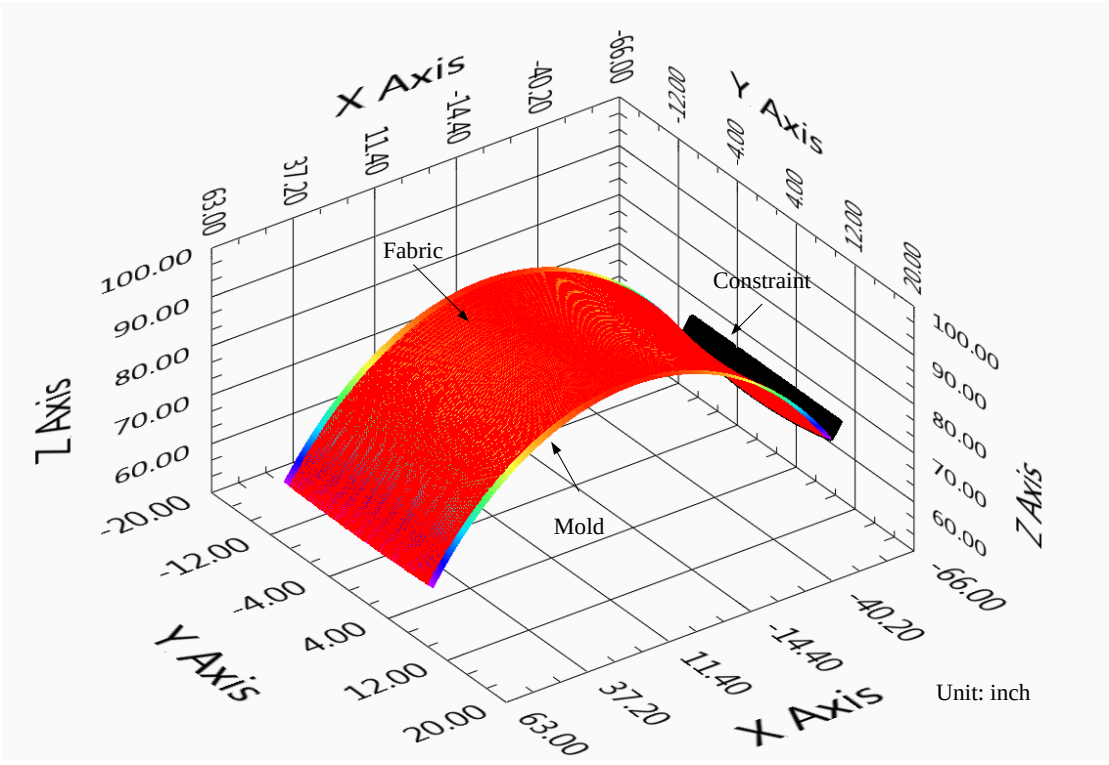

Figure 5. Layup simulation – fabric position

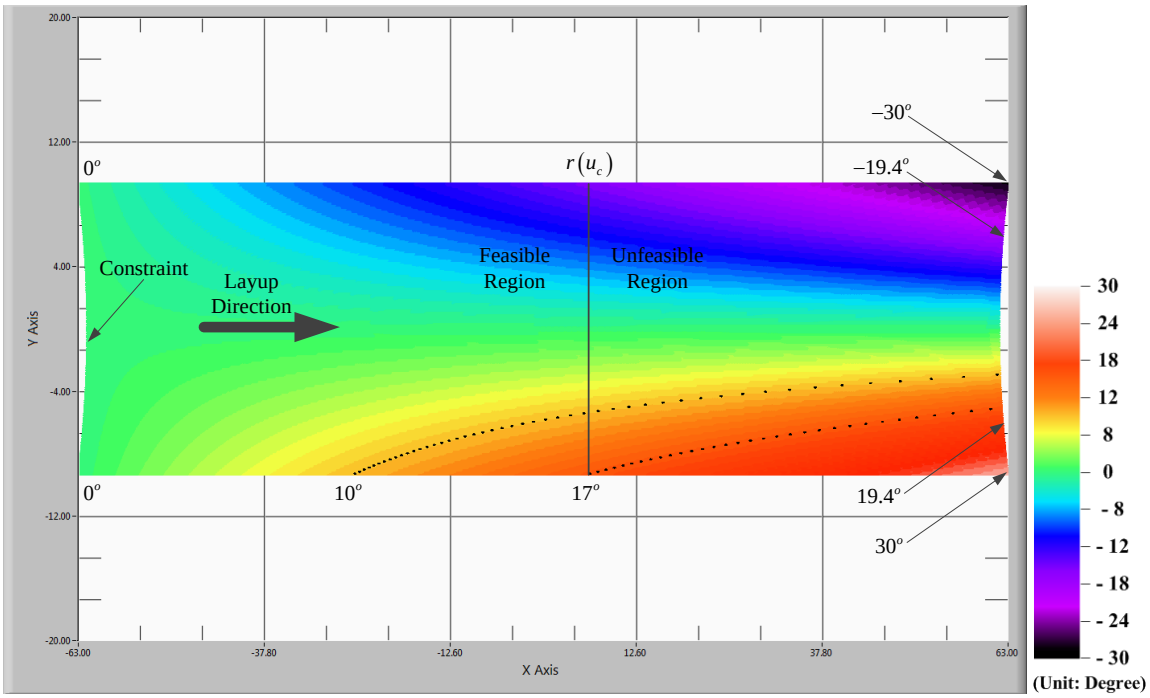

Figure 6. IPS distribution for naïve layup approach (top view)

4.4 In-process manipulation planning

Although the pre-shearing method [9] can improve the drapability of the fabric, the resulted layup process may still be unfeasible. The method of in-process manipulation planning provides a more robust solution to the feasibility problems of the layup process.. The manipulation involves two phases of actions. Firstly, in an unfeasible region, prescribed manipulations will further shear the fabric within the fabric surface, and the objective is to either drive IPS values to within the SLLs, or push the push the point where SLL is reached further down the mold. Secondly, these prescribed manipulation lengths are accommodated as acceptable waves in the neighboring upstream feasible region. This two-phased manipulation approach is applied to all the neighboring pairs of feasible-unfeasible regions along the lay direction, until all the IPS values are within SLLs.

4.4.1 Determination of feasible and unfeasible regions

Based on the shear angle distribution obtained from a given layup simulation, the first step of this method is to divide the fabric surface into feasible and unfeasible regions. The following parameters are defined:

$p(u)$ $(u_a \le u \le u_b)$: the layup guide curve, where u_a and u_b represent the starting and ending points, respectively.

$q(u)$: the plane at position u , which is orthogonal to $p(u)$,

$r(u)$: the intersection curve between $p(u)$ and the fabric surface.

$\alpha_{i,r(u)}$: the shear angle value for the i^{th} tow pair, on $r(u)$

A feasible region can be defined as a continuous region within the fabric surface such that $\underset{i}{Max}\left\{\left|\alpha_{i,r(u)}\right|\right\} \le \alpha_{SLL}$. For example, in Figure 6, the curve $r(u_c)$ divides the fabric into a feasible region ($u_a \le u \le u_c$), and an unfeasible region ($u_c < u \le u_b$).

4.4.2 Effect of manipulation at the unit cell level in the unfeasible region

Figure 7 shows the effect of in-process manipulation at the unit cell level for the unfeasible region, where $\alpha_{i,j}$ is the shear angle at the j^{th} pair of node ($N_{i,j}$ and $N_{i+1,j}$) on the i^{th} pair of neighboring tows, obtained from the naïve layup method; $\alpha_{Mi,j}$ is the shear angle after manipulation at the corresponding location, and Δl_i is the manipulation length. Geometrically, at the j^{th} pair of node,

$$\Delta l_i = -\left[\left(\tan\alpha_{i,j}\right)\times w - \left(\tan\alpha_{Mi,j}\right)\times w\right] = w\times\left(\tan\alpha_{Mi,j} - \tan\alpha_{i,j}\right), \forall j \qquad (1)$$

and therefore,

$$\tan\alpha_{Mi,j} = \tan\alpha_{i,j} - \frac{\Delta l_i}{w}. \quad (2)$$

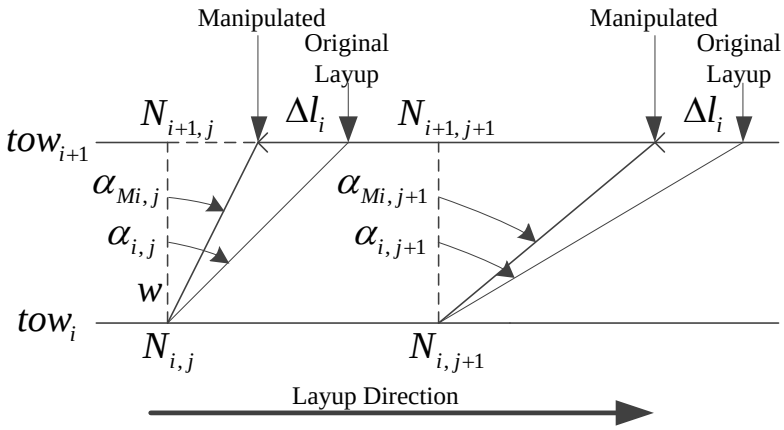

Figure 7. Effect of in-process manipulation on unit cell deformation

4.4.3 Algorithm: in-process manipulation length planning

To begin a presentation of the algorithm for the determination of Δl_i s', critical parameters are defined as follows:

$\underset{j\in UF}{Min}\{\tan\alpha_{i,j}\}$: the minimum tangent value among shear angles, obtained from the naïve layup, up to the j^{th} node within the unfeasible region, for the i^{th} tow pair.

$\underset{j\in UF}{Max}\{\tan\alpha_{i,j}\}$: the maximum tangent value among shear angles, obtained from the naïve layup, up to the j^{th} node within the unfeasible region, for the i^{th} tow pair.

$\underset{j\in UF}{R}\{\tan\alpha_{i,j}\} = \underset{j\in UF}{Max}\{\tan\alpha_{i,j}\} - \underset{j\in UF}{Min}\{\tan\alpha_{i,j}\}$: the range of tangent values among shear angles obtained from the layup after pre-shear up to the j^{th} node within the unfeasible region for the i^{th} tow pair.

Case A: $\underset{j\in UF}{R}\{\tan\alpha_{i,J}\}\le 2\times\tan\alpha_{SLL}$. In this case, the range of the tangent of shear angles is within twice the tangent of shear locking limit. Two sub-cases are possible.

Case A-I: $\underset{j\in UF}{Max}\left\{\left|\tan\alpha_{i,J}\right|\right\}\le\tan\alpha_{SLL}$, which means this i^{th} pair of tows are feasible. Thus, no manipulation is needed, so $\Delta l_i=0$.

Case A-II: $\underset{j\in UF}{Max}\left\{\left|\tan\alpha_{i,J}\right|\right\}>\tan\alpha_{SLL}$, then:

if $\underset{j\in UF}{Max}\left\{\tan\alpha_{i,J}\right\}>\tan\alpha_{SLL}$,

$$\Delta l_i=-w\times\left(\underset{j\in UF}{Max}\left\{\tan\alpha_{i,J}\right\}-\tan\alpha_{SLL}\right); \tag{3}$$

if $\underset{j\in UF}{Min}\left\{\tan\alpha_{i,J}\right\}<-\tan\alpha_{SLL}$,

$$\Delta l_i=-w\times\left(\tan\alpha_{SLL}+\underset{j\in UF}{Min}\left\{\tan\alpha_{i,J}\right\}\right). \tag{4}$$

The purpose of manipulation for Case A in the algorithm is to shift the interval of shear angles so that they are within the range of shear locking limits. For in-process manipulation, minimum shifting distances are desired, because accommodating these shifting distances will be at the cost of losing geometric conformity of the fabric surface, as will be shown in 4.4.4.

Case B: $\underset{j\in UF}{R}\{\tan\alpha_{i,J}\}>2\times\tan\alpha_{SLL}$. In this case, the range of the tangent of shear angles is outside twice the tangent of shear locking limit, therefore, the interval $\left[\underset{j\in UF}{Min}\{\tan\alpha_{i,J}\},\underset{j\in UF}{Max}\{\tan\alpha_{i,J}\}\right]$ cannot be shifted into the acceptable interval of

$[-\tan\alpha_{SLL}, \tan\alpha_{SLL}]$. A cumulative range checking method, as shown in Figure 14, was developed to determine the value of Δl_i for this case.

Starting from the first node within the unfeasible region, this method calculates $\underset{j\in UF}{R}\{\tan\alpha_{i,j}\}$ with increasing j value continuously, until the L^{th} node is reached, where $\underset{j\in UF}{R}\{\tan\alpha_{i,L}\} > 2\times\tan\alpha_{SLL}$. It can be proved (see *proof* in the Appendix) that only two sub-cases exist under this condition. Case B-I is $\underset{j\in UF}{Max}\{\tan\alpha_{i,L}\} > \tan\alpha_{SLL}$, where the pre-shearing length is determined as:

$$\Delta l_i = -\left(\underset{j\in UF}{Min}\{\tan\alpha_{i,L-1}\} + \tan\alpha_{SLL}\right)\times w. \tag{5}$$

Case B-II is $\underset{j\in UF}{Min}\{\tan\alpha_{i,L}\} < -\tan\alpha_{SLL}$, where the pre-shearing length is determined as:

$$\Delta l_i = \left(\tan\alpha_{SLL} - \underset{j\in UF}{Max}\{\tan\alpha_{i,L-1}\}\right)\times w. \tag{6}$$

The purpose of manipulation for Case B is to push the location of the problem ($\underset{j\in UF}{Max}\left\{\left|\tan\alpha_{i,j}\right|\right\} > \tan\alpha_{SLL}$) as far as possible downstream along layup direction, as shown in Figure 9.

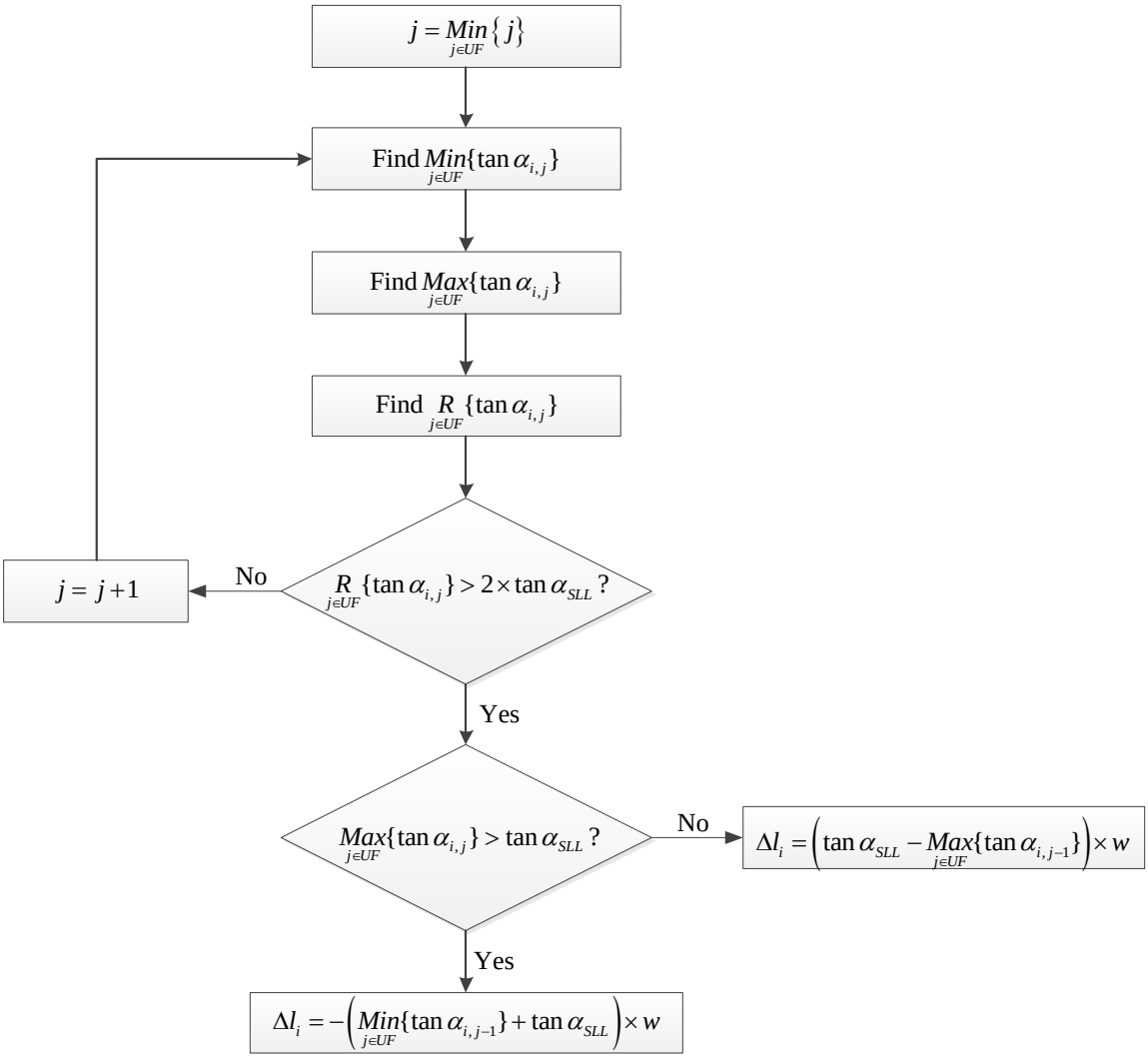

Figure 8. Cumulative range checking method for in-process manipulation

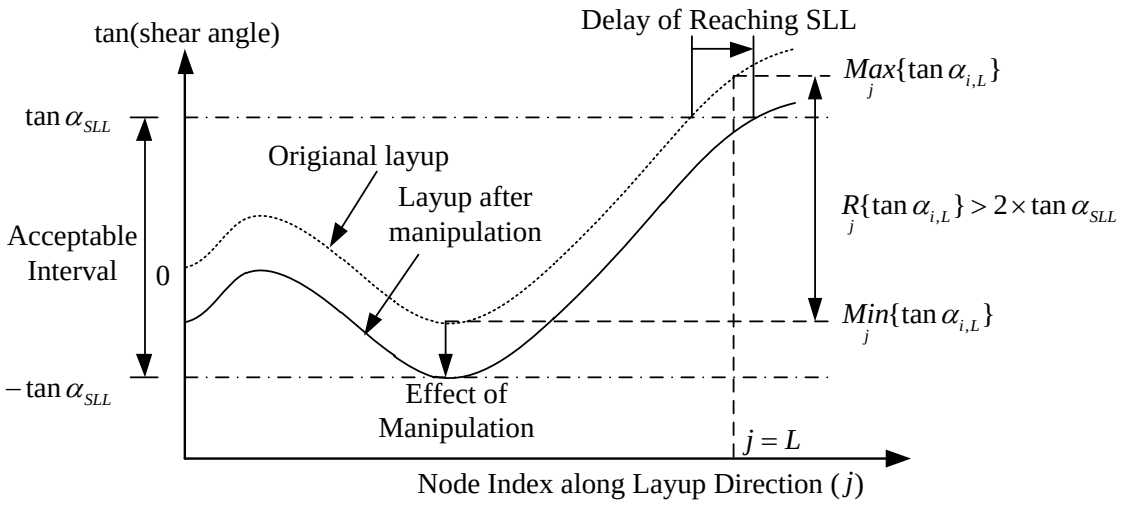

Figure 9. Effect of manipulation on IPS deformation in Case B

In addition to giving the needed length for in-process manipulation, the algorithm also shows that the unfeasible region can be modified to be feasible, or at least, be pushed downstream along the layup direction. This algorithm can be recursively applied to the unsolved unfeasible regions, until they all become feasible.

4.4.4 Accommodation of in-process manipulation length

The in-process manipulation length Δl_i for individual tow pairs was planned based on the shear angle distribution within the unfeasible regions. This Δl_i has to be accommodated into a single or multiple zones within the corresponding feasible regions. Two effects will be introduced by this accommodation. Firstly, the Δl_i changes the length difference between the i^{th} tow pair within the accommodation zones, where the tow pair (or at least one of them) will not be able to conform to the mold surface, resulting in OOM deformations. Secondly, shear angle distribution within and after the accommodation zone

will change due to the generation of OOM deformation, which is equivalent to layup on a mold with modified geometry.

Selection of the accommodation zone. Within the feasible region, the shear angle distribution map obtained from original layup (for example, the one in Figure 6) can be used to determine the capacity for accommodating Δl_i s'. If $\Delta l_i > 0$, the largest absolute length difference that can be accommodated at the j^{th} node on i^{th} tow pair is (maximum forward capacity):

$$Max\left|\Delta l_{i,j}\right| = \left[\left(\tan\alpha_{SLL}\right)\times w - \left(\tan\alpha_{i,j}\right)\times w\right]. \tag{7}$$

If $\Delta l_i < 0$, the largest absolute length difference that can be accommodated at the j^{th} node on i^{th} tow pair is (maximum backward capacity):

$$Max\left|\Delta l_{i,j}\right| = \left[\left(\tan\alpha_{SLL}\right)\times w + \left(\tan\alpha_{i,j}\right)\times w\right]. \tag{8}$$

The relative capacity (RC) is defined as:

$$RC_{i,j} = \frac{Max\left|\Delta l_{i,j}\right|}{\left|\Delta l_i\right|}, \tag{9}$$

and $RC_{i,j} = 100\%$ if $\Delta l_i = 0$. Because accommodating Δl_i within the interval between nodes $j = k - n$ and $j = k$ will result in the same change in the tangent value of shear angles at downstream nodes $j = k+1, k+2, ..., J$, the relative capacity in (9) has to be adjusted so that $RC_{i,j} \le RC_{i,k}$, for any $j < k$. The method to obtain the adjusted relative capacity (ARC) is by comparing the RC value upstream the layup direction, from the last pair of nodes within the feasible region: if $RC_{i,j} < RC_{i,j-1}$, then $ARC_{i,j-1} = RC_{i,j}$, otherwise $ARC_{i,j-1} = RC_{i,j-1}$. The ARC reflects the actual relative capacity in accommodating $\Delta l_i'$ s.

The manipulation length can also be distributed into multiple accommodation zones. Assuming that a number of M accommodation zones are selected, and let p_m be the fraction of the manipulation length to be accommodated in the m^{th} zone, then the following relationships must be satisfied: $\sum_{m=1}^{M} p_m = 1$, $\sum_{m=1}^{M} \left(p_m \times \Delta l_i \right) = \Delta l_i$. These fractions of manipulation length must be sequentially accommodated, and the order should follow their position along the layup direction, with the one nearest to the constraint accommodated first. This is because after each fraction of manipulation length is accommodated, the IPS map changes for the portion within and downstream the accommodation zone. Correspondingly, the ARC map changes, based on which the next fraction of the manipulation length is accommodated.

In addition to capacity, other factors should also be considered in the selection of accommodation zones. For example, in the fabrication of a load carrying composite structure, high stress regions should be avoided from accommodating the manipulation length.

Tow length determination in accommodation zones. The manipulation length is the length difference between certain pairs of tows that has to be created during manipulation. New tow lengths have to be determined in order to achieve the differences. The following parameters are defined to derive the new tow length within the accommodation zones:

Δl_i^o : original tow length difference between the i^{th} pair of tows within the accommodation zones.

Δl_i^N : new tow length difference between the i^{th} pair of tows within the accommodation zones.

l_i^o : original tow length for the i^{th} tow within the accommodation zones.

l_i^N : new tow length for the i^{th} tow within the accommodation zones.

For any neighboring pair of tows, the new length difference is equal to the length difference that has to be accommodated plus the original length difference within the accommodation zones. Therefore,

$$\Delta l_i^N = \Delta l_i^o + \Delta l_i \,. \tag{10}$$

Assume that within the accommodation zone, the new length of the first tow is $l_1^{N'} = 0$, then the tentative new length of the rest of the tows are:

$$l_i^{N'} = \sum_{k=1}^{i-1} \Delta l_i^N \,(i \geq 2)\,. \tag{11}$$

These tentative new tow lengths will be uniformly increased by the distance M, where

$$M = \underset{i}{Min}\left\{ l_i^{N'} - l_i^o \right\}, \tag{12}$$

in order to obtain the new tow lengths:

$$l_i^N = l_i^{N'} + M \,. \tag{13}$$

In this way, the new length(s) for tow(s) satisfying (12) will be equivalent to the original length, which means it (they) will conform to the mold surface. Whereas for the rest of the tows, their new lengths will be greater than the corresponding original lengths, so OOM deformation will be required in the accommodation zones.

Form of accommodation. When $l_i^N > l_i^o$, there can be infinitely many ways of arranging l_i^N into the accommodation zones. A baseline method is presented in this sub-section, which can be modified according to specific layup requirements to achieve optimal results.

For a specific accommodation zone on the i^{th} tow, the average normal direction can be found, which serves as the local Z direction. Selection of X and Y directions can be arbitrary. Then the original tow curve within the accommodation zone can be represented as $r_o(t)_i = \left(x_o(t)_i, y_o(t)_i, z_o(t)_i\right),\ t \in [0, 2\pi]$. The new tow can be represented as $r_N(t)_i = \left(x_N(t)_i, y_N(t)_i, z_N(t)_i\right),\ t \in [0, 2\pi]$, where $x_N(t)_i = x_o(t)_i$, $y_N(t)_i = y_o(t)_i$, and

$$z_N(t)_i = z_o(t)_i + A_i \times (1 - \cos t),\ t \in [0, 2\pi], \tag{14}$$

where A_i is determined as the value that makes the length of curve $r_N(t)_i$ equal to l_i^N.

Because the first order derivative of the function $g(t) = A \times (1 - \cos t)$ is equal to zero at $t = 0$ and $t = 2\pi$, the curve joined by $r_N(t)_i$ section and the original tow curve sections outside the accommodation zone will share a common tangent direction at the join point, which means the new curve will be of C^1 continuity. Each of these new tows may have a waved section or sections above its nominal position, and these waves together form the waved regions, which are the OOM deformations for the fabric surface.

4.4.5 Control of loss in geometric conformity

In the composite structure manufacturing industry, a common measure of geometric conformity is the size of the waves. Aspect ratio (AR) is typically utilized to indicate the

relative severity of a wave. AR is defined as twice of reciprocal of the local maximum absolute slope value over a waved tow,

$$AR_i = 2 \times \frac{1}{\underset{j}{Max}\left\{\left|dz_i / dw_{i,j}\right|\right\}}, \tag{15}$$

where $w_{i,j}$ is in the direction $W_{i,j}$, which is orthogonal to Z, and within the plane formed by Z and the tangent direction ($T_{i,j}$) of the i^{th} tow at node j (Figure 10).

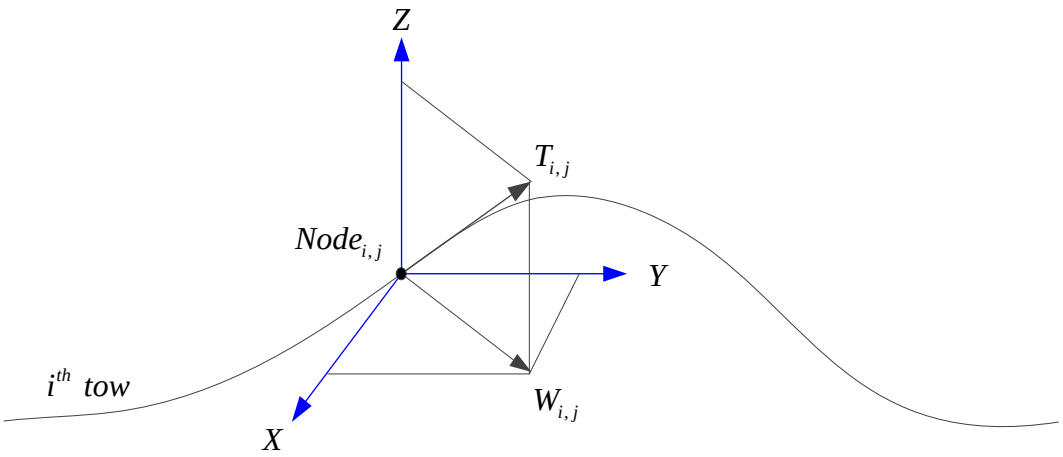

Figure 10. Local coordinate system for computing aspect ratio

It can be inferred from (15) that the larger AR is, the less severe the wave is, and therefore the fabric has better geometric conformity to the mold surface. In industrial practices, minimum AR values are designated as thresholds for different locations on mold. Waves with ARs greater than these threshold values at the corresponding locations are considered within the manufacturing tolerance, and therefore they are acceptable. Some guidelines are provided here to control the AR of prescribed waves:

(1) Use multiple accommodation zones, so that each zone has a fraction of the manipulation length $\Delta l_i'$ to be accommodated, resulting in less severe waves.

(2) Allocate the fractions of $\Delta l_i'$ according to the local threshold value of AR, so that local tolerance can be fully utilized to minimize the number of wave regions.

5. Implementation

The in-process manipulation method was implemented for the fabric-mold-layup process combination described in Section 3. The Algorithm was applied to shear angle distribution obtained from the naïve layup method given in Figure 6. Figure 11 (a) and (b) show the change in shear angle distribution due to manipulation within the unfeasible region. The manipulation lengths, $\Delta l_i's$ are given in Figure 12.

Following the parameters defined in 4.4.1, let $u \equiv \theta$, where θ is the angular position of the mold along the layup direction. Therefore, $-45^o \le u \le 45^o$ (see Figure 3), and $u_c = 4.01^o$. It can be verified by (7) and (8) that the entire feasible region shown in Figure 5 has $ARC \ge 100\%$ for each neighboring pair of tows. The region bounded by $r(-10^o)$ and $r(-5^o)$ was selected as the common accommodation zone of the manipulation length for all the tows. Following (10) ~ (13), the manipulation length and the new tow lengths can be calculated, which are shown in Figure 13 and Figure 14, respectively. These new tow lengths were accommodated in the form defined by (14). Figure 15 shows the new positions of all tows after manipulation, and Figure 16 shows the corresponding shear angle distribution. Figure 17 shows the positional deviation (measured along local normal direction of the mold surface) within the accommodation zone.

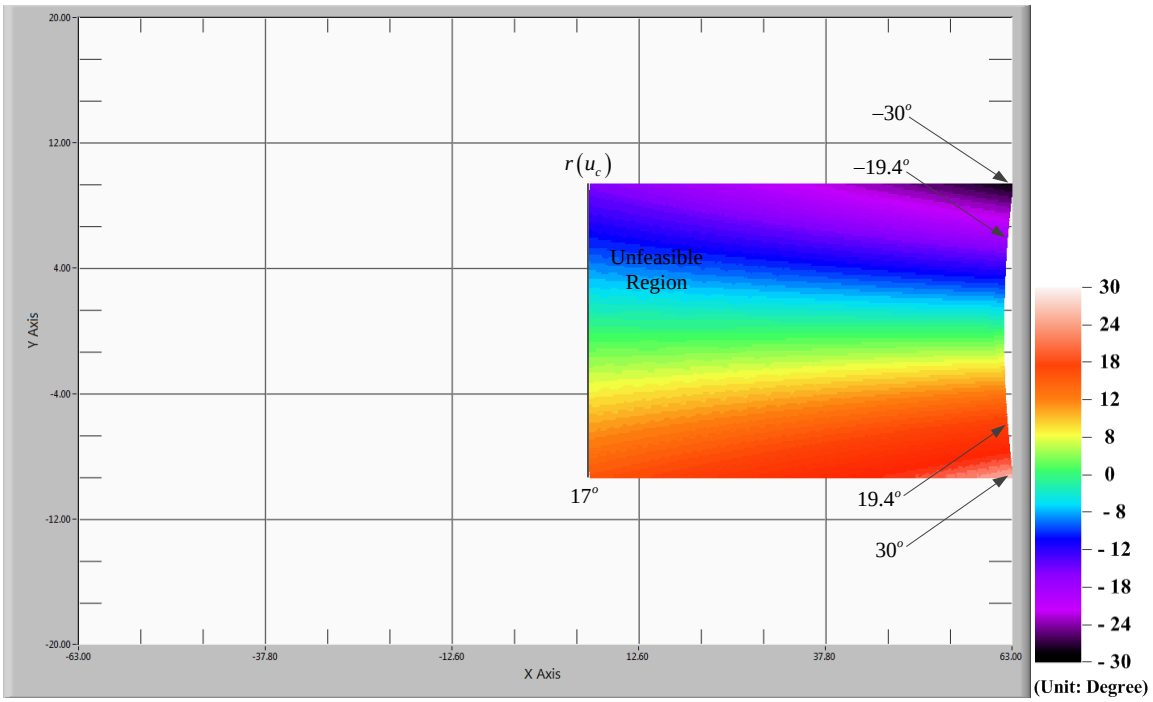

Figure 12 (a). Unfeasible region of Figure 6 before manipulation

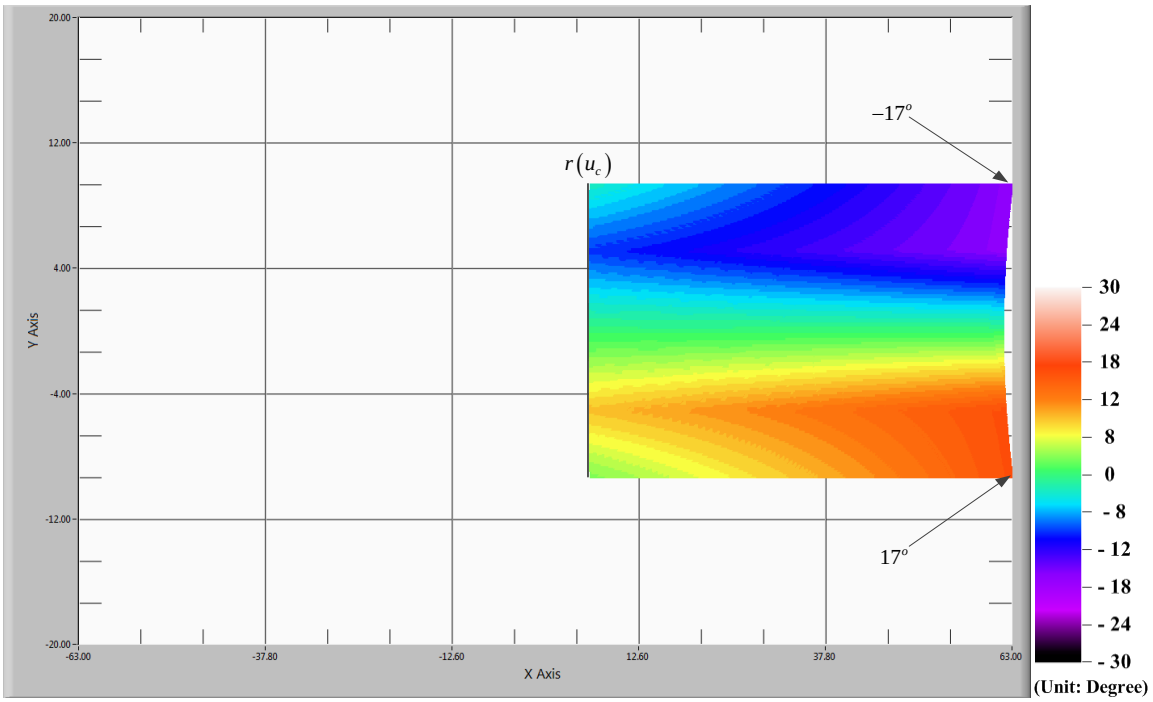

Figure 12 (b). Unfeasible region of Figure 6 after manipulation

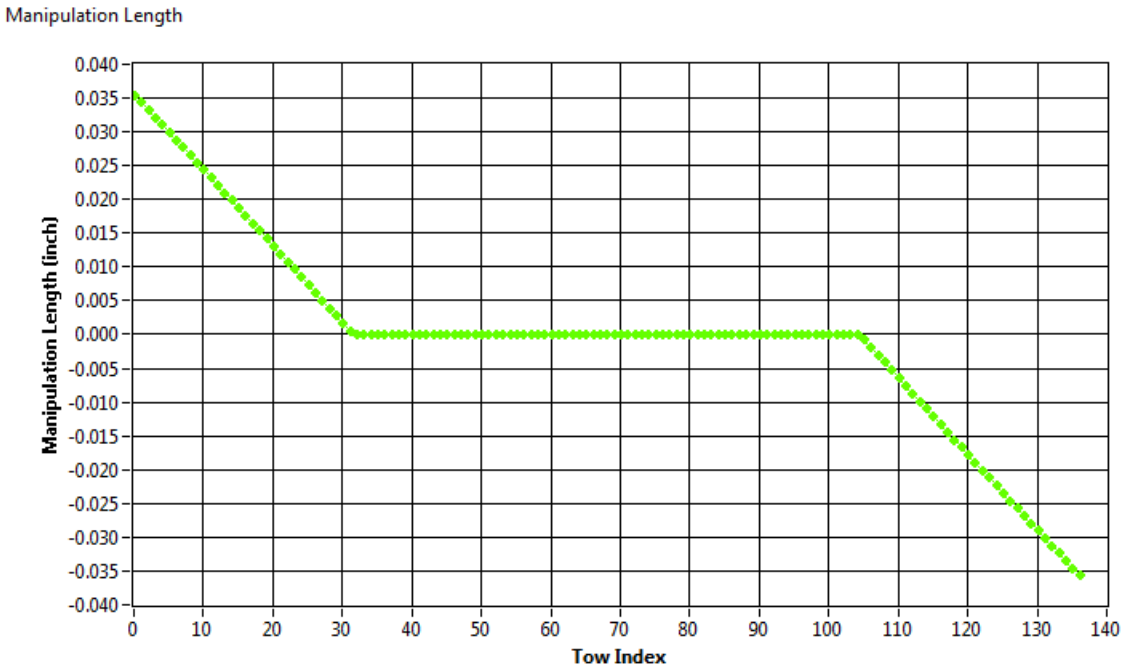

Figure 13 In-process manipulation lengths

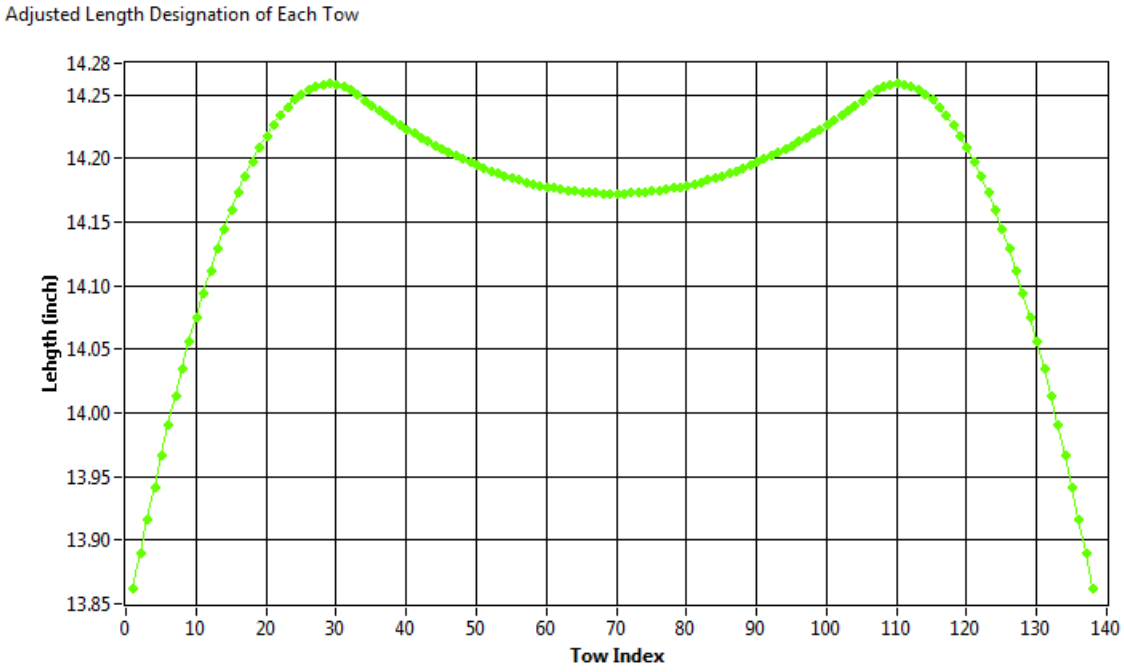

Figure 14. New tow lengths within the accommodation zone

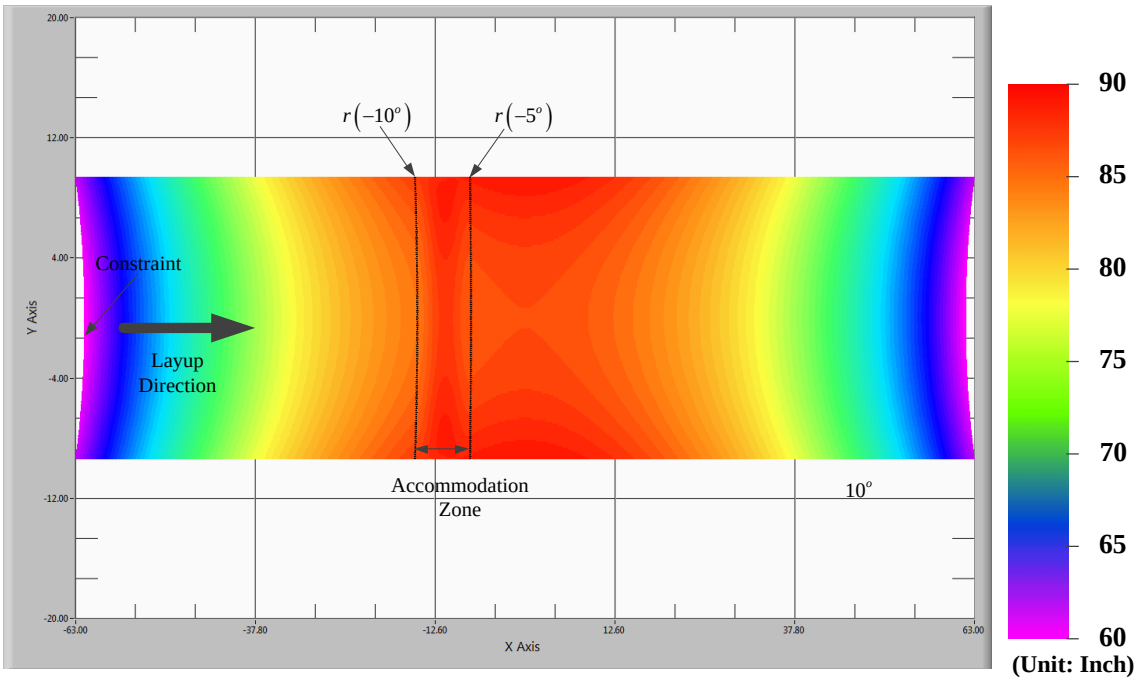

Figure 15. New tow positions after in-process manipulation

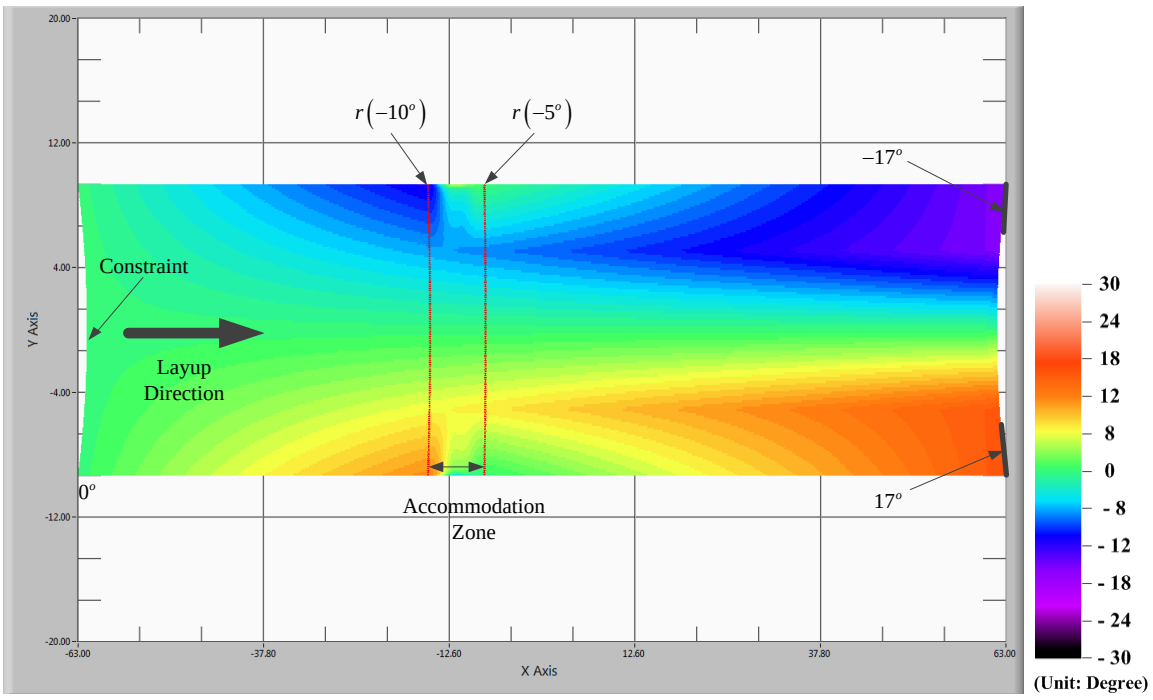

Figure 16. Shear angle distribution for na ïve layup after manipulation

– Sing accommodation zone

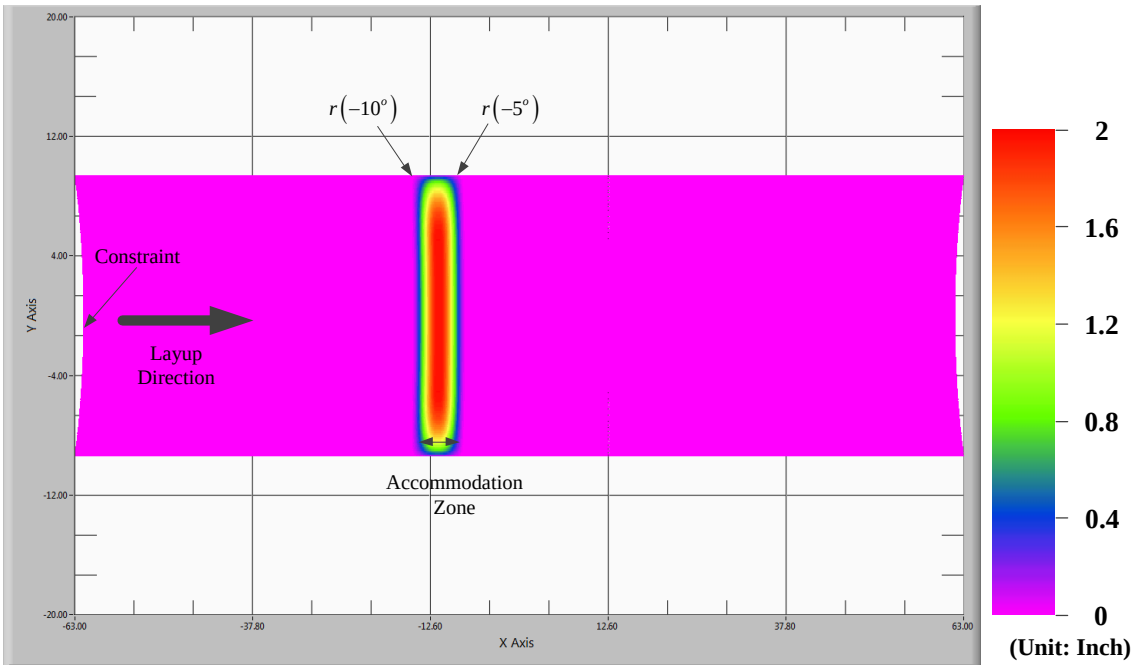

Figure 17. Position deviation map – Single accommodation zone

The changes from Figure 6 to Figure 16 demonstrates the effectiveness of the in-process manipulation method on the improvements over the naïve layup method, changing an unfeasible layup plan to a feasible one. Although it is shown in Figure 16 that all of the shear angle values are within the SLLs, allocating all the manipulation length into a single accommodation zone will introduce significant loss in geometric conformity. As seen in Figure 17, the maximum positional deviation is 1.64 inch, and the minimum AR is calculated to be 3.49; which could very easily fall outside of typical manufacturing tolerance.

In order to reduce the geometric conformity of the fabric, an alternative allocation scheme was also implemented, where the each of the manipulation length is divided into three equal length fractions and accommodated into three zones sequentially. Figure 18 – Figure 20 show the progressive change in IPS distribution across the fabric, where the unfeasible region shrinks and disappears. While satisfying the shear angle feasibility

requirement, Figure 21 shows that this new scheme has the maximum position deviation of 0.59 inch, and the minimum AR is calculated to be 4.64, which could be closer to within manufacturing tolerance; as compared to the first scheme.

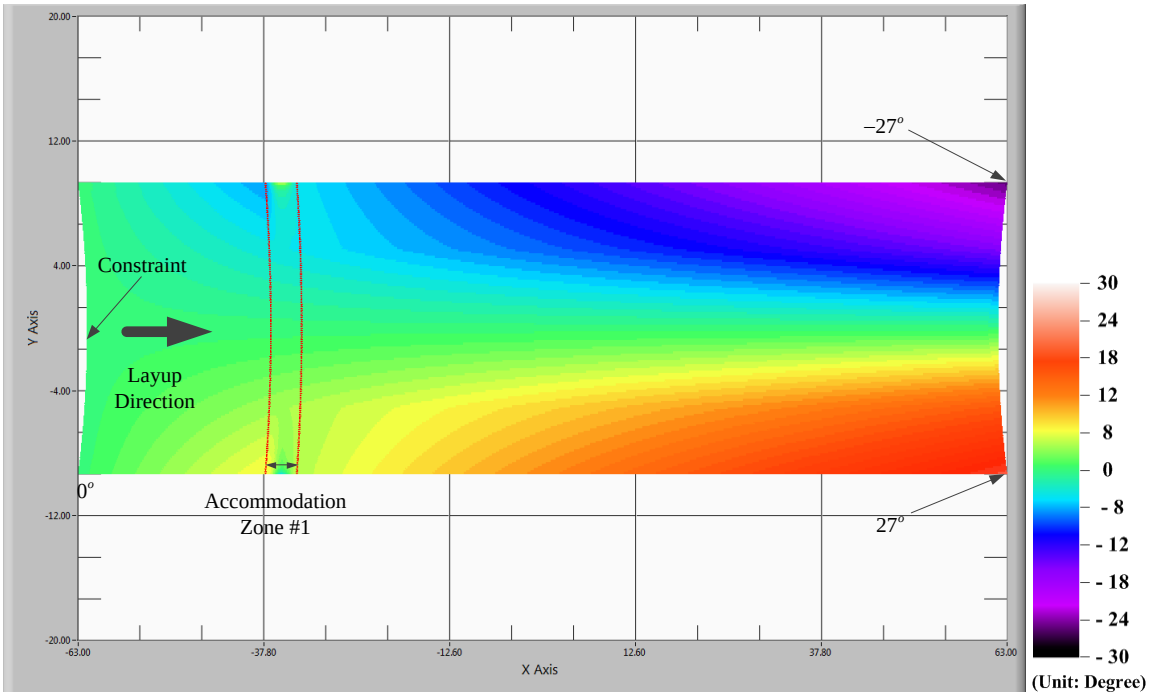

Figure 18. Shear angle distribution after the accommodation of first manipulation length fraction (Three accommodation zones design)

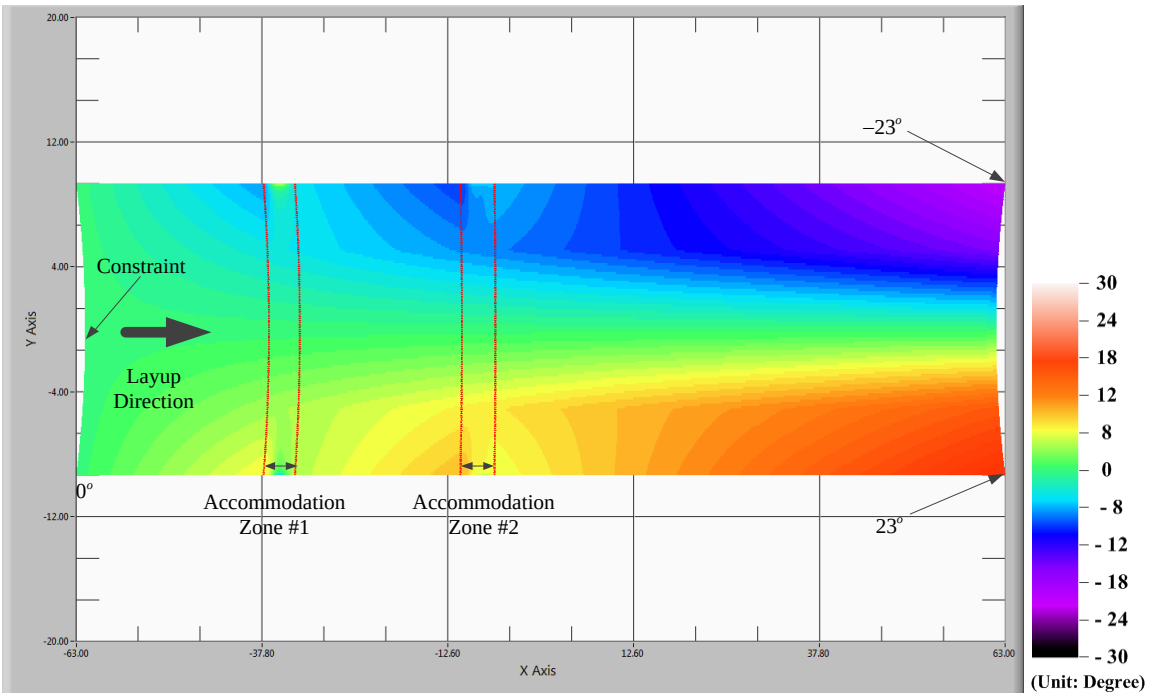

Figure 19. Shear angle distribution after the accommodation of first and second manipulation length fractions (Three accommodation zones design)

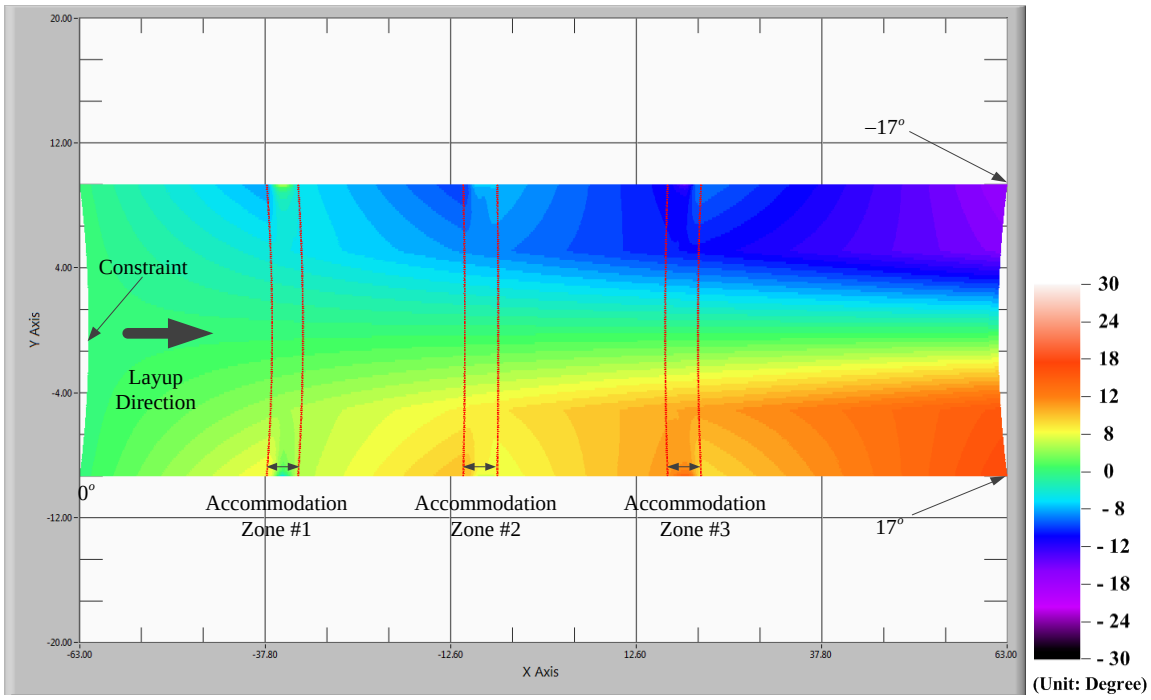

Figure 20. Shear angle distribution after the accommodation of all manipulation length fractions (Three accommodation zones design)

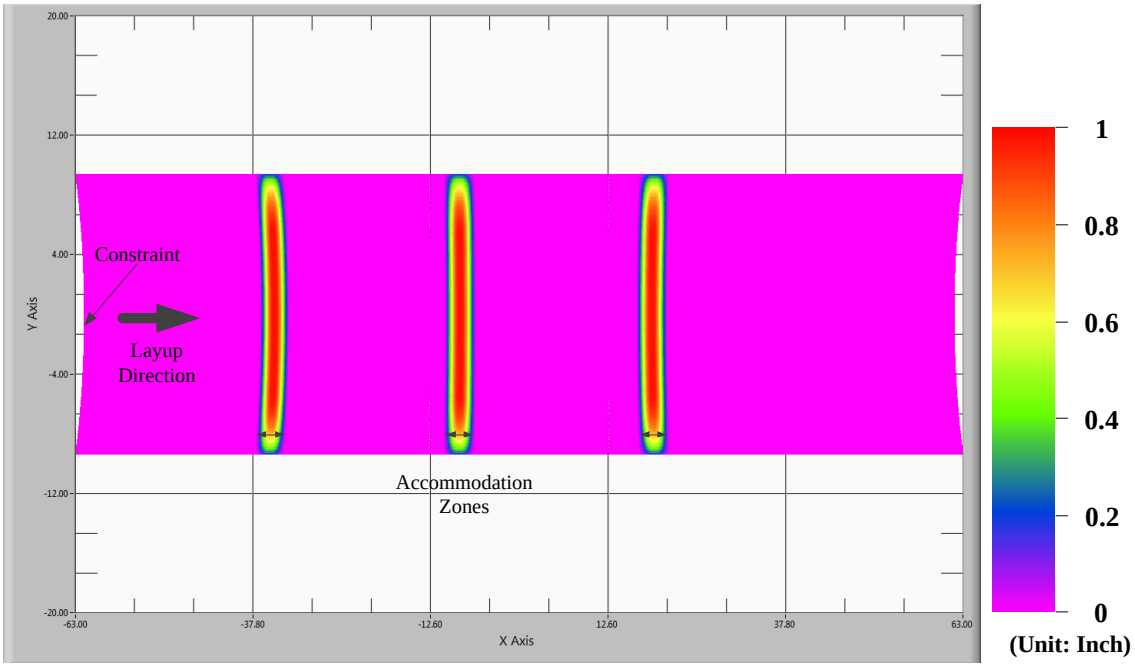

Figure 21. Positional deviation map – Three accommodation zones

The in-process manipulation planning method could be readily applied to the industry to improve the manufacture of composite structures; however, another application is to provide design considerations for manufacturability. For instance, typical design requirements in the aerospace and wind energy industries emphasize aerodynamic characteristics and structural strength. Sometimes the designed composite part cannot be produced at the layup stage, because the designed geometries are too complex for the fabric to conform. The example in Figure 6 shows that, if the naïve/direct layup method is applied, SLL will be reached in the middle of the layup process.

The positional deviation map, for example, the one in Figure 21, can be utilized as a mold shape design modification guide. The modified mold shape is obtained by superposing the positional deviation map to the original mold shape. Layup onto this modified mold shape will guarantee that the IPS angle is within in SLLs' at any location. This design for manufacturability approach was experimentally verified. The positional deviation map (Figure 21) was superposed to the original mold shape (Figure 2), in order to generate the 3D shape of modified mold. Figure 22 shows this modified mold's shape within one of the three accommodation zones. During the implementation, plastic patches were made according to this shape, and then attached to the original mold, as shown in Figure 23. Figure 24 shows the layup result following the naïve approach on the original mold, where a large-sized wave was generated when the IPS reached the SLL. Figure 25 shows the layup on the mold with modified shape. It can be seen that the fabric totally conformed to the mold surface, suggesting a successful layup result.

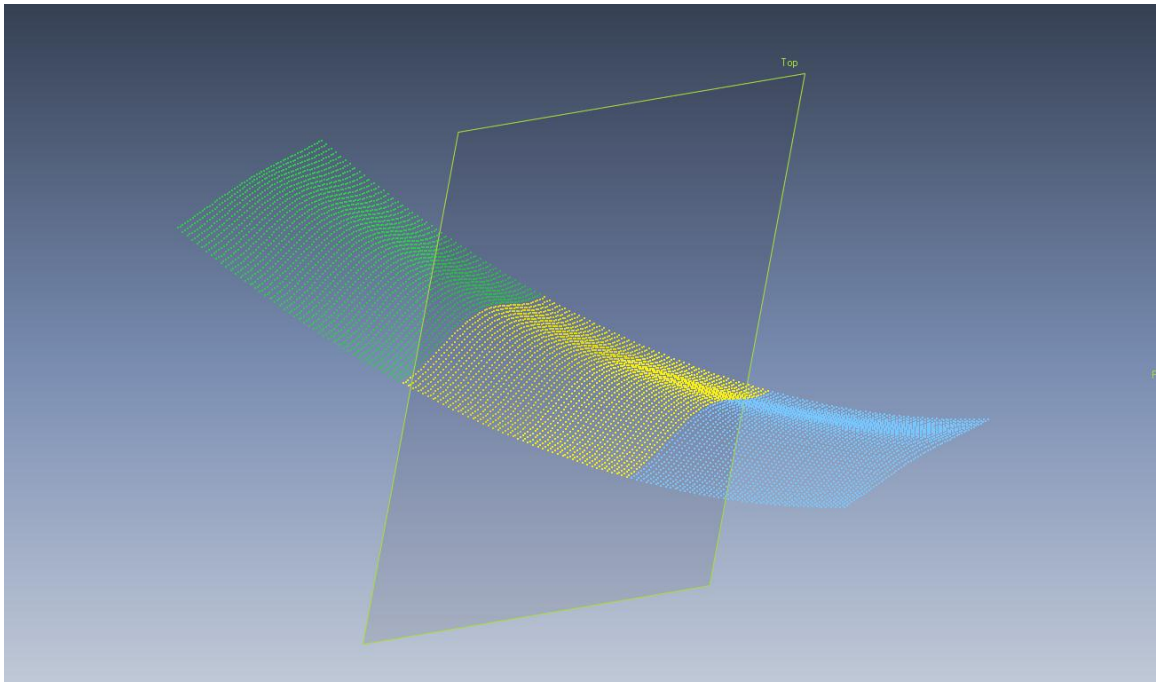

Figure 22. 3D shape of the modified mold in one accommodation zone

Figure 23. Plastic patch made for the modification of mold shape

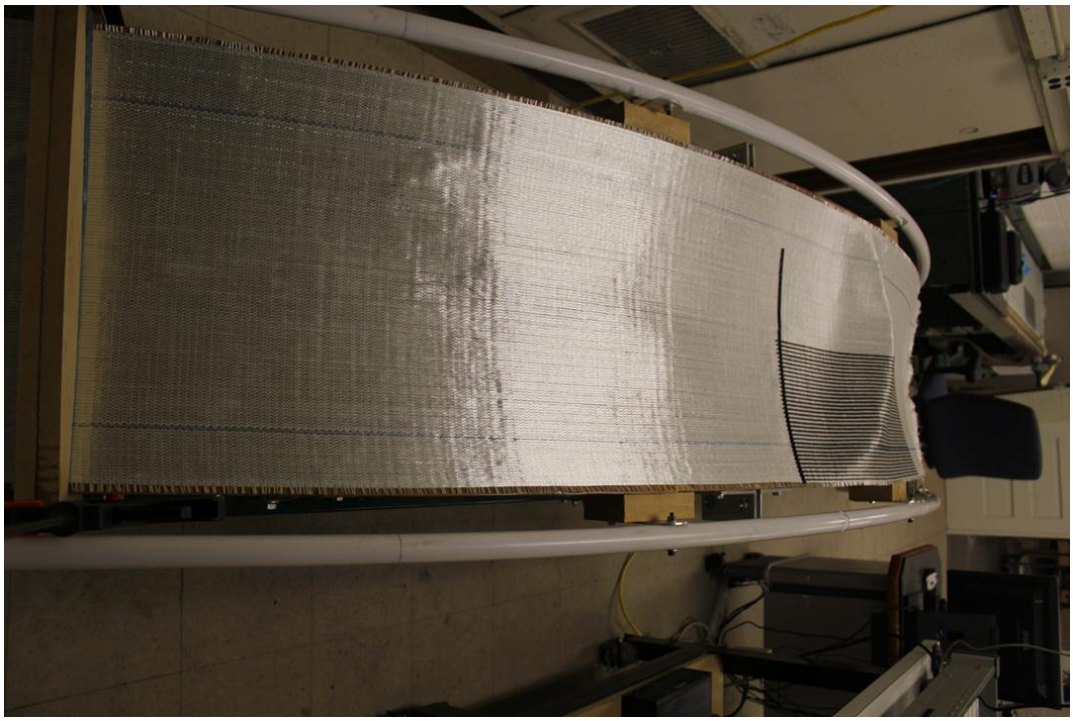

Figure 24. Layup result following the naïve approach

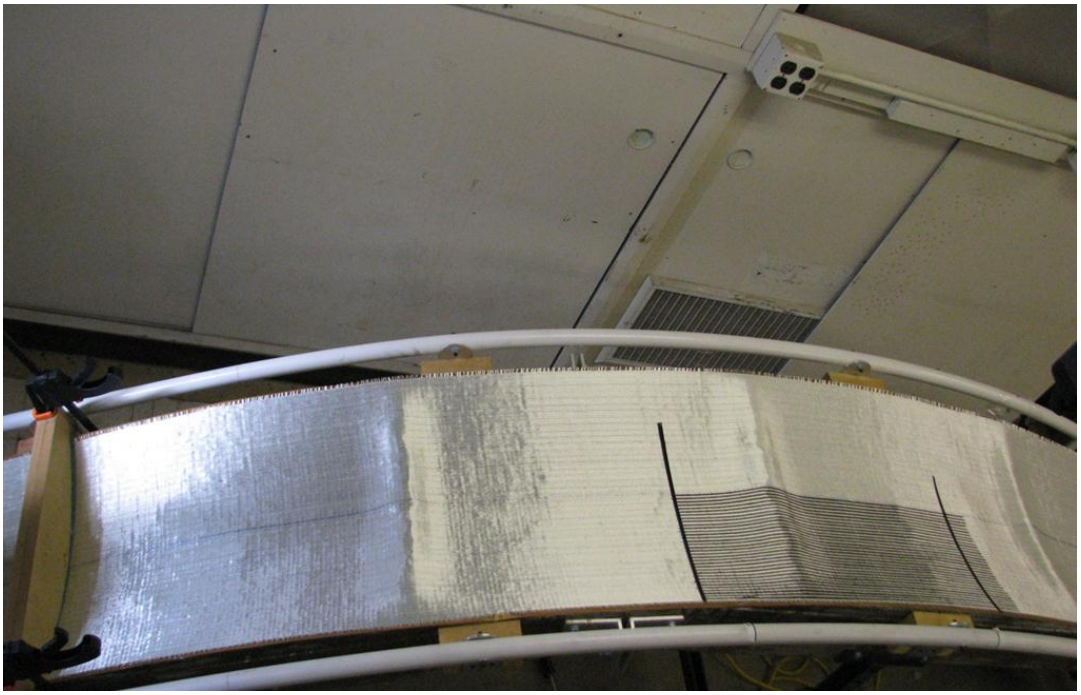

Figure 25. Layup result on the modified mold

6. Conclusion and Future Work

This work proposed a methodology of in-process manipulation planning for improving the drapability of fabric during composite layup. It has been verified via both simulation and experiment that by sacrificing a controlled amount of geometric conformity to the mold surface, this methodology is effective and robust in rectifying a given unfeasible layup plan. Essentially, the output of this methodology is a set of re-defined tow positions of the given UD fabric to be manipulated during the implementation of the layup process, following which will guarantee that the resulted IPS deformations are within the SLLs.

As a design for manufacturability tool, the in-process manipulation planning methodology can be integrated to traditional fabric layup simulation software packages. It will not only allow the composite structure designer to evaluate the fabric layup process on designed shape, but for the unfeasible cases, it will also automatically provide appropriate geometric modification suggestions on the original designed shape that will ensure the feasibility of the layup process.

The methodology of fabric manipulation developed in the current work accommodates the manipulation lengths as individual discrete OOM deformations to secure the feasibility of the layup process. Future work will search for an optimal method for continuous deposition of the manipulation lengths over the entire feasible region. This is equivalent to having a global modification to the mold shape; providing a feasible layup process while keeping the loss of geometric conformity at the minimum. A constraint to this optimization problem is that the resulted mold surface would need to meet the designed performance characteristics, but that would be outside the scope of this research area.

References

[1] Lubosny Z. Wind Turbine Operation in Electric Power Systems: Advanced Modeling (Power Systems). Berlin: Springer. 2003.

[2] Wang X, Wen Z, Wei J, Jens NS, Chen J. Shape optimization of wind turbine blades. Wind Energy 2009; 12; 8, 781-803.

[3] Potter K. In-plane and out-of-plane deformation properties of unidirectional preimpregnated reinforcement. Composites Part A 2002;33:1469-1477.

[4] Prodrodromou AG, Chen J. On the relationship between shear angle and wrinkling of textile composite preforms. Composites Part A. 1997;28(A):491-503.

[5] McBride TM, Chen J. Unit-cell geometry in plain-weave fabrics during shear deformations. Composites Part A. 1997;57:345-51.

[6] Mohammed U, Lekakou C, Bader MG. Experimental studies and analysis of the draping of woven fabrics. Composites Part A. 2000;31:1409-20.

[7] Potter K. The influence of accurate stretch data for reinforcements on the production of complex mouldings. Part 1: deformation of aligned sheets and fabrics. Composites 1979; July:161-167.

[8] Dong L, Lekakou C, Bader MG. Solid-mechanics finite element simulations of draping fabrics: sensitivity analysis. Composites Part A 2000;31:639-52.

[9] Meng F, Frank M, Peters F. Measurement, analysis and process planning for the layup of fabrics in wind turbine blades. Proceedings of the American Wind Energy Association Conference, Atlanta, GA 2012.

[10] Hancock SG and Potter KD. The use of kinematic drape modeling to inform the hand layup of complex composite components using woven reinforcements. Composites Part A 2006;37;413-422.

Appendix

Proof

For Case B, it is given that

$$\underset{j}{R}\{\tan\alpha_{Ni,J}\} > 2\times\tan\alpha_{SLL}$$

$$\Leftrightarrow \underset{j}{Max}\{\tan\alpha_{Ni,J}\} - \underset{j}{Min}\{\tan\alpha_{Ni,J}\} > 2\times\tan\alpha_{SLL} \quad \text{(B1)}$$

Suppose that

$$\underset{j}{Max}\{\tan\alpha_{Ni,J}\} \le \tan\alpha_{SLL} \text{ and } \underset{j}{Min}\{\tan\alpha_{Ni,J}\} \ge -\tan\alpha_{SLL}$$

$$\Rightarrow \underset{j}{Max}\{\tan\alpha_{Ni,J}\} - \underset{j}{Min}\{\tan\alpha_{Ni,J}\} \le 2\times\tan\alpha_{SLL}\text{, which is a contradiction to (B1)}$$

$$\Rightarrow \text{It is TRUE that } \underset{j}{Max}\{\tan\alpha_{Ni,J}\} > \tan\alpha_{SLL} \text{ or } \underset{j}{Min}\{\tan\alpha_{Ni,J}\} < -\tan\alpha_{SLL}\text{.}$$

CHAPTER 7. GENERAL CONCLUSION AND FUTURE WORK

This dissertation presented a three phased study toward the development of automated and optimal process planning tools for the layup of unidirectional fabrics onto three-dimensional mold surfaces.

In this first phase of the study, a modified laser scanning system and analysis technique were developed, with the capability of measuring the in-plane shear and out-of-plane deformations of UD fabrics at the resolution of between-tows level. The fine resolution and capability of measuring three-dimensional fabric deformations achieved by this measurement methodology allows the second phase of study, where the relationship between in-plane shear and out-of-plane deformations at unit cell level was analyzed.

The second phase of the study analyzed the effects of process parameters on the generation of different deformation modes and the transformation between them. It was found that the when local IPS angle value reached the shear locking limit, an OOM deformation was initiated. This OOM deformation in turn decreased magnitude of the IPS deformation. A volume conservation unit cell model based simulation method was proposed and validated utilizing the measurement data. Under this model, it was mathematically shown that the IPS angle at a given unit cell can be computed by using the layup constraint position, and the tow lengths from the constraint. This technique enabled an analytical explanation for the IPS angle distribution for the given mold geometry and the starting position of the layup. These two important findings from the analysis were further explored, in order to provide generalized solutions for improving the process of fabric layup in the third phase of the study,

where two process planning tools were developed: the pre-shearing planning and in-process manipulation planning.

The methodology of pre-shearing planning targets the manipulation of unidirectional fabrics prior to the layup process, with the purpose of obtaining optimal IPS angle distribution on the draped fabric, for a given three dimensional mold geometry-fabric property-layup process plan combination. The pre-shearing pattern is obtained quantitatively utilizing the shear angle distribution map obtained from kinematic drape simulation of commonly applied naïve/direct layup approach. It has been shown that the pre-shearing can make an unfeasible layup process feasible, or, at least, it can increase the drapability of the unidirectional fabric, reducing the effort on the smoothing operation during the layup process. The fabric pre-shearing method developed in this work can be applied in several aspects in the composite manufacturing industry. Firstly, as an add-on optimization package for the existing layup simulation software, the method presented in this work is able to automatically suggest the optimal shear angle distribution, and how this optimal result can be achieved via pre-shearing the fabric by following the pre-shearing profile generated from the package. Secondly, the pre-shearing method virtually increased the drapability of a given UD fabric, so that designs with more complex geometric features are allowed without switching to more expensive fabrics with better shear qualities. This is particularly important for the aerospace and wind turbine designers, who can be given lesser material and manufacturing constraints, so that better aerodynamic characters can be achieved. Lastly, the pre-shearing method can be implemented efficiently by different types of automated processes. If integrated with the pre-shearing function, the capability of traditional automated fabric

placement and smoothing machines can be significantly extended to perform layup on molds with more complex geometries.

The methodology of in-process manipulation planning was the second tool developed in the third phase of the study. Specifically, this process planning method considers the layup process which is predicted to be unfeasible by common computer layup simulations. By sacrificing a controlled amount of geometric conformity to the given three-dimensional mold, this method modifies the shear angle distribution within the unfeasible region, so that all the shear angle values can be controlled within the shear locking limits. The fabric's loss of geometric conformity to the mold is represented as out-of-mold deformations, and each of the deformation regions consists of tows with out-of-plane waves with respect to their nominal positions. Essentially, the method of in-process manipulation redefines the position of each individual tow in three-dimensional space, so that the feasibility of the layup process is guaranteed by having all the in-plane shear deformation angles within the shear locking limits, while keeping the loss of the geometric conformity within the manufacturing tolerances. As a design for manufacturability tool, the in-process manipulation planning methodology can be integrated to traditional fabric layup simulation software packages. It will not only allow the composite structure designer to evaluate the fabric layup process on designed shape, but for the unfeasible cases, it will also automatically provide appropriate geometric modification suggestions to the original designed shape that will ensure the feasibility of the layup process.

Future work should explore utilizing and extending the process planning tools developed in this work. Essentially, the output of these tools defines what to be achieved. The pre-shearing planning defines the two-dimensional shear deformation pattern to be

obtained within the fabric prior to the layup process, and the in-process manipulation planning defines the three-dimensional tow positions to be obtained for the layup process, in order to increase the fabric drapability and secure the process feasibility. For industrial automation applications, however, more factors should be considered on how to achieve the process plans. For example, the magnitude of force required for pre-shearing tows within a long fabric panel can be much larger than the force required in traditional fabric gripping and transferring systems. In addition, the gripping force on the tows must be uniformly distributed, in order to achieve a consistent shear deformation between the neighboring pair of tows under manipulation. A mechanical system with a special gripping device must be carefully designed to facilitate the realization the outcomes defined by the process planning tools.

Solutions out of this study were developed under a kinematic framework, where the simulations and analyses emphasized fabric deformations, mold geometries, constraint positions, and layup directions. As a possible venue of improvement, a dynamic approach could be integrated into the development of layup process planning tools. By considering additional factors including aerial density, tensile, shear and bending moduli of the fabric material, more advanced process planning tools can be expected to further improve the layup process.

ACKNOWLEDGEMENTS

This dissertation would not have been accomplished without the support of many people. I owe my gratitude to all those who have made this dissertation possible and because of whom my graduate experience has been one that I will cherish forever.

First and foremost, I would like to express my sincere appreciation to my major professors Dr. Frank Peters and Dr. Matthew Frank. Their expert guidance, mentorship and encouragements have made this an inspirational, thoughtful and rewarding journey.

I also would like to acknowledge Dr. Dayal, Dr. Vardeman, and Dr. Meeker for numerous discussions and lectures on related topics that helped me improve my knowledge in the area.

My parents Qingzhi Meng and Xiaoqin Wang for them bringing me up and giving me their immense love. I realize how lucky I am to have such great parents who sacrifice so much and persistently give me the best they have for my life and education.

The most special thanks belong to my wife Yanjun Liu, for her understanding, selfless love and support through the duration of my graduate study, and the patience, encouragement and company during the preparation of this dissertation.

Last but not least, my thankfulness extends to Kevin Brownfield, Wade Johanns, Ben Wollner, Daniel Chrusciel, and Thomas McGee, for supporting the of the development of laboratory equipment and the preparation of experiment materials.